MERCURY TOXICITY AND DETOXIFICATION IN *THERMUS THERMOPHILUS* HB27

By

JAVIERA A. NORAMBUENA MORALES

A dissertation submitted to the

School of Graduate Studies

Rutgers, The State University of New Jersey

In partial fulfillment of the requirements

For the degree of

Doctor of Philosophy

Graduate Program in Microbial Biology

Written under the direction of

Tamar Barkay

And approved by

____

____

____

____

New Brunswick, New Jersey

October 2018

ABSTRACT OF THE DISSERTATION

Mercury toxicity and detoxification in *Thermus thermophilus* HB27

by Javiera A. Norambuena Morales

Dissertation Director:

Tamar Barkay, Ph.D.

Mercury (Hg) is one of the most toxic and widely distributed heavy metals. To detoxify this metal the mercury (*mer*) resistance operon is present some Bacteria and Archaea. This is the most studied mechanism of Hg-detoxification. This dissertation describes how the *mer* operon is regulated in *Thermus thermophilus* HB27, how two of the genes present in this operon (*oah2* and *merR*) are involved in Hg(II) resistance, as well as low molecular weight (LMW) thiol and reactive oxygen species (ROS) responsive systems. *T. thermophilus* HB27 is a Gram-negative thermophile that has a very peculiar *mer* operon, it consists of *merA* (mercuric reductase), an hypothetical protein (*hp*), *merR* (regulator), and *oah2*, which encodes for an enzyme that synthesizes homocysteine. Therefore, the *mer* operon in *T. thermophilus* HB27 links mercury resistance to low-molecular weight (LMW) thiols biosynthesis. To determine the role of each gene in Hg-detoxification, mutant strains were constructed and their response to Hg was analyzed. I found that the *mer* operon has two promoters, one appears to be independent of regulation by MerR and in the other, MerR mediates response to Hg(II) as a repressor/activator. It was also determined that *oah2* as well as other LMW thiols biosynthetic genes (*oah1*, *bshA*, *bshB* and *oas*) and the thioredoxin system are involved in Hg resistance. I discovered that bacillithiol (BSH) is the major LMW thiol in strain HB27 and showed that Hg(II) caused depletion of the reduced BSH pool. This depletion was associated with an increase in ROS upon Hg(II) exposure and free iron concentration in the cytoplasm. I showed that ROS were triggered by Hg(II) and that superoxide dismutase and pseudocatalase, both known ROS detoxifying enzymes that maintain intracellular redox state, are involved in Hg(II) resistance. These results suggest that small thiols play a role in *T. thermophilus* HB27's response to Hg stress, possibly providing a buffer for Hg that is later removed by MerA. If thiols are oxidized by Hg(II), oxidative stress is produced leading to an increase in ROS. Collectively, the research presented in this dissertation describes how Hg(II) regulates the *mer* operon, interacts with LMW thiols and produces ROS in the extremophile *T. thermophilus*. Studying the physiology of *T. thermophilus* provides clues about the origin and evolution of mechanisms for mercury resistance and toxicity, as we as the oxidative stress response.

ACKNOWLEDGEMENTS

I would like to thank everyone that helped me during this process. First and foremost, I would like to thank my advisor Dr. Tamar Barkay for allowing me to work with her and be part of her lab. I would like to thank her and my co-advisor Dr. Jeff Boyd for all their feedback, encouragement and time spent discussing my research and new ideas. I am forever in debt with them. I would also like to thanks to the Barkay's and Boyd's Lab members, especially Zuelay, Spencer, Ameya, and Nicole, for their help and company through the years. I would specially like to thank Dr. Tom Hanson, for all his invaluable feedback and help with my research; as well as life. To Dr. Gerben Zylstra for all his time and invaluable feedback through the years and on this dissertation, but I would also like to thank him for all his guidance navigating the microbial biology program.

I would like to thank people that helped to make this research possible: Dr. Peter Kahn for providing access to and guidance in the use of the spectrophotometer used to measure MerA activity, Dr. Alexei M. Tyryshkin for his help with the EPR experiments and Dr. Akira Nakamura for kindly providing us with a plasmid harboring the Hygromycin B resistance which was fundamental for complementation and construction of double knock out strains.

Many thanks to all the different sources of funding that support me through the years, especially Fulbright and Becas Chile that made this possible. To the Graduate School of New Brunswick, as well as, the many Alumni and friends of the Department that, through their generous donations, made fellowships, scholarships, and travel awards possible. I am deeply grateful for the all their financial support. A special thanks to

Department of Biochemistry and Microbiology for providing me with the opportunity to be a teaching assistant over the year. It was an honor and pleasure to work with Dr. Natalya Voloshchuk.

Finally, I would like to thank to all family and friends that were routing for me from far away; especially to my mom, my aunt Nany, my brother, Pablo, Pamela and Isabel. Without you this would not have been possible.

TABLE OF CONTENTS

Abstract ii

Acknowledgements iv

List of Tables vii

List of Figures ix

Preface xii

Introduction 1

Chapter 1 – Expression and regulation of the *mer* operon by mercury in *Thermus thermophilus* HB27 7

Chapter 2 – Low-molecular-weight thiols and thioredoxins are important players in Hg(II) resistance in *Thermus thermophilus* HB27 32

Chapter 3 – Superoxide dismutase and pseudocatalase promote Hg(II) resistance in *Thermus thermophilus* HB27 by maintaining the reduced bacillithiol pool 66

Concluding Remarks 88

Appendix A – Supplementary Material for Chapter 1 93

Appendix B – Supplementary Material for Chapter 2 101

Appendix C – Supplementary Material for Chapter 3 178

References 123

LIST OF TABLES

CHAPTER 1

Table 1.1. *mer* operon transcript stability following cessation of de-novo transcription. 17

CHAPTER 2

Table 2.1 PCR primers used for construction of *T. thermophilus* HB27 knockout mutants in Chapter 2. 39

Table 2.2 qPCR primers used to measure gene expression of the listed genes in Chapter 2. 42

APPENDIX A

Table 1.S1 Primers used on Chapter 1. 97

Table 1.S2 Primers used for knockout construction on Chapter 1. 99

APPENDIX B

Table 2.S1. *gyrA* Ct values obtained in qPCR experiments for the WT strain of *T. thermophilus* HB27. 110

Table 2.S2. Fold induction of *trx* genes in *T. thermophilus* HB27 at different times after exposure to 1 μM Hg(II). 111

Table 2.S3. Concentrations of LMW thiols and effect of exposure to Hg(II) in *T. thermophilus* HB27 and in some of its mutants. 112

Table 2.S4. Structure of *mer* operons in Deinococcus-Thermus. 113

Table 2.S5. Alphaproteobacterial *mer* operons containing *gor*, the gene encoding for glutathione reductase (GR). 114

Table 2.S6. Locus tags of the proteins used to construct *Thermus* phylogenies. 116

Table 2.S7 Locus tag used to construct alphaproteobacterial phylogenies. 117

APPENDIX C

Table 3.S1. Primers used to construct mutant strains for Chapter 3. 121

Table 3.S2. Primers and parameters used for qPCR in Chapter 3. 122

LIST OF FIGURES

INTRODUCTION

Figure 1. Metal uptake and resistance mechanisms in prokaryotes. 3

CHAPTER 1

Figure 1.1. Hg-dependent induction of the *mer* operon. 16

Figure 1.2. Multiple promoter sequences are present in the *mer* operon. 18

Figure 1.3. Two different transcripts are synthesized from the *mer* operon. 19

Figure 1.4. *T. thermophilus's* MerR acts as a repressor/activator for P_{mer}. 22

Figure 1.5. The *mer* operon is transcribed constitutively from P_{oah2}. 24

Figure 1.6. Mercury affects *mer* operon operon expression. 30

CHAPTER 2

Figure 2.1. The *mer* and *met* operons, and the methionine metabolism pathways in *T. thermophilus*. 35

Figure 2.2. Thiol systems are induced by Hg(II). 48

Figure 2.3. Sensitivity to Hg(II) increased in mutant strains lacking LMW thiol synthesis genes or thiol homeostasis systems. 52

Figure 2.4. BSH is the primary LMW thiol in *T. thermophilus* and LMW thiols are responsive to Hg(II). 55

Figure 2.5. Decreased thiol availability enhances Hg(II) toxicity. 57

Figure 2.6. Molecular phylogenetic analysis of Oah proteins in *Thermus* spp. by the Maximum Likelihood method. 60

Figure 2.7. Proposed model for a two-tiered response to Hg(II) toxicity in *T.* 63

thermophilus.

CHAPTER 3

Figure 3.1. Mercury exposure induces ROS and increased SOD and Pcat expression. 75

Figure 3.2. ROS mutants are more sensitive to Hg(II) and have increased ROS levels upon Hg(II) exposure. 78

Figure 3.3. *T. thermophilus* strains lacking Sod or Pcat have decreased reduced BSH. 80

Figure 3.4. Mercury stress results in aconitase inactivation and increased intracellular free iron. 82

Figure 3.5. Working model for ROS generation by Hg(II). 85

CONCLUDING REMARKS

Figure 4.1. Proposed mechanism of Hg(II) toxicity and detoxification in *T. thermophilus*. 89

APPENDIX A

Figure 1.S1. Schematics of the *mer* operons and *rrsB* loci of the different strains used on Chapter 1. 93

Figure 1.S2. Differential expression of *mer* operon's genes in response to Hg(II) exposure. 94

Figure 1.S3. Control reactions for gene junction PCR. 95

Figure 1.S4. Convergent *mer* operons possess multiple promoters. 96

APPENDIX B

Figure 2.S1. LMW thiol biosynthesis genes are not induced by ROS or disulfide 101 stress.

Figure 2.S2. Thiol related genes are not induced by Hg(II) in *E. coli*. 102

Figure 2.S3. Resistance to Hg(II) in complex medium. 103

Figure 2.S4. MerA activity is not affected by exposure to Hg(II) in the Δ*oah2* strain. 104

Figure 2.S5. HPLC chromatograms of small thiol pools in *T. thermophilus*. 105

Figure 2.S6. Effect of diamide on Hg(II) toxicity. 106

Figure 2.S7. Molecular Phylogeny of Oah proteins in different *Thermus* spp. by the Maximum Likelihood method. 107

Figure 2.S8. Molecular phylogeny of GR proteins from Alphaproteobacteria obtained by the Maximum Likelihood method. 108

Figure 2.S9. Construction of HB27 knockout strains. 109

APPENDIX C

Fig 3.S1. Δ*sod* and Δ*pcat* strains are more sensitive to ROS than the WT strain. 118

Fig 3.S2. Genetic complementation of Δ*sod* and Δ*pcat* strains. 119

Figure 3.S3. A strain lacking Nfo is more sensitive to Hg(II). 120

PREFACE

Chapter 1 is in preparation for publication as “Expression and regulation of the *mer* operon by mercury in *Thermus thermophilus* HB27”, by J. Norambuena, J.M. Boyd and T. Barkay, to be submitted to Frontiers in microbiology.

J Norambuena contribution: All data used to generate figures and tables included in this chapter, except for the construction of Δ*merR* strain.

Chapter 2 has been published as “Low molecular weight thiols and thioredoxins are important players in Hg(II) resistance in *Thermus thermophilus* HB27.”, J. Norambuena, Y. Wang, T. Hanson, J.M. Boyd and T. Barkay. 2018. Appl Environ Microbiol. 84(2): e01931-17. PMID: 29150497.

J Norambuena contribution: All data used to generate figures and tables, except for Table 2.S4 and 5.

Chapter 3 is in preparation for publication as “Superoxide dismutase and pseudocatalase promote Hg(II) resistance in *Thermus thermophilus* HB27 by maintaining the reduced bacillithiol pool.”, J. Norambuena, T. Hanson, T. Barkay and J.M. Boyd, to be submitted to mBio.

J Norambuena contribution: All data used to generate figures and tables.

.

INTRODUCTION

Metals are classified as essential and non-essential to biological systems. Essential metals are required for growth due to their role as catalysts, enzyme co-factors, redox mediators and stabilizers of protein structures. Metals can easily become toxic to the cell (Nies, 1999). There are five known defense mechanisms that cells exploit to avoid metal toxicity (Figure 1), (1) efflux pumps, (2) enzymatic conversion, (3) cellular sequestration, (4) exclusion, and (5) reduced sensitivity of cellular targets (Nies, 1999, Dopson, 2003).

In mechanism 1, there are three main types of efflux pumps that decrease metal concentrations inside the cell (a) A- or P-type ATPases, (b) RND (root, nodulation, cell division) superfamily, and (c) CDF (cation-diffusion facilitator) family. The P- and A-type ATPases use ATP to pump metals out; the P-type ATPases can act as an uptake pumps as well. On the other hand, the heavy metal efflux RND family use proton gradient to pump metals out. The CDF family is driven by concentration gradient, chemiosmotic gradient, $\Delta\psi$, pH or potassium gradient (Nies, 2003).

Metals cannot be transformed or metabolized to innocuous compounds as organic contaminants are; the only way that some of them can be detoxified is by affecting environmental mobility, a process that may be carried out by enzymatic reduction (mechanism 2) or by the production of chelating molecules such as hydrogen sulfide. For reduction, the redox potential of the metal has to be close to that of the reducing agents present in the cytoplasm. One example is mercury (Hg) that is reduced from Hg(II) to elemental mercury, Hg(0), by mercuric reductase (MerA). Hg(0) has low aqueous solubility and high vapor pressure and thus is highly volatile leaving the immediate environment of the cell (Barkay *et al.*, 2003). On the other hand, some reduced products are more toxic to the cell than the original form of the metal, like arsenite (Nies, 1999). Cellular sequestration (mechanism 3) may occur extracellularly or intracellularly whereby the metal is sequestered, preventing cell damage. Intracellularly, the main buffering systems are small thiol molecules such as glutathione (GSH) or bacillithiol (BSH), which also act as redox buffers (Nies, 1999). Some specialized proteins bind metals, e.g., metallothioneins (MT), which are rich in cysteine (Cys) residues (Nies, 1999, Cassier-Chauvat & Chauvat, 2014). These intracellular molecules have been shown to be involved in metal resistance; a heavy metal multi-resistant yeast had higher levels of GSH when challenged with metals (Ilyas & Rehman, 2015). In *Cyanobateria*, metallothioneins respond to cadmium (Cd), cobalt (Co), chromium (Cr), copper (Cu), Hg, nickel (Ni), lead (Pb) and zinc (Zn) (Cassier-Chauvat & Chauvat, 2014).

In many microbes the influx of toxic metals can be avoided by exclusion (mechanism 4). For example, a mutation in a transporter gene reduced the import of arsenite (Dopson, 2003). Finally, it has also been described that the metal targets can be modified (mechanism 5), so the metal does not interfere in the target cellular processes; this is the case for a specific cytochrome *c*-oxidase that renders the cell more tolerant to Hg(II) among acidophilic organisms (Dopson, 2003).

Mercury is toxic to cells that has no known cellular role. Resistance to Hg, encoded by the *mer* operon, is wide spread over the bacterial and archaeal kingdoms. The most studied *mer* operons are specified by the proteobacterial Tn*21* and Tn*501* (Barkay et al., 2003). These operons encode for defense mechanism type 2 and can also encode for

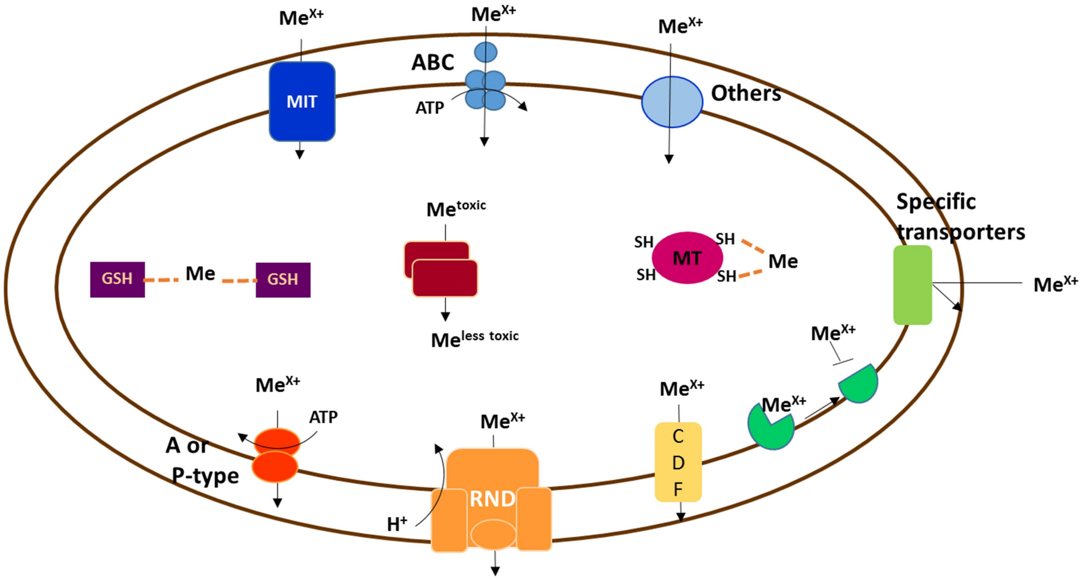
Me^X+
MIT
Me^X+
ABC
ATP
Me^X+
Others
Specific transporters
Me^X+
GSH
Me
GSH
Me^toxic
Me^less toxic
SH
SH
MT
SH
SH
Me
Me^X+
Me^X+
Me^X+
ATP
A or P-type
Me^X+
RND
H+
Me^X+
C
D
F

Figure 1. Metal uptake and resistance mechanisms in prokaryotes. Uptake systems are shown in blue and are usually transporters of essential metals. MIT (metal inorganic transport, dark blue) are unspecific transporter. ABC (ATP-binding cassette, blue), and other specialized transporters (light blue). The resistance mechanism are (mechanism 1) efflux pumps (various orange colors); (mechanism 2) enzymatic conversion (dark red); (mechanism 3) cellular sequestration is represented by GSH (dark purple) and proteins like metallothioneins (MT) (light purple); (mechanism 4) exclusion (green); and (mechanism 5) sensitivity reduction of cellular targets (light green). Adapted from Dopson et al., 2003 and Nies, 1999.

type 3 (Figure 1). Mechanism 2 includes the aforementioned *merA* and *merB* which can detoxify organomercurial compounds. For type 3, there is *merP* which encodes for a periplasmic protein that can scavenge Hg(II) (Steele & Opella, 1997), but it is not present in all *mer* opeons. The *mer* operon also encodes for transcriptional regulator, *merR*. MerR acts as a repressors/activator depending on the presence of Hg(II) and for *merD*, a secondary regulator that can act as a repressor (Barkay *et al.*, 2003).

Mercury is a “sulfur loving” metal and its toxicity is in part due to its high affinity for low-molecular weight (LMW) and protein thiols (Valko *et al.*, 2005, Jan *et al.*, 2011, LaVoie *et al.*, 2015). Thus, the main biological effects of Hg are related to this high affinity for sulfhydryl groups (Valko *et al.*, 2005), which results in thiol oxidation (Carvalho *et al.*, 2008, Wang *et al.*, 2013, Rodríguez-Rojas *et al.*, 2016, Norambuena *et al.*, 2018). There are two main systems that are able to reduce intracellular disulfide bonds, maintaining the cellular redox state of the cytoplasm, thioredoxin and glutathione systems. The thioredoxin system, present in all Bacteria, consist of thioredoxins (Trx 1 and/or Trx2, encoded by *trxA* or *trxC*, respectively) that are directly involved in disulfide bond reduction and thioredoxin reductase (TR or *trxB*) which utilize electrons from NADPH to reduce disulfide bonds in thioredoxins (Ritz & Beckwith, 2001). The glutaredoxin system predominates in Gram negative bacteria; it has three components: GSH, glutaredoxins (Grx) and glutathione reductase (GR). GSH reduces protein disulfides resulting in oxidized GSH dimers (GS-SG) or mixed disulfides with proteins. The later can be resolved by Grx. The oxidized GSH can be reduced by GR utilizing NADPH (Ritz & Beckwith, 2001). These systems have previously been documented to be involved in Hg(II) resistance (Valko *et al.*, 2005, Jan *et al.*, 2011, Wang *et al.*, 2013, LaVoie *et al.*, 2015).

Mercury must be detoxified to prevent cellular damage. Mercury cannot perform Fenton chemistry, but in animal models Hg(II) exposure resulted in oxidative stress (Lund *et al.*, 1991, Miller *et al.*, 1991, Ariza *et al.*, 1998, Ariza & Williams, 1999, Valko *et al.*, 2005). Oxidative stress occurs when there is an imbalance between pro-oxidants and antioxidants, shifting the balance towards pro-oxidants, like reactive oxygen species (ROS). ROS are produced by reduction of dioxygen by intracellular flavoproteins (Imlay, 2013). A one electron transfer to oxygen produces superoxide (O_2^-), which if not detoxified by superoxide dismutase (SOD) damages methionine, cysteine and iron-sulfur (Fe-S) clusters (Imlay, 2008, Imlay, 2014). While a two electron transfer produces hydrogen peroxide (H_2O_2) that can damage Fe-S clusters (Imlay, 2008). H_2O_2 is also produced by SOD and it can be detoxified by catalases, peroxidases or peroxiredoxins (Imlay, 2008). A three electron transfer to oxygen can be catalyzed by redox active divalent transition metals such as copper and iron (Fe) via Fenton and Haber-Weiss reactions to produce hydroxyl radicals ($HO^•$). These radicals cannot be detoxified by cellular enzymes, and rapidly react with multiple cellular constituents (Imlay, 2008, Imlay, 2014). Disturbance in LMW thiol redox buffers can be detrimental to the cell; these systems normally quench ROS that are generated during normal cellular metabolism. Mercury binding to the LMW thiols can disturb redox homeostasis causing ROS (Cassier-Chauvat & Chauvat, 2014).

Thermus thermophilus is a deep-branching thermophilic aerobe, a member of the Deinococcus-Thermus phylum that together with the Aquificae constitute the earliest aerobic bacterial lineages. This organisms that serves as a model for early-diverged bacteria (Hartmann *et al.*, 1989), whose natural heated habitat may contain Hg of geological origins (Geesey *et al.*, 2016). *T. thermophilus* HB27 possesses a very unique *mer* operon, it consists of *merA*, *merR*, a hypothetical protein (*hp*) and *oah2* (Wang *et al.*, 2009, Norambuena *et al.*, 2018). *merA* encodes for a mercuric reductase that reduces

Hg(II) to elemental Hg (Wang *et al.*, 2009) and *oah2* encodes for an *O*-acetyl-L-homoacetylserine sulfhydrylases that produces the low molecular weight thiol homocysteine (Iwama *et al.*, 2004). Both genes confer Hg(II) resistance (Wang *et al.*, 2009, Norambuena *et al.*, 2018). In other organisms MerR acts as transcriptional regulator that modulates transcription of the *mer* operon and the role of *hp* is currently unknown. In this dissertation, I studied the regulation of the *mer* operon and the role of MerR in its regulation (Chapter 1), the role of Oah2 and other LMW thiols in Hg(II) resistance (Chapter 2) (Norambuena *et al.*, 2018), and how ROS-detoxifying enzymes are involved in Hg(II) resistance through BSH (Chapter 3).

Research Goal and Objectives. The overarching goal of my research was to examine the responses of *T. thermophilus* to Hg stress; as well as, to understand how its particular *mer* operon is regulated by Hg(II). The work presented here reports on:

- How the *mer* operon is regulated in *T. thermophilus* by Hg – Chapter 1.
- The role of low molecular weight thiol and thioredoxins in mercury stress – Chapter 2.
- How ROS are generated upon Hg stress and how BSH is involved in this process – Chapter 3.

CHAPTER 1

EXPRESSION AND REGULATION OF THE *MER* OPERON BY MERCURY IN *THERMUS THERMOPHILUS* HB27

Abstract

Mercury (Hg) is a one of the most toxic and widely distributed heavy metals. Some Bacteria and Archaea possess the mercury resistance (*mer*) operon, specifying detoxification by the reduction of ionic Hg to elemental volatile Hg(0). The *mer* operon of the thermophile *Thermus thermophilus* HB27, representing an early lineage among the Bacteria, encodes for a mercury reductase (*merA*), a gene related to low molecular weight thiol biosynthesis (*oah2*), a hypothetical protein (*hp*), and a regulatory gene, *merR*. This study shows that *T. thermophilus mer* operon has two promoters, which are differentially regulated. The upstream promoter, P_{oah}, transcribes *oah2*, *merR, hp* and *merA*, the first two genes are constitutively expressed by this promoter, but *hp* and *merA* can also be expressed. A second promoter, P_{mer}, located in *merR*, is responsive to Hg(II). In P_{mer}, MerR acts as a repressor and activator, the presence of Hg significantly increasing *merA* transcripts in presence of Hg(II), but it requires MerR for its transcription. When P_{mer} along with MerR are removed, transcription initiated from P_{oah} constitutively expresses *merA*. These results suggest that the transcription regulation of *mer* in *T. thermophilus* is both similar to, and different from, the well-documented expression of the proteobacterial *mer* system, possibly representing an intermediate step in the evolution of *mer* regulation.

Introduction

Resistance to mercury (Hg) by the mercury resistance operon, *mer* operon is widely spread in the bacterial and archaeal kingdoms (Barkay *et al.*, 2003, Boyd & Barkay, 2012). The *mer* operon in *Thermus thermophilus* HB27, a Gram-negative thermophilic bacterium from an early lineage among the Bacteria, consists of *merA*, *merR*, a hypothetical protein (*hp*) and *oah2* (Wang *et al.*, 2009, Norambuena *et al.*, 2018). *merA* encodes for a mercuric reductase that reduces Hg(II) to the volatile elemental form, Hg(0), and *oah2* encodes for an *O*-acetyl-L-homoacetylserine sulfhydrylases that catalyzes the production of the low molecular weight thiol homocysteine (Wang *et al.*, 2009, Norambuena *et al.*, 2018). Both genes confer Hg(II) resistance (Wang *et al.*, 2009, Norambuena *et al.*, 2018). MerR in other microorganisms is a transcriptional regulator that modulates transcription of the *mer* operon (Barkay *et al.*, 2003). In Proteobacteria, MerR acts as a homodimer and is both a repressor and an activator depending on the presence of Hg(II). When Hg(II) is not present, MerR binds to the operator and blocks *mer* transcription (Summers, 2009), but when Hg(II) is present an allosteric change occurs in MerR's configuration (Guo *et al.*, 2010) underwinding the promoter (Ansari *et al.*, 1992) resulting in an increased transcription of *mer* (Summers, 2009). MerR in some Gram-positive bacteria operates very similarly to the proteobacterial system in spite of protein sequence and structural dissimilarities (Wang *et al.*, 2016); but little is known about how MerR regulates *mer* expression in early microbial lineages. In Achaea MerR acts only as a repressor (Schelert *et al.*, 2006), as it does in the Actinobacteria (Brünker *et al.*, 1996). The regulation of the *mer* operon in *T. thermophilus* by MerR may provide useful information on *mer* regulation in an early bacterial lineage.

The regulation of the *mer* operon has been well studied in proteobacterial systems. Transcription of *merR* is divergent from the rest of the *mer* genes with an overlapping promoter region that separates the two transcriptional units. This promoter region has two promoters, one promoter transcribes additional *mer* genes ($P_{merTP(C)AD}$) in one direction and the other promoter transcribes only *merR* (P_{merR}) in the other direction. This arrangement allows MerR to regulate its own synthesis, as well as that of the *mer* genes (Brown *et al.*, 2003). In absence of Hg(II), MerR binds 26-bp upstream from the transcription start of the *mer* genes (Ansari *et al.*, 1992). There, MerR attracts the RNApol to the promoter and bends the promoter away from the RNApol as a stable none-transcribing pre-initiation complex (Heltzel *et al.*, 1990, Barkay *et al.*, 2003). When the MerR-RNApol complex is bound to the operator/promoter in $P_{merTP(C)AD}$ the -35 and -10 regions are projected in opposite directions, this configuration changes when Hg(II) binds to MerR underwinding the DNA and facing the -35 and -10 regions in the same direction aligning (Ansari *et al.*, 1992). The angle of the operator/promoter when Hg(II) is bound to MerR is similar to the one found in an 18-bp promoter (Ansari *et al.*, 1992). Usually bacterial promoters have a 16 to 18 bp spacer between the -35 and -10 regions, but $P_{merTP(C)AD}$ has a 19-bp spacer, making MerR necessary for the activation of the promoter. When the spacer is altered, MerR is no longer needed for activation of $P_{merTP(C)AD}$ (Shewchuk *et al.*, 1989, Ansari *et al.*, 1992).

MerR has three distinct protein domains each with its own unique function. The N-terminal domain of MerR binds to DNA, an intervening region that plays a role in repression and conformational change to the activator state, and the Hg(II) binding domain present the C-terminal domain (Zeng *et al.*, 1998). Mercury binding occurs in a trigonal coordination between cysteines 126 and 117 of one monomer and cysteine 82 of the other in proteobacterial MerR (Zeng *et al.*, 1998). When C126 is replaced by a serine, the MerR mutant had less affinity to Hg(II), but has the same DNA binding affinity than the WT strain (Shewchuk *et al.*, 1989). This MerRC126S strain did not activate *merA* transcription, but had nearly WT levels of repression in absence of Hg(II) (Shewchuk *et al.*, 1989). Similar results were found when the cysteine was replaced by tyrosine (Ross *et al.*, 1989).

The *mer* operon in *T. thermophilus* has a convergently transcribed *merR* gene homolog, but its role in gene regulation, including whether it acts as a repressor/activator (as among the Proteobacteria and the bacilli) or only as a repressor (as in Archaea and some Actinobacteria), is not known. This study provides evidence that MerR in *T. thermophilus* HB27 is proteobacterial type regulator, that interacts with two distinct promoters which are differentially controlled by Hg(II) through MerR.

Methods

Bacterial strains and growth conditions

Thermus thermophilus HB27 (DSMZ 7039) and its mutants were cultured at 65°C in 461 Castenholz TYE medium as previously described (Wang *et al.*, 2009, Norambuena *et al.*, 2018). When grown in liquid media cells were cultured in 3 mL of medium in 13 mL tubes and shaken at 200 rpm. Solid culture TYE medium was supplemented with 1.5% agar. When present, kanamycin was added to 25 µg/ml (Sigma) and Hygromycin B to 40 µg/ml (Sigma).

RNA extraction, cDNA synthesis and qPCR

The OD_{600} of an overnight (O.N.) cultures was adjusted to 0.1 with TYE medium and cultures were grown to OD of ~0.4 when 1 µM of $HgCl_2$ was added and incubation continued for 7.5, 15 or 30 minutes; each experiment included an unexposed control. RNA extraction, cDNA synthesis and qPCR were performed as previously described by Norambuena *et al* (2018). The annealing temperature and primer sequences are shown in Table 1.S1. Results of at least three biological replicates were averaged in all experiments.

RNA degradation, coding strand assay and junction PCR

It was determined in our laboratory that *T. thermophilus* is sensitive to the RNA polymerase inhibitor rifampicin (not shown). The OD_{600} of a 24 hours culture of the wild type (WT) strain was adjusted to 0.1 and grown to an OD of ~0.4 when 1 µM Hg(II) was added. Incubations continued for 15 min prior to the addition of 500 µg/ml rifampicin (Sigma) (Dressaire *et al.*, 2013). Three-ml samples of exposed cultures were withdrawn at 0, 20 and 30 min after the addition of the antibiotic followed by RNA extraction, cDNA synthesis and qPCR analysis as described (Norambuena et al., 2018). Experiments included at least triplicate exposed cultures and an unexposed control and transcript copy number was calculated from a calibration curve run in parallel for each gene transcript.

DNA-free RNA from 15 minutes uninduced and Hg-induced cultures was used as template for cDNA synthesis in coding-strand assays. Primer-specific cDNA was synthesized using 1 µg of RNA and reverse primers (Table 1.S1) for *oah2*, *merR* and *merA* (these only matched the coding RNA sequence). cDNA synthesis was carried with

High-Capacity cDNA Reverse Transcription Kit (Applied Biosystems) as manufacturer's instructed. For the following PCR reaction primer sets specific for *oah2*, *merR* or *merA* were used (Table 1.S1). The PCR reaction was set up as follows: 12.5 µl of 2X Master Mix (Promega), 1 µl cDNA and 1 µM of each primer, in a 25 µl reaction. The thermal cycling conditions were: initial denaturation at 95°C for 5 min, followed by 30 cycles of denaturation (95 °C for 15 sec), annealing (15 sec), extension (72 °C for 15 sec), and a final extension at 72 °C for 10 minutes. Employed annealing temperatures for each set of primers are listed in Table 1.S1. PCR products were visualized in a 2% agarose gel.

To determine to length of transcripts, junction targeted PCR, cDNA from Hg(II)-exposed and unexposed cultures was used for the PCR reactions. PCR was performed as stated above and PCR products were visualized in a 1.5% agarose gel. Primers used are listed in Table 1.S1.

5' RACE PCR

The OD_{600} of an O.N. grown cultures was adjusted to 0.1 in complex medium and grown to an OD_{600} of 0.4 when 1 µM of Hg(II) was added and incubations continued for 15 min when RNA was prepared as described above. For 5' RACE PCR, DNA-free RNA was ligated with 0.3 µg/µL of 5' RNA adapter (Table 1.S1) using T4 ligase (NEB) as manufacturer's instructed. Ten µL of the ligated RNA was used for cDNA synthesis with Superscript III kit (life technologies). The outer PCR reaction was performed as described in the previous section using 1 µL of the cDNA for 35 cycles and primers listed in table S1. The inner PCR was performed with 1:50 dilution of the outer PCR product for 30 cycles (primers are listed in Table 1.S1). PCR products from the inner PCR reaction were gel purified and cloned into TOPO-TA (life technologies) as manufacturer's instructed. Ten to 20 clones were sequenced (Genewiz, South Plainfield, NJ) for the Hg-treated and untreated cultures.

Mutant construction

Construction of the Δ*merA* mutant was previously described (Wang *et al.*, 2009) and transformation procedures were performed as previously described (Norambuena *et al.*, 2018). Primers used for mutant construction are listed in Table 1.S2. For the MerRC128S replacement the mutation was introduced amplifying *merR* with mutagenized primers and the assembly of the construct was performed as all the other mutants. All transformants were confirmed by sequencing (Genewiz, South Plainfield, NJ). For genetic complementation the 16S rRNA gene, the *rrsB* locus (TT_C3024), was replaced with the complementing gene constructs. It was previously reported that *T. thermophilus* HB27 is capable of surviving with a single copy of its two *rrs* genes (Gregory & Dahlberg, 2009). Figure 1.S1 depicts the different strains used in this study.

Mercury resistance and pre-incubation assays

The OD_{600} of an O.N. grown cultures was adjusted to 0.1 in fresh medium and exposed to $HgCl_2$ concentrations of 0 to 10 µM for 14-24 hours. For the pre-incubation assays, O.N. grown cultures were diluted to OD_{600} of 0.2 and cells were incubated, or not, with 0.2 µM of $HgCl_2$ for 2 hours. Cultures were then spun down, washed once with fresh medium and resuspended to OD_{600} of 0.1 before $HgCl_2$ exposure for 24 hours. To quantitate

Hg(II) resistance, growth of each strain at 0 μM was considered 100%. Unless otherwise stated, experiments were performed in at least triplicate independent cultures.

MerA activity

The assay was performed as previously described by Norambuena *et al*. (2018). Oxidation of NADH by crude-cell extracts was monitored each second at 340 nm for 60 seconds at 70 °C (AVIV, biomedical spectrophotometer, model 14 UV-VIS). Specific activities were defined as units (U)/mg of protein; 1U corresponded to 1 mmol of NADH oxidized per min. Bradford assay (Bio-Rad Laboratories Inc., Hercules, CA) was used to determine protein concentrations.

Promoter prediction

Promoter prediction of the *mer* operon was performed with BPROM software (Solovyev, 2011).

Statistical analysis

Two-group comparisons were performed using t-test. For multiple-group comparisons, One-way analysis of variance (ANOVA) followed by Tukey test, was performed.

Results

The mer operon is induced by Hg(II) and mer genes have differential expression patterns

The *mer* operon in *T. thermophilus* HB27 consists of *merA*, *merR*, *oah2* and a hypothetical protein (*hp*) (Figure 1.1A). It was previously suggested that this operon is expressed as a single transcriptional unit when cells were exposed to Hg(II) (Wang *et al.*, 2009). To further understand how Hg(II) affects *mer* expression, the transcript abundance of each gene was quantified in cells that had been exposed to 1 μM Hg(II) for 7.5, 15 and 30 minutes. The abundances of *oah2* and *merR* transcripts displayed the highest induction after 7.5 min of exposure to Hg(II), which corresponded to ~ 6-fold induction. In contrast, *merA* was maximally induced at 15 minutes and at a much higher level (~ 400-fold induction) (Figure 1.1B).

The differences in fold induction and time at which transcript accumulation peaked suggest a differential expression pattern. The stability of *mer* operon's transcripts was measured to evaluate if there is a differential transcript stabilities that could explain these differences. For this, cells were exposed for 15 min to 1 μM Hg(II) when rifampicin was added to stop further transcription and cells were collected for RNA extraction after 0, 20 or 30 min of additional incubation. Indeed, *oah2* and *merR* transcripts were found less stable than *merA* or *gyrA* transcripts (Table 1.1); 20 min after rifampicin addition, only 38% and 13% of *oah2* and *merR* transcripts remained, respectively; while no significant changes were observed in *merA* or *gyrA* transcript copy numbers even after 30 min. This suggests that transcripts of *mer* genes located at the 5' end of the operon are less stable than those of genes located downstream or other *Thermus* genes; this could explain the temporal variation, but not likely the >60 fold difference in fold induction (Figure 1.1B), in *mer* gene transcription.

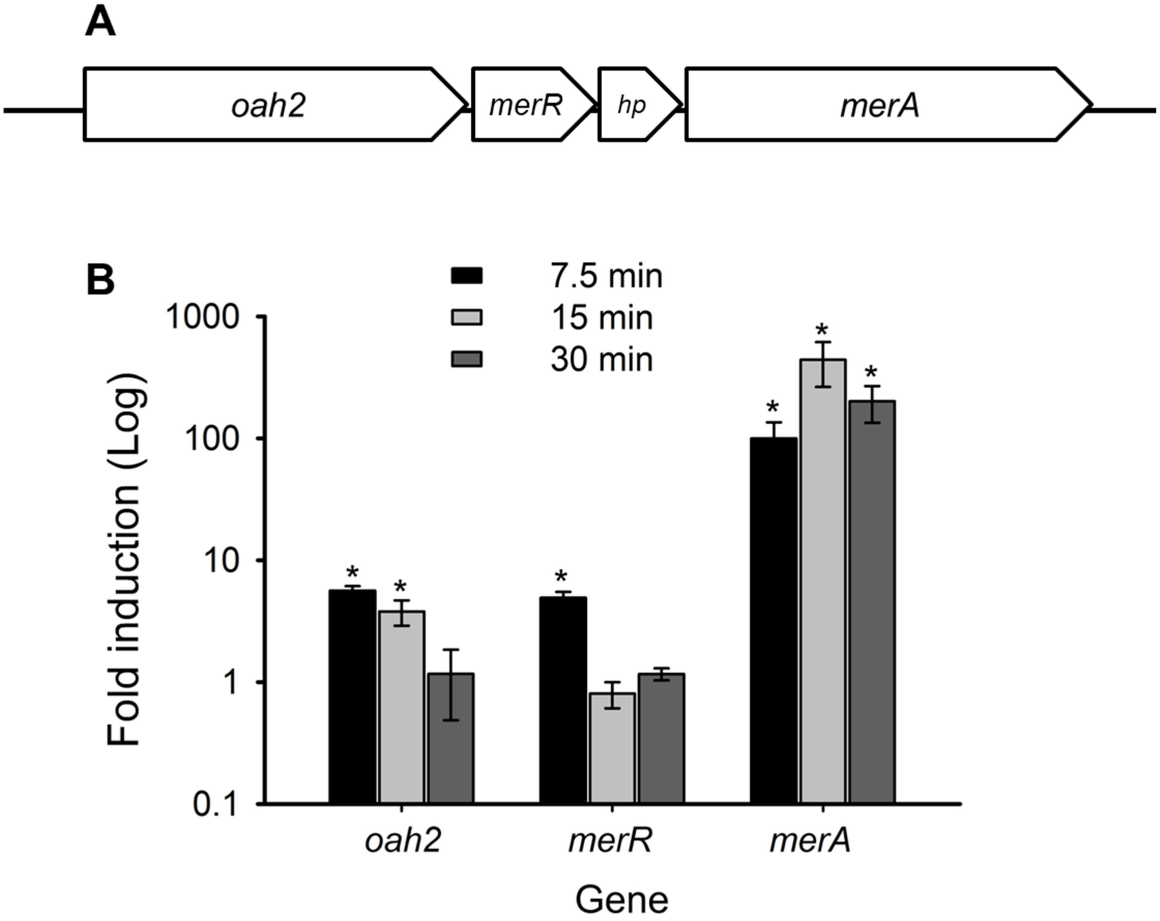

Figure 1.1. Hg-dependent induction of the *mer* operon. (A) Diagram of the *mer* operon in *T. thermophilus* HB27. This operon includes *oah* (TTC0792), *merR* (TTC0791), hypothetical protein (*hp*, TTC0790) and *merA* (TTC0789) genes. The arrow indicates the direction of the transcript. (B) Expression of *mer* operon genes was evaluated in the WT strain 7.5, 15 and 30 min after Hg(II) exposure. Gene expression was normalized to *gyrA* transcripts and presented as logarithm of fold-induction relative to respective unexposed controls (ΔΔCt method) (Norambuena *et al.*, 2018). Statistical analysis was conducted using the two-tailed t test. *, P ≤ 0.03.

Table 1.1. *mer* operon transcript stability following cessation of de-novo transcription.

Time after rifampicin addition (min)	**Copy number**			
	oah2	*merR*	*merA*	*gyrA*
0	3,413 ±470	1180 ±250	40,090 ±7,343	35,956 ±8,475
20	1,358 ±252*	160 ±43.4*	40,846 ±17,838	35,209 ±10,328
30	1,004 ±434*	200 ±29.5*	44,369 ±19,340	44,139 ±10,764

One way ANOVA followed by a Tukey test comparing each time to 0 min after rifampicin addition for each gene. * P <0.001.

The differential fold induction can be explained by either a low basal transcription of *merA* in absence of Hg(II) and/or the presence of a second promoter that regulates *merA* transcription separately from *oah2* and *merR*. To test the first possibility, cDNA was synthesized using only primers for the coding sequence. As expected, *oah2* and *merR* are expressed in presence and absence of Hg(II), but *merA* is only expressed when Hg(II) is present (Figure 1.S2). The low level of *merA* transcript in absence of Hg(II) and the high copy number of *merA* transcript (Table 1.1), compared to *oah2* and *merR,* can explain why the fold induction is so high. These results are consistent with fewer *merA*, relative to *oah2* and *merR*, reads reported for a transcriptome analysis of strain HB27 obtained in absence of Hg(II) (Swarts *et al.*, 2015).

Next, the possibility of multiple promoters was evaluated using the BPROM software. Two putative promoters were identified, one located upstream of *oah2* and the second promoter in *merR* (Figure 1.2A and C). The functionality of both promoters was confirmed by 5’ RACE-PCR (Figure 1.2B and D). The first, or *oah* promoter (P_{oah}) was

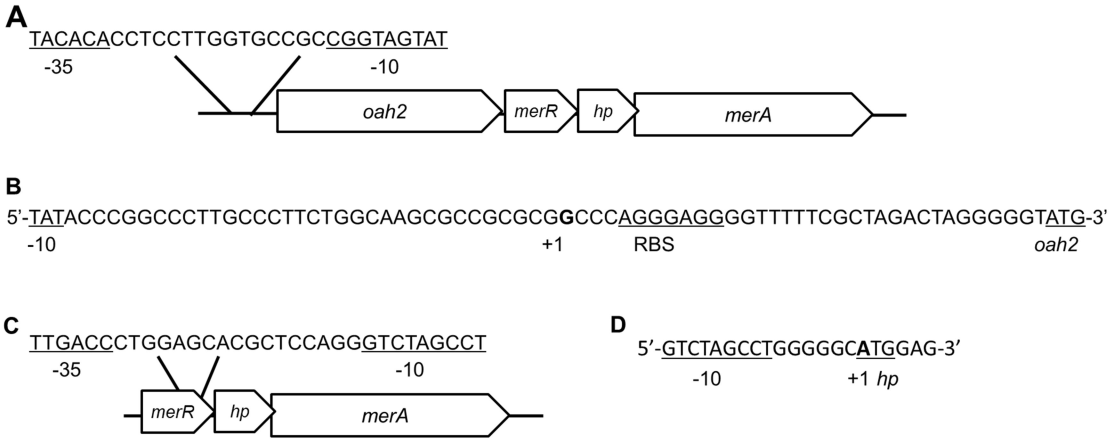
A
TACACACCTCCTTGGTGCCGCCGGTAGTAT
-35
-10
oah2
merR
hp
merA
B
5'-TATACCCGGCCCTTGCCCTTCTGGCAAGCGCCGCGCGGCCCAGGGAGGGGTTTTTCGCTAGACTAGGGGGTATG-3'
-10
+1
RBS
oah2
C
TTGACCCTGGAGCACGCTCCAGGGTCTAGCCT
-35
-10
merR
hp
merA
D
5'-GTCTAGCCTGGGGGCATGGAG-3'
-10
+1 hp

Figure 1.2. Multiple promoters are present in the *mer* operon. Putative promoters were determined bionformatically (A and C) and confirmed by RACE 5'-PCR (B and D). One promoter was located upstream of *oah2* (A and B) and the second promoter (C and D) at the 3' end of *merR* (400 bp). -35, -10 sites and ribosome binding site (RBS) are underlined and +1 sites are indicated by bold-face letters.

detected in PCRs samples prepared from cells exposed and unexposed to Hg(II), indicating that this promoter is active independently of Hg(II) and has a +1 site, signifying translation initiation, before the ribosomal binding site. Interestingly, most of the sequenced colonies started on the first codon of *oah2* (80% of the sequences), not in the +1 site. On the other hand, the *merR*-located promoter (P_{mer}) was only detected when Hg(II) was present; the +1 site for this promoter was found on the first codon of *hp* (Figure 1.2D).

To further understand how this operon is regulated by Hg(II), primers were design for the junctions between the 4 genes in the operon, as indicated in Figure 1.3A. cDNA was prepared for cells exposed, or not, to 1 µM of Hg(II) for 15 minutes; the sets of primers used to amplify cDNA are shown in Figure 1.3B. *oah2* and *merR* are constitutively expressed, as shown by the presence of a band in presence and absence of Hg(II) (Figure 1.3C). On the other hand, bands for the junctions between *merR* and *hp* or

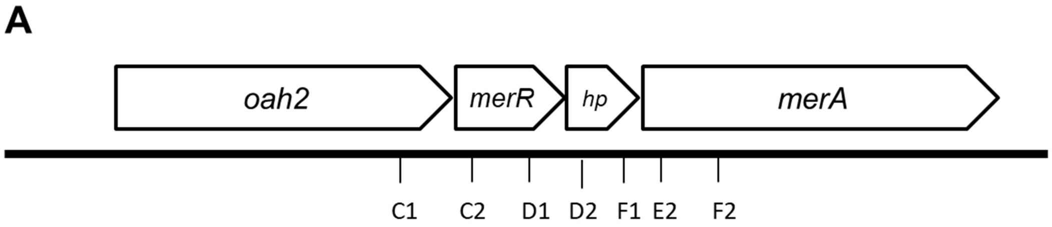

B

Primer set	Size (bp)	Gene junction targeted	PCR product
C1-C2	159	*oah2-merR*	C
D1-D2	169	*merR-hp*	D
D1-E2	211	*merR-merA*	E
F1-F2	333	*hp-merA*	F

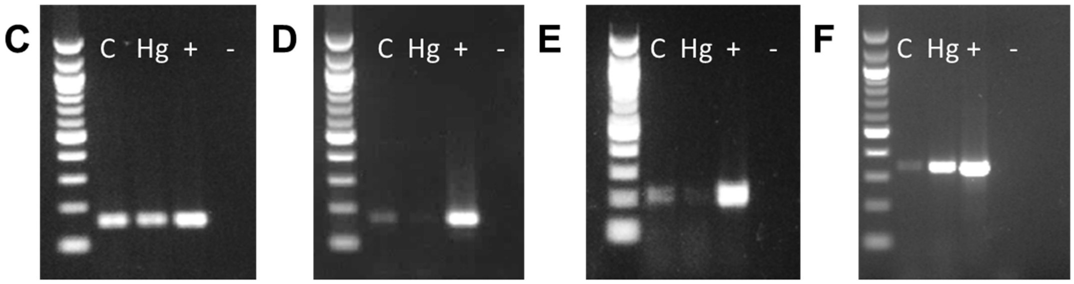

Figure 1.3. Three different transcripts are synthesized from the *mer* operon. (A) Sequence locations of the primers used for transcript determination. (B) primers sets used to amplify specific gene junctions. (C-F) PCR of cDNA from cells exposed (Hg) or not (C) to 1 µM Hg(II) for 15 min, primer sets used are indicated in B. +, positive control (DNA) and -, negative control (no template). These PCRs are representatives of at least 5 independent experiments. PCR products were visualized in a 1.2 % agarose gel and 100bp ladder was used.

merA, weakly present in absence of Hg(II), are almost undetectable when Hg(II) was added to the growing culture (Figure 1.3D and E). PCR reactions set with only RNA from the samples had no products (Figure 1.S3), indicating that contaminating DNA was not present in cDNA preparations used as a template in gene junction PCR. Results show that there is some basal transcription of *hp* and *merA* in absence of Hg(II), possibly attributed to a long transcript that is initiated from P_{oah} and includes all operon's genes. This transcript is not the only one made in absence of Hg(II), *oah2* and *merR* transcripts are more abundant than *hp* and *merA*, as shown by the lower intensity of the band, suggesting that a short transcript of *merR* and *oah2* is preferentially made from P_{oah}. Finally, the *hp*-*merA* junction increases when Hg(II) is added to the culture (Figure 1.3F), suggesting that the short transcript initiated from P_{mer}, shown by 5' RACE-PCR (Figure 1.2D), is induced by Hg(II). It is worth noticing that when Hg(II) is present, the intensity of the *merR*-*hp* or *merR*-*merA* junctions fades, this further suggest that in presence of Hg(II) the transcription of *merA* from P_{oah1} is suppressed.

MerR acts as a repressor/activator for P_{mer}

To corroborate the role of MerR in Hg(II)-dependent regulation of *mer* in *T. thermophilus*, a knock out strains were constructed. As aforementioned, P_{mer} is a part of *merR*, so to determine the role of MerR in the regulation of this promoter the knock out strain constructed had intact P_{mer} but lacked the N-terminal and middle domains of *merR* (this strain was named Δ*merRprom* – Figure 1.S1). When tested for Hg(II) resistance, the Δ*merRprom* strain was more sensitive to Hg(II) than the WT strain, with IC_{50} of ~3 μM and ~4 μM, respectively (Figure 1.4A). The Δ*merRprom* strain behaved similarly to the

Δ*merA* strain, although the Δ*merA* strain was slightly more sensitive to Hg(II) with an IC_{50} of ~2.5 µM (Figure 1.4A). To confirm that this phenotype was due to MerR and not to faulty *merA* transcription, the Δ*merRprom* strain was complemented with a native *merR*. This *merR* was expressed from its own promoter (P_{oah2}) and replaced *rrsB* loci; this strain was named Δ*merRprom merR::rrsB*. As expected, strain Δ*merRprom merR::rrsB* that was pre-exposed to 0.2 µM Hg(II) for 2 hours was as resistance to 4 µM Hg(II) as the WT strain, while pre-exposure to Hg(II) in the Δ*merRprom* had no effect in Hg(II) resistance (Figure 1.4B). Thus, MerR is needed for, and likely the activator of, transcription of *merA* from P_{mer}.

To test if MerR is also a repressor of P_{mer}, two approaches were used; the first one was to compare *merA* transcript copy numbers between the Δ*merRprom* and the WT strains. If MerR acts as a repressor, in the absence of Hg(II) the copy number of *merA* transcripts in the WT strain should be lower than in the Δ*merRprom* strain due to repression by MerR. Indeed, the *gyrA*-normalized *merA* transcript copy number was ~ 6 times lower in the WT strain than in the Δ*merRprom* strain (Figure 1.4C). Moreover, in the presence of Hg(II), no change in the *merA*/*gyrA* transcripts ratio was detected relative to the unexposed control in the Δ*merRprom* strain, while a significant 100-fold increase in this ratio occurred in the WT strain (Figure 1.4C), confirming MerR as an activator of *merA* transcription.

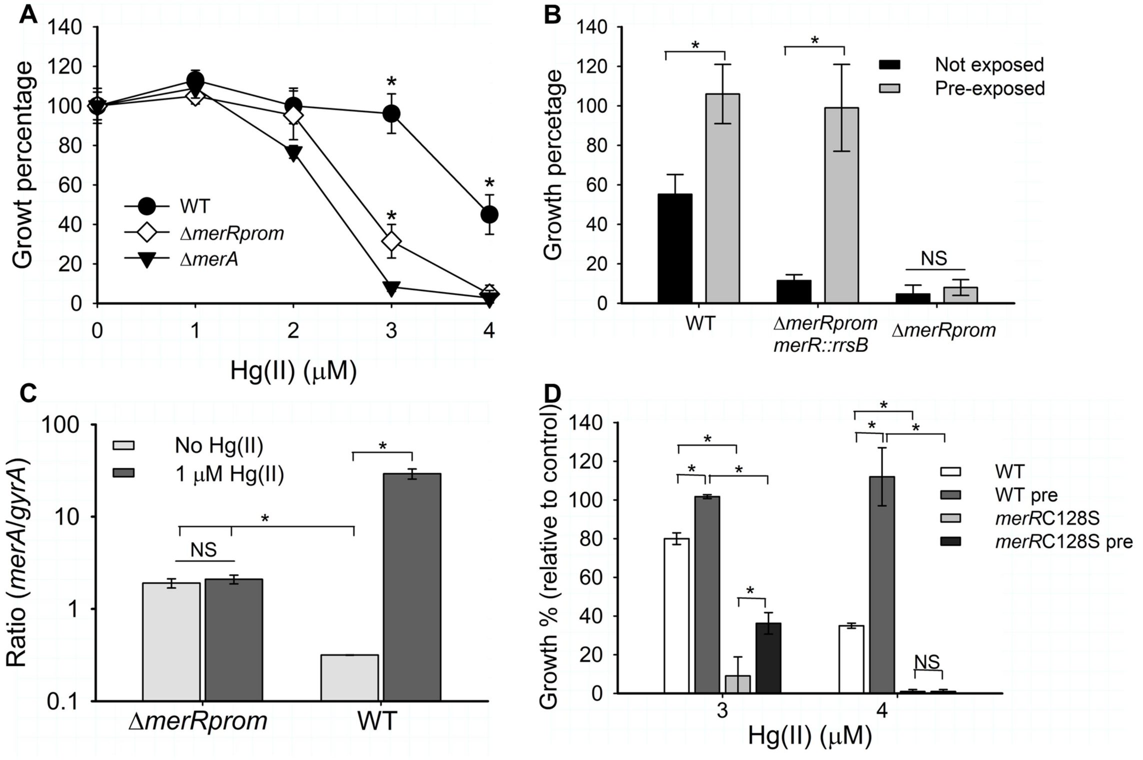

Figure 1.4. *T. thermophilus*'s MerR acts as a repressor/activator for P_{mer}. (A) Effect of growth on Hg(II) was measured in the WT, Δ*merA* and Δ*merRprom* strains after 22 hours of incubation. (B) WT, Δ*merRprom* and the complemented Δ*merRprom merR::rrsB* strains were pre-induced with 0.2 μM of Hg for 2 hours (grey) or not (black). Pre-induced cells were then grown in 4 μM Hg(II) for 22 hours. (C) Copy number of *merA* and *gyrA* transcripts were measured in WT or Δ*merRprom* strains exposed (grey) or not (white) to 1 μM Hg(II) for 15 min. (D) Growth on the WT or *merR*C128S strains was evaluated in presence of 3 and 4 μM Hg(II) after 20 hours of incubation. Growth with 0 μM of Hg (II) was considered 100% growth for each strain. Each point represents the average of three independent experiments. Bars represent standard deviations. t-test, *P≤ 0.01, NS: not significant.

The second approach used to confirm the role of MerR as a repressor of P$_{mer}$ was the construction of a MerR unresponsive to Hg(II). It has been previously shown that replacement of the last cysteine for serine in the metal binding domain of proteobacterial MerR caused lost in affinity to Hg(II), without affecting MerR's DNA binding ability (Shewchuk *et al.*, 1989). A *T. thermophilus* MerRC128S mutant, named *merR*C128S, was constructed replacing the native MerR of *T. thermophilus*. The *merR*C128S strain was as sensitive to Hg(II) as the Δ*merA* strain (not shown) with an IC$_{50}$ of 2.5 µM of Hg(II) (data not shown). Above, we have shown that MerR is a repressor/activator, so pre-exposure of cells for 2 hours to 0.2 µM Hg(II) before exposure to different Hg(II) concentrations should allow the expression of *merA* and an increase in Hg(II) resistance. As shown in figure 1.4D, pre-exposure to Hg(II) of strain *merR*C128S did not result in an increase in Hg(II) resistance as did for the WT strain at 3 and 4 µM of Hg(II), indicating that the substitution of cysteine 128 with serine makes MerR act only as a repressor, losing the ability to be activated by Hg(II).

Taken together, these results clearly show that MerR in *Thermus* acts as a repressor/activator MerR, in absence of Hg(II) it binds to P$_{mer}$ and represses the expression of *merA*, but when Hg(II) is present it acts as an activator of *merA*.

P$_{oah2}$ constitutively produce merA

To determine if *merA* could be constitutively expressed from P$_{oah2}$, a strain lacking all *merR* (including the P$_{mer}$; this strain was named Δ*merR*) was constructed. In this strain, the transcription could only be initiated from P$_{oah2}$. As shown in Figure 1.5A the Δ*merR* strain was more than two times more resistant to Hg(II) than the WT strain

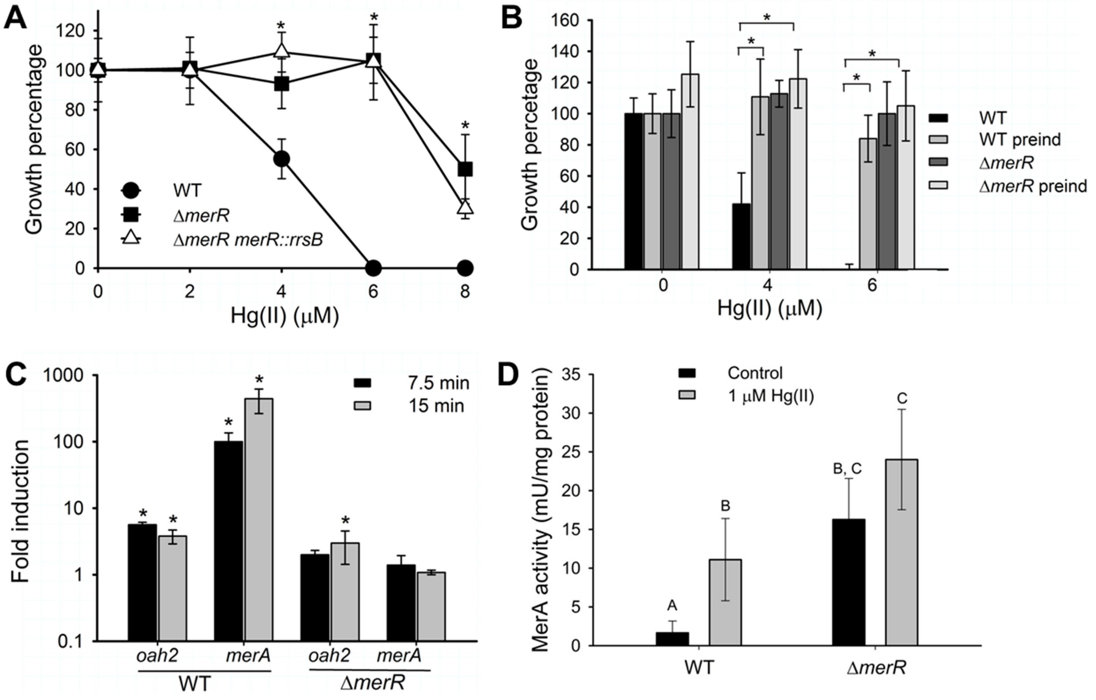

Figure 1.5. The *mer* operon is transcribed constitutively from P_{oah2}. (A) Growth was measured in presence of different Hg(II) concentrations after 22 hours of incubation for the WT (circle), Δ*merR* (square) and the complemented Δ*merR merR::rrsB* strains (triangle). (B) WT and Δ*merR* cells were pre-induced with 0.2 μM of Hg for 2 hours in complex medium. Pre-induced cells were then grown for 24 hours in different Hg(II) concentrations. Growth at 0 μM of Hg (II) was considered 100% growth. (C) Expression of *mer* operon genes was evaluated in WT and Δ*merR* strains 7.5 and 15 min after exposure to 1 μM Hg(II). Gene expression was normalized to *gyrA* gene and graphed by logarithm of fold-induction relative to their respective controls (ΔΔCt method). (D) Cells were exposed (grey), or not (black), to 1 μM Hg(II) for 30 min, prior to cell rupture and MerA activity measurements. One unit of MerA activity was defined as Hg(II)-dependent oxidation of 1 μmol of NADH per min. Each point represents the average of three independent experiments. Bars represent standard deviations. One-way ANOVA

followed by a Tukey test analysis was performed; letters indicate statistical difference between groups. $P < 0.05$.

with IC_{50} of 8 and 3 µM, respectively. When *merR* was complemented in the Δ*merR merR::rrsB* strain, no significant change was observed in Hg(II) resistance suggesting that MerR does not act on P_{oah2} (Figure 1.5A). To test if the high resistance in the Δ*merR* strain was due to constitutive expression of *merA*, WT cells were pre-exposed to 0.2 µM Hg(II) for 2 hours prior to growth at 0, 4, or 6 µM Hg(II). As shown in figure 1.5B, WT cells that were previously exposed to Hg(II) displayed increased resistance to Hg(II), at levels very similar to those of strain Δ*merR*. The pre-exposure of Δ*merR* strain to Hg(II) did not result in increased Hg(II) resistance in the Δ*merR* strain, suggesting that there was no repression and/or induction of *merA* when P_{mer} and MerR were absent. When *merA* is under control of P_{oah2}, no significant difference in *merA* expression, relative to the control, was observed in presence of Hg(II) (Figure 1.5C). The functionality of MerA was corroborated by the enzyme's specific activity in crude cell extracts. This analysis showed that MerA activity is ~4-fold higher in Hg(II)-exposed (30 min to 1 µM Hg[II]) WT (Figure 1.5D), but MerA activity was elevated in the Δ*merR* strain irrespective of pre-exposure to Hg(II) indicating that MerA is constitutively expressed in the Δ*merR* strain.

In summary, expression of the *mer* operon in *T. thermophilus* HB27 is derepressed when *merR* and the P_{mer} promoter are removed from the operon which is now exclusively and expressed from P_{oah} independently of Hg(II).

Discussion

The regulation of the *mer* operon has been mostly studied in proteobacterial systems (Ni'Bhriain *et al.*, 1983, Heltzel *et al.*, 1987, Lund & Brown, 1989, O'Halloran *et al.*, 1989, Ross *et al.*, 1989, Shewchuk *et al.*, 1989, Shewchuk *et al.*, 1989, Shewchuk *et al.*, 1989, Heltzel *et al.*, 1990, Ansari *et al.*, 1992, Gambill & Summers, 1992, Park *et al.*, 1992, Lee *et al.*, 1993, Livrelli *et al.*, 1993, Parkhill *et al.*, 1998, Zeng *et al.*, 1998, Kulkarni & Summers, 1999, Barkay *et al.*, 2003, Song *et al.*, 2007), to some degree in actinobacterial (Brünker *et al.*, 1996, Ravel *et al.*, 2000) and bacilli (Chang *et al.*, 2015) systems, and in only one thermophilic archaeon (Schelert *et al.*, 2003). In addition, a constitutive expression of *mer* was documented in the early bacterial phylum Aquificae (Freedman *et al.*, 2012). In this study we provide evidence for the regulation of the *mer* operon in *T. thermophilus* HB27 where MerR acts as a repressor/activator similar to the proteobacterial MerR and unlike the archaeal MerR which acts only as a repressor (Schelert *et al.*, 2006). MerR in *T. thermophilus* represses the expression of *merA* in absence of Hg(II) and activates its transcription from P_{mer} in its presence (Figure 1.4). The uniqueness of the regulation of transcription of the *T. thermophilus mer* operon is found in its convergent transcription of *merR* with other genes in the operon (Figure 1.1) and on the presence and transcription form two promoters (Figure 1.2) that are differentially regulated by Hg(II) (Figures 1.3, 4 and 5).

Convergently-transcribed *merR* is less common than divergent *merR*s and is mostly found among *mer* operons of the Firmicutes, Deinococcus/Thermus, and the Alphaproteobacteria (Boyd & Barkay, 2012). Nine representative *mer* operons with convergent *merR* are shown in Figure 1.S4 and all have a promoter upstream of the entire operon. In seven of these, *merR* is located upstream of *merA* and of these, 6 had more than one promoter identified by BPROM, with one located upstream of *merR* and at least one additional one on *merR*. Interestingly most of these operons are found in the Firmicutes, and *Streptomyces* is the only studied system in that Phylum, this organism has a divergent *merR* (Brünker *et al.*, 1996). How these other operons are regulated remains unknown, but they might act as repressor-activator similar to *Thermus* and these promoters might have differential responses to Hg(II).

It is interesting to consider that P_{mer} has 17-bp between -35 and -10-bp regions (Figure 1.2C) instead of the 19-bp of the promoter found in Proteobacteria and the 20 bp in a Firmicute (Chang *et al.*, 2015). This longer than the common separation has been proposed to facilitate MerR's unique mode of activating transcription upon binding of Hg(II) by allowing a turn in this region of the operator/promoter to an angle similar to the one found in a 18-bp promoter (Ansari *et al.*, 1992). So, how MerR acts as an activator from P_{mer} in *Thermus* is unknown. In Proteobacteria when MerR-RNApol complex is bound to the operator/promoter in $P_{merTP(C)AD}$ the -35 and -10 regions are projected in opposite directions, but when Hg(II) binds to MerR the -35 and -10 region unwinds and face the same direction (Ansari *et al.*, 1992). We propose that *Thermus* MerR might just be necessary to project the -35 and -10 regions in the same direction. Further research is needed to understand how *Thermus* MerR activates transcription of P_{mer}.

The Δ*merRprom* strain behave similarly to the Δ*merA* strain, although the *merA* strain was slightly more sensitive to Hg(II) (Figure 1.4A). This is expected because an intact *merA* is present in Δ*merRprom* but not in Δ*merA*; in the Δ*merRprom* strain *merA* can be somewhat expressed from P_{oah} in absence of Hg(II), as shown by the presence of an amplicon in the *merR*-*merA* junction in the Hg(II)-unexposed WT strain (Figure 1.3E). The recovery of Hg(II) resistance in the *merR*-complemented strain (Figure 1.5A) further corroborates the role of MerR as an activator. As mentioned, the Δ*merRprom merR::rrsB* strain was more sensitive to Hg(II) than the WT strain when not pre-exposed (Figure 1.4B). This might be due to the effect of the HygR cassette-*merR* fusion on rates of *merR* transcription. It can also be explained by the presence of 2 P_{mer} to which MerR can bind, one in the *mer* operon that lacks a full MerR and the other in the *merR* sequence that was trans complementated to *rrsB,* in which a full MerR is encoded. The 2 P_{mer} present in one genome and only of full *merR,* might require more MerR to properly regulate both promoters, explaining why pre-exposure of the Δ*merRprom merR::rrsB* strain recovers WT levels of Hg(II) resistance (Figure 1.5B). As expected, MerR also acted as a repressor of the operon, as shown by a lower copy number of *merA* transcripts in the WT strain as compared to the Δ*merRprom* strain in absence of Hg(II) (Figure 1.5C). In proteobacterial MerR the replacement of C126S resulted in MerR that acted only as a repressor, but could not activate *merA* transcription (Shewchuk *et al.*, 1989). We obtained similar results when the homologue cysteine in *Thermus*'s MerR, C128S, (Figure 1.5D) and the strain was less resistant to Hg(II) with the same IC_{50} as the *merA* strain (data not shown). This MerRC128S might not have lost all the activation properties, due to higher levels of resistance in the pre-induced in the *merR*C128S, a double cysteine mutant MerR might have a more decisive phenotype. Together our results show that MerR acts as a repressor/activator controlling transcription from P_{mer} and that the whole operon can be constitutively expressed from P_{oah} (Figure 1.6).

The presence of two transcriptional units in *T. thermophilus* allows a fast and efficient response to Hg(II) with constitutive expression from P$_{oah2}$ assuring presence of MerR to repress and activate expression from P$_{mer}$ in response to Hg(II). A gradient in the relative abundance of various gene transcripts was previously shown in the *merTPCAD* of Tn*21* with lower abundance of promoter-distal transcripts relative to promoter-proximal ones (Gambill & Summers, 1992). In vivo mRNA degradation rates did not significantly changed, but mRNA synthesis rates varied considerably from the beginning to the end of the Tn*21* operon; promoter-proximal genes achieved a maximum *in vivo* synthesis rate fast, but the synthesis rates of mRNA from promoter-distal genes (like *merA*) were lower. So, *T. thermophilus* might have found an efficient way to maximize the response to Hg(II) by the presence of a secondary promoter closer to *merA*.

In conclusion, we have shown that the *mer* operon in *T. thermophilus* HB27 has two promoters which differentially regulate transcription in response to Hg(II). We propose the following model for the regulation of this operon (Figure 1.7). In absence of Hg(II), P$_{oah2}$ produces two transcripts: a long transcript from *oah2*-*merA* and a short transcript from *oah2*-*merR* (Figure 1.7A). P$_{oah2}$ may initiate a long transcript containing *oah2* to *merA* (Figure 1.3E) in absence of Hg(II), as shown by the constitutive expression of *merA* in the Δ*merR* strain (Figure 1.6). But, most of the transcripts made from P$_{oah2}$ in absence of Hg(II) are from *oah2* to *merR* (Figure 1.3B, thick PCR band). This allows constitutive expression of *oah2* and *merR*, which can partially explain why the fold induction of these genes is lower than that of *merA* (Figure 1.1B; Figure 1.3E, faint PCR band). Furthermore, the rapid degradation of the 5’ end of the transcript shown by the high amount of 5’-RACE clones that started at the first codon of *oah2* and not the +1 site,

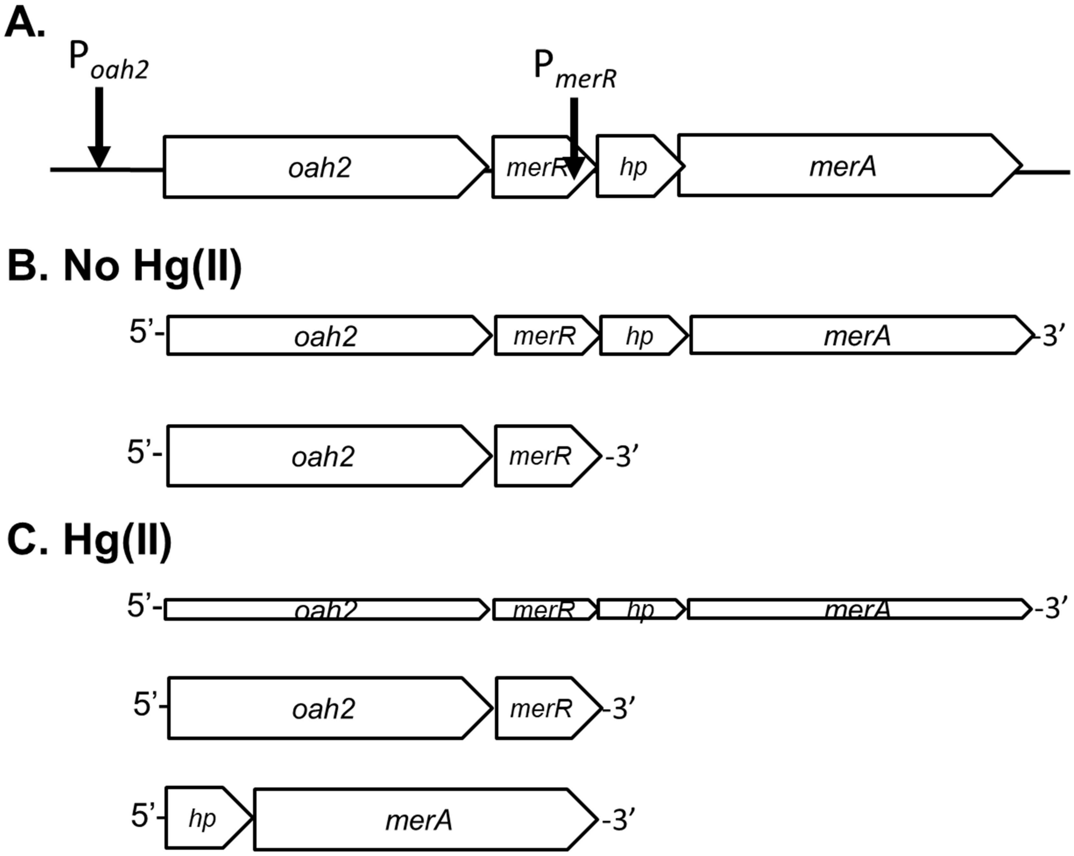
A.
P oah2
P merR
oah2
merR
hp
merA
B. No Hg(II)
5'-
oah2
merR
hp
merA
-3'
5'-
oah2
merR
-3'
C. Hg(II)
5'-
oah2
merR
hp
merA
-3'
5'-
oah2
merR
-3'
5'-
hp
merA
-3'

Figure 1.6. Mercury affects *mer* operon operon expression. (A) *mer* operon with the 2 promoters identifeid by RACE-PCR. (B) Transcripts producced in absence of Hg(II). (C) Transcripts producced in presence of Hg(II). The thickeness of the line represents the abundance of the respective transcript under the respective conditions.

and the lower transcript stability as compared to the *merA* gene, can explain why transcripts of these genes have shorter induction times. In presence of Hg(II), P_{mer} is activate (Figure 1.6B) and it favors the transcription of a short transcript of *hp* and *merA* (Figures 1.2D and 3F). In presence of Hg(II), the long *oah2-merA* transcript is still made (Figure 1.3E, fainter band in presence of Hg[II]), but most of the transcripts synthesized from P_{oah2} is *oah2-merR* (Figure 1.3C). The differential regulation of the operon can be explained by MerR; in P_{mer} MerR acts as a repressor/activator regulator (Figure 1.5), which modulate expression of *merA* without significantly affect *oah2* and *merR*. This also allows a fast and efficient response to Hg(II) exposure, in which a promoter closer to *merA* allows a fast transcription of this gene.

CHAPTER 2

LOW-MOLECULAR-WEIGHT THIOLS AND THIOREDOXINS ARE IMPORTANT PLAYERS IN HG(II) RESISTANCE IN *THERMUS THERMOPHILUS* HB27

Norambuena J, *et al*.. 2018. Appl Environ Microbiol. PMID: 29150497.

Abstract

Mercury (Hg), one of the most toxic and widely distributed heavy metals, has a high affinity for thiol groups. Thiol groups reduce and sequester Hg. Therefore, low molecular weight and protein thiols may be important cell components used in Hg resistance. To date, the role of low molecular weight thiols in Hg-detoxification remains understudied. The mercury resistance (*mer*) operon of *Thermus thermophilus* suggests an evolutionary link between Hg(II) resistance and low molecular weight thiol metabolism. This *mer* operon encodes for an enzyme involved in methionine biosynthesis, Oah. Challenge with Hg(II) resulted in increased expression of genes involved in the biosynthesis of multiple low molecular weight thiols (cysteine, homocysteine, and bacillithiol), as well as the thioredoxin system. Phenotypic analysis of gene replacement mutants indicated that Oah contributes to Hg resistance under sulfur limiting conditions, and strains lacking bacillithiol and/or thioredoxins are more sensitive to Hg(II) than the wild type. Growth in presence of either a thiol oxidizing agent or a thiol alkylating agent increased sensitivity to Hg(II). Furthermore, exposure to 3 μM Hg(II) consumed all intracellular reduced bacillithiol and cysteine. Database searches indicate that *oah2* is present in all *Thermus* spp. *mer* operons. The presence of a thiol related gene was also detected in some

alphaprotobacterial *mer* operons, in which a glutathione reductase gene was present, supporting the role of thiols in Hg(II) detoxification. These results have led to a working model in which LMW thiols act as Hg(II) buffering agents while Hg is reduced by MerA.

Introduction

Mercury (Hg) is one of the most toxic and widely distributed heavy metals. Mercury toxicity is due, in part, to its high affinity for low molecular weight (LMW) thiols including homocysteine, N-acetylcysteine, cysteine, and thiol-based cellular redox buffers like glutathione (GSH) (Valko *et al.*, 2005, Jan *et al.*, 2011) . Not surprisingly, free thiol groups have a high binding constant for Hg(II) (Oram *et al.*, 1996, Helbig *et al.*, 2008). Mercury can also bind thiols present in proteins (Valko *et al.*, 2005, Jan *et al.*, 2011, LaVoie *et al.*, 2015), and oxidize thioredoxins (Carvalho *et al.*, 2008, Wang *et al.*, 2013). Thus, the main biological effects of Hg are related to this high affinity toward sulfhydryl groups (Valko *et al.*, 2005).

Bacteria commonly possess two main thiol systems that maintain the redox state of the cell. The first is a LMW thiol system, typically utilizing GSH (Quastel *et al.*, 1923) or bacillithiol (BSH) (Gaballa *et al.*, 2010), and the second is a thioredoxin system (Ritz & Beckwith, 2001). LWM thiol systems vary among bacteria, are present at millimolar concentrations, and act as redox buffers in the cell (Ritz & Beckwith, 2001, Fahey, 2013). Thioredoxins are present among all kingdoms, and the system consists of thioredoxin protein(s) and an enzyme, thioredoxin reductase (Ritz & Beckwith, 2001, Lu & Holmgren, 2014). In *Escherichia coli* there are two thioredoxins: Trx1 (*trxA*) and Trx2 (*trxC*), which differ in an extra N-terminal extension (Ritz & Beckwith, 2001).

Thioredoxins become oxidized when their targets are reduced, and thioredoxin reductase (*trxB*) uses electrons from NADPH to maintain thioredoxins in a reduced state system (Ritz & Beckwith, 2001, Lu & Holmgren, 2014).

To overcome Hg toxicity, some Bacteria and Archaea employ the Hg resistance (*mer*) operon (Valko *et al.*, 2005). The composition of the *mer* system varies among organisms, but they all have *merA*, which encodes for a mercuric reductase that reduces inorganic Hg(II) to Hg(0); Hg(0) is volatile and is partitioned out of the cell. Proteobacterial *mer* operons are the most studied (Barkay *et al.*, 2003). These operons have several genes that can encode for transcriptional repressors/activators (*merR* and *merD*), specific transporters (*merC, merE, merF, merG*, *merP* and *merT*) and *merA* (Boyd & Barkay, 2012). Some *mer* operons can detoxify organomercurial compounds, in addition to Hg(II), by the inclusion of an organomercurial lyase (*merB*). With the advance of whole genome sequencing new *mer* operons were discovered, and simpler operons were found in early microbial lineages (Boyd & Barkay, 2012). These simpler operons were found in some thermophilic microbes, like the crenarchaeota *Sulfolobus solfataricus* (Schelert et al., 2006), some bacteria belonging to the Aquificaceae (Freedman *et al.*, 2012) and in *Thermus thermophilus* (Wang *et al.*, 2009). These organisms were subsequently shown to have *merA*-dependent resistance to Hg(II).

The *mer* operon in *T. thermophilus* HB27 is unique, because it consists of two classical *mer* operon genes (*merA* and *merR*) and the thiol biosynthesis-related gene (*oah2*) (Figure 2.1A) (Wang *et al.*, 2009). In the *mer* operon of *T. thermophilus* HB27, *merA* encodes for a mercuric reductase; suggested by protein homology to other MerA (Wang *et al.*, 2009, Barkay *et al.*, 2010), higher susceptibility to Hg(II) of the Δ*merA*

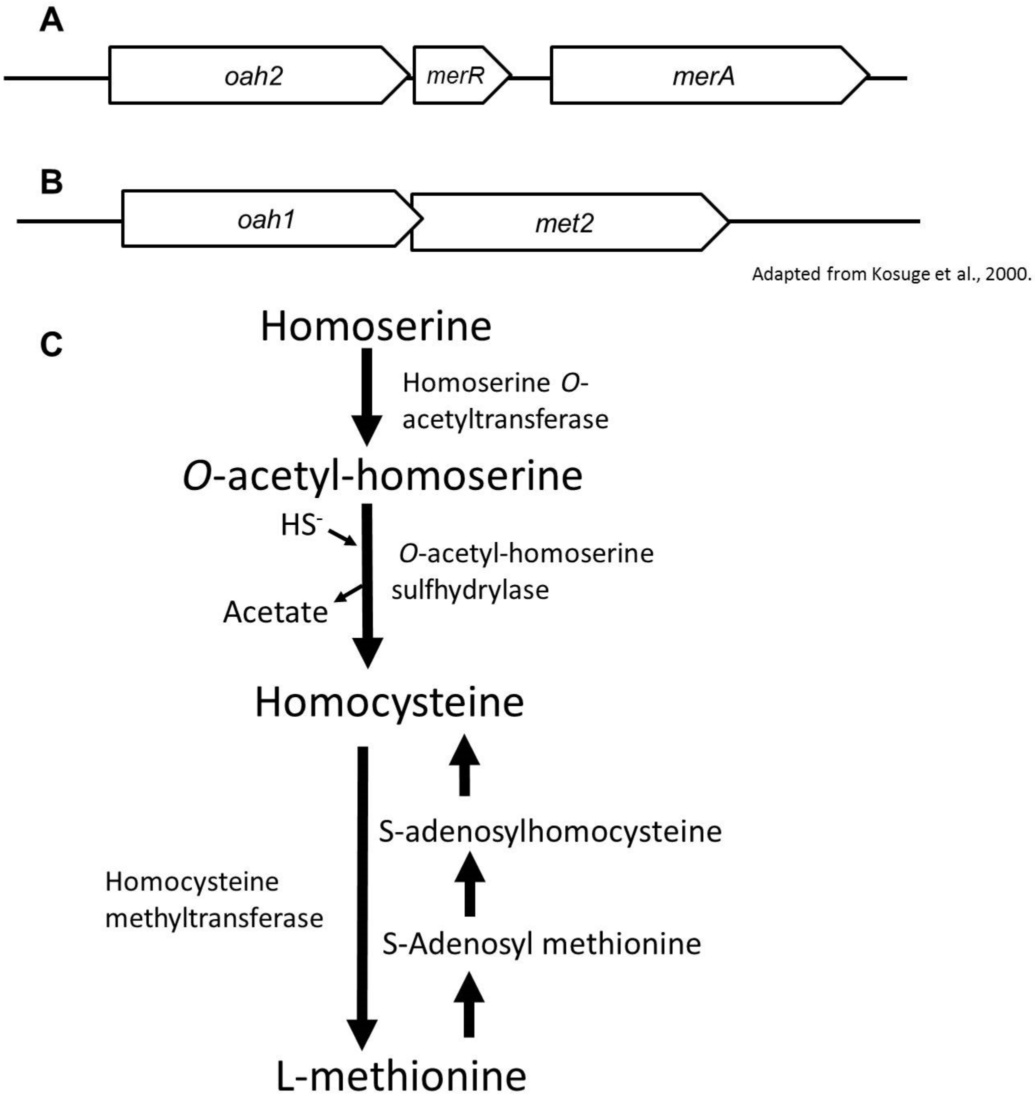
A
oah2
merR
merA
B
oah1
met2
C
Homoserine
Homoserine O-acetyltransferase
O-acetyl-homoserine
HS-
Acetate
O-acetyl-homoserine sulfhydrylase
Homocysteine
S-adenosylhomocysteine
Homocysteine methyltransferase
S-Adenosyl methionine
L-methionine

Adapted from Kosuge et al., 2000.

Figure 2.1. The *mer* and *met* operons, and the methionine metabolism pathways in *T. thermophilus*. (A) Diagram of the *mer* operon in HB27, which is composed of *oah2* (TT_C0792), *merR* (TT_C0791), and *merA* (TT_C0789). (B) Diagram of the *met* operon in HB27 composed of *oah1* (TT_C0408) and *met2* (TT_C0407). Arrows indicate direction of transcription. (C) Methionine metabolism in *T. thermophilus* (21). The *met2* gene encodes for homoserine *O*-acetyltransferase and the *oah* genes encode for *O*-acetyl-homoserine sulfhydrylase.

mutant and the lack of MerA activity in this mutant (Wang *et al.*, 2009). Although, the function of MerR in *T. thermophilus* has not been established, protein homology suggests that it encodes for the transcriptional regulator of the *mer* operon. The third member of the *mer* operon, *oah2*, encodes for an *O*-acetyl-L-homoacetylserine sulfhydrylase (Oah) that synthesizes homocysteine (Figure 2.1C) (Iwama *et al.*, 2004), an intermediate in methionine biosynthesis (Kosuge *et al.*, 2005). Our previous work found that *oah2, merR,* and *merA* are expressed as a polycistronic unit in presence of Hg(II) (Wang *et al.*, 2009). The co-localization and co-expression of *oah2* with the *mer* genes suggests a link between Hg(II) resistance and the biosynthesis of LMW thiol compounds.

The genome of *T. thermophilus* encodes for two Oah orthologs, *oah2* and *oah1*. *oah1* is located in an operon with *met2,* which encodes for an enzyme that catalyzes the first step in methionine biosynthesis (Figure 2.1B and C) (Kosuge *et al.*, 2005). It was determined that Oah1 and Oah2 have sulfhydrylase activity *in vitro* (Shimizu *et al.*, 2001, Iwama *et al.*, 2004); however, Oah2 had a lower K_M for the substrates homoserine and sulfide (Iwama *et al.*, 2004). This information suggested that these enzymes may have similar, but possibly not identical, cellular function. Here, the hypothesis that LMW thiols and the thioredoxin system play a role in Hg(II)-resistance in *T. thermophilus* was tested, by using a combination of gene expression, phenotypic, and metabolite analyses. We report that exposure to Hg(II) induced the expression of LMW thiols biosynthesis and thioredoxin genes, and decreased the bioavailability of reduced bacillithiol and cysteine. Moreover, phenotypic analysis found that strains lacking Oah, BshA/C, or TrxA were more sensitive to Hg(II) than the wild type strain. Database searches indicate that all

Thermus spp. *mer* operons have an *oah2* and that this phenomenon is not exclusive to *Thermus* spp.

Materials and Methods

Bacterial stains and growth conditions

T. thermophilus HB27 (DSMZ 7039) and its mutants were cultured at 65°C in 461 Castenholz TYE medium (complex medium) as described by Wang *et al.* Chemically defined media was prepared as described by Tanaka *et al.* When cultured in liquid media, cells were grown in 3 mL of medium in 13 mL test tubes shaken at 200 rpm. Solid culture media was supplemented with 1.5% noble agar (Sigma). When present, kanamycin (Kan) was supplemented at 25 µg/ml (Sigma). *E. coli* strains were grown at 37°C in Luria-Bertani (LB) medium. Liquid cultures were shaken at 180 rpm and solid media was supplemented with 1.5% agar.

Mutant construction

Construction of the Δ*merA* mutant was previously described (Wang *et al.*, 2009). To create gene replacement of *oah2, oah1, bshA, bshC, trxA1* and *trxA2* with the kanamycin resistance gene (Δ*gene*::HTK, are noted as Δ*gene*), the upstream and downstream flanking regions of the target gene were PCR amplified and products fused with the thermostable Kan-resistance gene, HTK (Wang *et al.*, 2009) (Figure 2.S9). Two strategies were used to fuse the PCR products. For the *oah2* gene different restriction sites were added to the 3’ end of PCR fragments; for the other five genes, fusion PCR was performed (Hoseki *et al.*, 1999). The final constructs were cloned into pUC19 and used to transform MAX Efficiency® DH5α™ Competent Cells (Invitrogen) with transformants selected on LB plates supplemented with 100 µg/ml ampicillin (Amp; Sigma). Transformants were grown in liquid LB medium supplemented with 100 µg/ml Amp, plasmids were extracted using Wizard® Plus SV Minipreps DNA Purification System (Promega), and purified plasmids were used to transform *T. thermophilus* as described by Koyama *et al.* (Lau *et al.*, 2002). *T. thermophilus* was grown for 2-3 days on complex medium plates containing 25 µg/mL of Kan until transformed colonies appeared. The in-frame replacement of the gene was confirmed by sequencing the insert with primers named 5 and 6 for each strain (Table 2.1). All transformants have the respective native promoter controlling the expression of the HTK cassette. Primers used for the knock out strains are listed in Table 2.1.

Mercury resistance in complex and defined media

Cells were grown over night (O.N.) in complex medium, diluted to $O.D_{600}$ of 0.1 in fresh complex medium or in defined medium supplemented with sulfate, and $HgCl_2$ was added to individual tubes at concentrations ranging from 0 - 10 µM. Growth was followed at $O.D_{600}$ (Spectronic 20 Genesys spectrophotometer, Spectronic Instruments). Resistance was assessed as the percentage of growth observed 18 or 20 hrs after Hg(II) addition relative to no Hg(II) control cultures (100% of growth). All experiments were performed in triplicate, unless otherwise stated.

Table 2.1 PCR primers used for construction of *T. thermophilus* HB27 knockout mutants in Chapter 2.

Mutant strain	Primer	Sequence[1]	Size (bp)	Target
Δoah2	oas 720 RI for1	GGATGCAGCAGCCCTGGAATTCGTAGTAGG	418	oah2 upstream sequence
	oas 1100 KpnI Rev1a	GTCTTCGGGAAGCCCGGCGAGGGTACCGAGGGTGGTGTA		
	pUC-HTK 670 for	GCTTGCATGCGGGGTACCCTAGAATTCAT	800	HTK
	pUC-HTK 1450 Xba Rev	GAGGTCATCGTCTAGAATGGTATGC		
	oas 2310 XbaI for2	CCTGGAGGCGGTCCATATGCTCTAGACCAT	470	oah2 downstream sequence
	oas 2750 PstI Rev2	GGTTCTTCTCCATGCCTGCAGGCTAGACC		
	oas del for3	GGTCTTCACGGGCTTGCCCTGAAAGG	595	Sequencing
	HTK 5′ rev	GCTGAACTCTACTCCCTCTGTTGACAGAACAC		
Δoah1	A HTKoah1upfor	GACTTTGGAAAGGAGGCCAAGGATGAAAGGACCAATAATAATGA	761	HTK
	B HTKmet2rev	CGAGGGCGATCTCGCTCATTCAAAATGGTATGCGT		
	E oah1uprev	TCATCCTTGGCCTCCTTTCCAAAGT	559	oah1 upstream sequence
	1 oah1 ecoRI	CCTCGAATTCCACGTCCCCG		
	F met2for	ATGAGCGAGATCGCCCTCG	366	oah1 downstream sequence
	4 met2rev	GGCGGGGTCCAGGATCC		
	htkoah1uprev	TCATTATTATTGGTCCTTTCATCCTTGGCCTCCTTTCCAAAGTC	1772	Sequencing
	htkmet2for	ACGCATACCATTTTGAATGAGCGAGATCGCCCTCG		
ΔbshC	B spo htk rev	CTAACCCTTCTTCAAAATGGTATGCGTTTTGAC	786	HTK
	A crp htk for	TAGGCTTTAAAGCATGAAAGGACCAATAATAATGAC		
	E htk crp rev	GGTCCTTTCATGCTTTAAAGCCTAAAGTTCC	513	bshC upstream sequence
	1 crp bamHI for	CTCGTCGGGATCCACCGG		
	F htk spo for	GCATACCATTTTGAAGAAGGGTTAGGATGTTCG	378	bshC downstream sequence
	4 spodown psti rev	AGGTAGTCCTGCAGGGGAAGG		
	5 bshC for	GTCCTTTGCGCTTGAGGCG	1774	Sequencing
	6 bshC rev	ACGGCCTGGGCCTTCA		
ΔbshA	A perm HTK for	CTAGGCTTAGGGCATGAAAGGACCAATAATA	785	HTK
	B bshA htk rev	GGGCGTAGACTCAAAATGGTATGCG		
	E htk perm rev	TTATTGGTCCTTTCATGCCCTAAGCCTAG	458	bshA upstream sequence
	1perm ecoR1 for	GCGCCGGGAATTCCGG		
	F HTK bshA for	ACCATTTTGAGTCTACGCCCAGG	714	bshA downstream sequence
	4 prot PstI rev	GAGAAGGACCTGCAGGCCTAC		
	5 perm upins for	AGACCCTCACCCTCAAGGACT	2062	Sequencing
	6 pro downins rev	GCCCTCCTCCGCAAGG		
ΔtrxA2	A trx2upHTK	GCGGAGGGGGTACCTATGAAAGGACCAATAATAAT	796	HTK
	B hsp20HTK rev	TCCCTTCTAGGTAGGGCCTTCAAAATGGTATGCG		
	E HTKuptrx2 rev	ATTATTGGTCCTTTCATAGGTACCCCCTCCG	539	trxA2 upstream sequence
	1 trx2 ecoR1 for	GAAAGGGAATTCCAGCTTGCGGG		
	4 hsp20 bamH1 rev	CGGGGGATCCGCACCT	403	trxA2 downstream sequence
	F HTKtrx2for	GCATACCATTTTGAAGGCCCTACCTAGAAGG		
	5 trx2upst for	CTTCTGGACCTGAGGGCGA	1465	Sequencing
	6 hsp20downst rev	TTTCCTGAATGGGTATCCGCACG		
ΔtrxA1	A trx1 htk for	CGTAGAGTAGGGGGGTATGAAAGGACCAATAATAATG	791	HTK
	B2 trx1	GTCCAGGGCGATGCGCATCCTCAAAATGG		
	E htktrx1 rev	ATTGGTCCTTTCATACCCCCCTACT	486	trxA1 upstream sequence
	1 trx1 ecoR1 for	CGCGGGTGAATTCCGCG		
	F htkphos for	CATACCATTTTGAGGATGCGCATCGC	397	trxA1 downstream sequence
	4 phos bamH1 rev	TCAAGCTGGGGATCCCCAC		
	5 trx1 upsisn for	GGACCTTCGCCGAGCTCC	1752	Sequencing
	6 Phos downins rev	GGACGAGGAAGGAAGGGCG		

Mercury resistance under sulfur limiting conditions

All strains were grown O.N. in complex medium, washed twice in chemically defined medium without sulfate and resuspended in this medium to O.D_{600} of 0.1. Cell suspensions were divided into different tubes and 10 μM of homocysteine, a concentration determined in preliminary experiments to be growth limiting, were added to each tube. Finally, $HgCl_2$ was added from 0 - 6 μM. Resistance was assessed as the percentage of growth (O.D$_{600}$) observed 24 hrs after the addition of Hg(II) relative to no Hg(II) control cultures.

Diamide and NEM assays

Cells were grown O.N. in complex medium, diluted to O.D$_{600}$ of 0.1, and divided into different tubes containing 0-2 mM diamide (Sigma) or 0-0.4 mM N-ethylmaleimide (NEM). $HgCl_2$ was added (ranging from 0 to 4 µM) and growth at O.D$_{600}$ was measured after 16 (diamide) or 24 (NEM) hrs of growth. For exposed cultures, including those exposed only to diamide or NEM, growth in absence of Hg(II) was considered 100%.

RNA extraction and cDNA synthesis

Cells from O.N. culture of *T. thermophilus* were diluted to O.D$_{600}$ 0.1 in complex medium and incubated to O.D$_{600}$ ~0.4 when 1 µM $HgCl_2$ was added. For *E. coli* K12 strain, an O.N culture was diluted to O.D$_{600}$ 0.1 in LB medium and incubated to O.D$_{600}$ ~0.8 when 2 µM $HgCl_2$ was added. Three mL aliquots of cell suspensions were removed 7.5, 15, 30 or 60 minutes after the addition of Hg(II); an unexposed control was included at each time point. The removed aliquots were mixed with 0.5 volumes of RNA protect (QIAGEN) and incubated for 5 minutes at room temperature. Cells were washed once with TE buffer (10 mM Tris-HCl, 1 mM EDTA, pH 8.0), resuspended in 300 µL of lysis buffer (20 mM sodium acetate, 1 mM EDTA, 0.5% SDS, pH 5.5), and incubated for 5 min at 65°C. Then, 1 ml of TRIzol (Invitrogen) was added and RNA extraction was performed as instructed by the manufacturer. RNA integrity was checked in a 1.5% agarose gel and concentration was measured by nanodrop (ND-1000 Spectrophotometer, NanoDrop Technologies Inc, Wilmington, DE). RNA was treated with Turbo DNA-free kit (Ambion) to remove DNA and the DNA-free RNA was used to synthesize cDNA with High-Capacity cDNA Reverse Transcription Kit (Applied Biosystems) using 1 µg of RNA for *T. thermophilus*. For *E. coli*, 2 µg of RNA were used to synthesize cDNA with the SuperScript^{TM} III First-Strand Synthesis System (Life Technologies). For both kits, cDNAs were synthesized following manufacturer's instructions.

Quantitative PCR

T. thermophilus transcripts of *oah2* (WP_011173224), *oah1* (WP_011172856), *met2* (WP_041443334), *metH* (WP_041443334), *oas* (WP_011174005), *bshA* (WP_011173182), *bshB* (WP_011173270), *bshC* (WP_011173609), *trxA1* (WP_011173768), *trxA2* (WP_011173531) and *trxB* (WP_011173929) were quantified by qPCR using cDNA as template and primers specific for each gene (Table 2.2). For *E. coli* transcripts of *gor* (Ga0175964_11222), *trxB* (Ga0175964_112966), *gshA* (Ga0175964_111051), *gshB* (Ga0175964_11784), *cysK* (Ga0175964_111321), *malY* (Ga0175964_112139), *cysM* (Ga0175964_111314) and *zntA* (Ga0175964_11254), were quantified as for *T. themophilus*. Reactions contained: 12.5 µl of 2X SYBR$^{®}$ Green JumpStart™ *Taq* ReadyMix™ (Sigma), 1 µl cDNA, and an optimized concentration of each primer set (Table 2.2), in a final volume of 25 µl. Thermal cycling (iCycler iQ, Bio-Rad Laboratories Inc., Hercules, CA) conditions were: initial denaturation at 95°C for 5 min, followed by 30 cycles of denaturation (95°C for 15 sec), annealing (for 15 sec, temperature as in Table 2.2), extension (72°C for 15 sec) followed by fluorescence measurement and a final melt curve (60–99°C). At least three biological replicates were

Table 2.2 qPCR primers used to measure gene expression of the listed genes in Chapter 2.[*]

Primer	Sequence	C (µM)[**]	T_A (°C)	Size (bp)
gyrase-F	GGGCGAGGTCATGGGC	1	61	134
gyrase-R	CGCCGTCTATGGAGCCG	0.25		
oah2-F3	GAGCTCTGGCGGAACTAC	0.25	56	104
oah2-R3	AAGGTGCGGACCCTTTC	1		
merR4-F	AGCTTGAGGACATCGCCTGGAT	0.5	61	214
merR4-R	TCCAAATAGACGCAGCGGTCCC	1		
merA for	GCCTTCAAGATCGTGGTGGACGAAGAG	0.5	62	186
merA rev	CCTGGGCCACGAGCCTTATCC	0.25		
oah1-F2	GGAGCTCGCCTTCATCGTCA	1	59	137
oah1-R2	TGTTTTCCACGTGACGCTCG	0.25		
met2-F	GAATCGCCATGATGAGCTACC	1.25	57	92
met2-R	CTGGTAGTCCAGGTAGGTTTCC	1.25		
oas-F	CGCTACCTCAAGGAAAGGATC	1.25	56	145
oas-R	GGGAAAGGTCCAGGTTCTCG	1.25		
metH-F	CCTCTTTGACCTCCTTACCTTCC	2.5	57	98
metH-R	TCTCCCGTAGCTCCTCTATGG	2.5		
bshA-F	CTAGACCTGAGCGCAAGAGG	2.5	58	128
bshA-R	GAGGCGCTTCCGGATTT	2.5		
bshB-F	CGCCGTTACTTTGGGAACTA	2.5	58	76
bshB-R	GCACGTAGAGCACGGGAAG	2.5		
bshC-F2	GGAGGCGGAGACGCTTTC	1.25	55	81
bshC-R2	GGGTCAAAGGGCACAAGC	1.25		
trxB-F	GGTGCGGCTTAAGAACCTAAAG	1.25	58	100
trxB-R	CTTGAGGAAAGCGGTGTTGG	1.25		
trxA1-F	GACCAGAACTTTGACGAGACCC	1.25	60	132
trxA1-R	AAGCTTCCCCTCGTACTCTTTGG	1.25		
trxA2-F	CCCACCCTGGTCCTCTTCC	1.25	60	105
trxA2-R	CCTCCCTTCTAGGTAGGGCCTG	1.25		
gor-R e coli	GCCGTGAATACCGACAATCT	0.4	60	130
gor-F e coli	CGACGATCAGGTGAAAGTGTAT	0.4		
trxB-F e coli	ACAGTCGGGTATTCATGGTAATG	0.4	60	110
trxB-R e coli	CTGTACCGGCCGAAGTAATG	0.4		
gshB-F e coli	CCCATCGCAAACATCAACATC	0.4	60	101
gshB-R e coli	AGATCGCCCATCTCCATATAGT	0.4		
gshA-F e coli	CGGATGTGGCCGTTAAGTAT	1	60	91
gshA-R e coli	TAAAGCGTCCGGTGTTAGAAG	1		
zntA-F	ATCAGGTGCAGGTGTTGTT	1	60	113
zntA-R	TTCATCGCGCAGGGAATAG	1		
cysM-F ecoli	ATACGCCTCTGGTGAAGTTG	0.5	60	89
cysM-R ecoli	CGAACCTGCCGGGTTATT	0.5		
cysK-F ecoli	CGATCTCAAGCTGGTCGATAAA	0.4	60	116
cysK-R ecoli	CAGCTGCTCCAGAAGAGATAC	0.4		
MalY-F ecoli	GATGAGTTTCTCGCGGCTATT	0.5	60	93
MalY-R ecoli	GATGACAGAAGGGCCATACAC	0.5		
ssrA-F Ecoli	CGCCCGTCACGAATACTTTA	0.4	60	110
ssrA-R Ecoli	ACGTAGCTGTCGCTGATATTG	0.4		

*All primers were designed in this study, except for *merA* primers that were taken from Wang et al. 2009.

**Final concentration of the primers.

averaged in all cases. A reaction mixture with DNA free RNA was run as control for detecting DNA contamination. Transcript abundance was normalized to *gyrA* (TT_C0990) for *T. thermophilus* (Cusick *et al.*, 2015), and to *ssrA* (Ga0028711) for *E. coli* (Onnis-Hayden *et al.*, 2009), using the ΔΔCt method (Livak & Schmittgen, 2001).

Mercuric reductase assay

Cells from an O.N. culture were diluted in fresh complex medium to $O.D_{600}$ of 0.1 and grown to an O.D of ~0.4 when 1 µM of $HgCl_2$ was added and cultures were incubated for 30 additional minutes. Each experiment included an unexposed control. Cultures (35 mL) were centrifuged and washed once in PBS buffer (8.01 g/L NaCl, 0.2 g/L KCl, Na_2HPO_4 1.78 g/L and 0.27 g/L KH_2PO_4, pH 7.4) and cell pellets were frozen until further use. Crude cell extracts were prepared as previously described (Vetriani et al., 2005). MerA assays were performed at 70°C as described by Wang et al. using 200 µM NADH and 20 µL of protein extracts. Oxidation of NADH was monitored spectroscopically (at 340 nm; AVIV, biomedical spectrophotometer, model 14 UV-VI) each second for 1 min. Control reactions were set up with NADH and cell extract, but no $HgCl_2$, and the cell extract only activities were subtracted from rates of complete assay mixtures to determine Hg(II)-dependent NADH oxidation. Specific activities were defined as units (U)/mg of protein with a unit corresponding to 1 µmol of NADH oxidized per min. Bradford assay (Bio-Rad Laboratories Inc., Hercules, CA) was used to determine protein concentrations.

Thiol content assay

Cells from an O.N. culture were diluted to $O.D_{600}$ of 0.1 and grown to an O.D ~0.4 when 0-3 µM of $HgCl_2$ was added and growth continued for additional 30 or 60 min. Cells from a 25 mL culture were harvested and washed twice with PBS buffer. Cell pellets were resuspended in 500 µL of D-mix (9.4 mM monobromobimane [mBrB; Sigma], 50% acetonitrile, 50 mM HEPES, 5 mM EDTA, pH 8.0) and incubated for 15 min at 60°C in the dark. Derivatization was stopped by adding methanesulfonic acid to a final concentration of 25 mM. Samples were stored at -20°C until high-performance liquid chromatography (HPLC) analysis. Reversed phase HPLC analysis and fluorescence detection of the bimane derivatization products was performed as previously described by Rethmeier *et al.*

Bioinformatic analysis

The presence of *oah2* gene homologs in all Finished, Permanent Draft and Draft Deinococcus-Thermus genomes available in the IMG/MER (https://img.jgi.doe.gov/cgi-bin/mer/main.cgi) on June 8, 2017, was determined as follows. First, *mer* operons were identified using blastx (https://img.jgi.doe.gov/cgi-bin/mer/main.cgi?section=FindGenesBlast&page=geneSearchBlast) with MerA of HB27 (accession TTC0789) as a query, and a cutoff value of 1e-50. Hits were manually examined for the presence of amino acid residues characteristic of MerA (Barkay *et al.*, 2003) and neighboring genes examined for the presence of Oah2 homologs in JGI's gene detail page.

The presence of the GSR gene in the finished and assembled Alphaproteobacteria genomes was determined on Apr. 18, 2017 using a blastp search (https://img.jgi.doe.gov/cgi-bin/mer/main.cgi?section=FindGenesBlast&page=geneSearchBlast) and MerA of *Aurantimonas mangagnoxydans* S185-9A1 (accession EAS49959.1) as a query and a cut off value of 1e-50. Hits were manually examined for the presence of amino acid residues characteristic of MerA (Barkay *et al.*, 2003) and neighboring genes examined for the presence of GSR homologs using JGI's gene detail page.

Phylogenetic analysis

Protein sequences of Oah and GR were aligned using ClustalX (ver. 2.0) (Jeanmougin *et al.*, 1998, Larkin *et al.*, 2007) . The resulting alignments were used for phylogenetic analysis, which was inferred by using the Maximum Likelihood method based on the JTT matrix-based model (Jones *et al.*, 1992). Initial tree(s) for the heuristic search were obtained automatically by applying Neighbor-Join and BioNJ algorithms to a matrix of pairwise distances estimated using a JTT model, and then selecting the topology with superior log likelihood value. Evolutionary analyses were conducted in MEGA7 (Kumar *et al.*, 2016).

For both trees, all positions containing gaps and missing data were eliminated. The Oah tree was constructed of 21 amino acid sequences including a total of 248 positions in the final dataset. The outgroup used was *O*-acetylserine sulfhydrylases (Oas) enzymes because they carry out similar reaction but have a different substrate specificity than Oah (Shimizu *et al.*, 2001). Met17 was used as an internal outgroup for the Oah1 proteins due to its high homology to the later (Shimizu *et al.*, 2001). For the GR tree the analysis included 30 amino acid sequences with a total of 323 positions in the final dataset. For the outgroup, LpdA was used as it is considered ancestral enzyme to GR in the FAD-dependent pyridine nucleotide-disulfide oxidoreductases family (Gleason & Holmgren, 1988, Fahey, 2013).

Statistical analysis

One-way ANOVA followed by a Tukey test analysis was performed for multiple group comparison. For two group comparison, t-test was run.

Results

Transcription of thiol-related genes is induced by Hg(II)

To begin examining the role of thiols in Hg(II) resistance in *T. thermophilus*, the effect of Hg(II) on transcript levels of genes that encode for thiol-related enzymes was evaluated. Bioinformatic analysis determined that the genome of strain HB27 lacks GSH biosynthesis genes, as has been reported for *Deinococcus radiodurans* (another member of the *Deinoccucus*/*Thermus* phylum) (Newton *et al.*, 2009). Three putative genes for the biosynthesis of bacillithiol (BSH) were detected (*bshA*, *bshB* and *bshC*), as were *cysE* (Kobayashi *et al.*, 2004) and *cysK*/*oas* (Kosuge *et al.*, 2005) for cysteine biosynthesis and *met2*, *oah2*, *oah1* and *metH* for methionine biosynthesis (Figure 2.1C) (Kosuge *et al.*, 2005). Also, two thioredoxins (*trxA1* and *trxA2*) and one thioredoxin reductase (*trxB*) homologs were present in the genome (for locus tag identifiers of these genes, please see Materials and Methods section on qPCR).

mRNA transcripts were quantified in WT cells exposed to 0 or 1 μM Hg(II) for 7.5, 15 or 60 minutes, and transcript abundances were normalized to that of *gyrA* (Table 2.S1) (Cusick *et al.*, 2015). Mercury treatment increased transcript levels of all thiol-related genes tested, from over 10-fold for *oah1* and *trxA1* to about 2-fold for *bshC* (Figure 2.2). For LMW thiol genes, the highest induction was achieved after 7.5 minutes of Hg(II) exposure followed by a decrease at 15 min. With regards to methionine biosynthesis genes (Figure 2.2A), *met2* showed similar fold-induction as *oah1* at all time points tested, suggesting that these two genes are likely expressed as an operon. As expected, *oah2* was induced(Wang *et al.*, 2009) ~5-fold, the same fold induction reached by *metH*. These data suggest that methionine and homocysteine biosynthesis genes are induced by short exposure to Hg(II). Likewise, *oas* was induced ~7-fold by Hg(II). Transcript levels of *bshA* and *bshB* increased by approximately 4-fold (Figure 2.2B) upon Hg(II) exposure. Furthermore, transcript levels of thioredoxin related genes increased at 7.5 min (Table 2.S2), but the highest fold induction was at 15 min, reaching ~10-fold for *trxA1* and *trxB* and ~7-fold for *trxA2* (Figure 2.2C).

GSH and thioredoxins are oxidized or consumed when they reduce and sequester Hg(II) (Wang *et al.*, 2009, LaVoie *et al.*, 2015, Cappello *et al.*, 2016, Rodríguez-Rojas *et al.*, 2016), this interaction with Hg can lead to disulfide stress. Mercury exposure can also produce reactive oxygen species (ROS), such as superoxide and hydrogen peroxide (Wang *et al.*, 2009, Cappello *et al.*, 2016, Rodríguez-Rojas *et al.*, 2016). Therefore, we evaluated the possibility that in *T. thermophilus* the 7.5 min induction of LMW-thiol genes was due to these indirect effects triggered by Hg(II). For this purpose, known stressor agents that produce disulfide stress (diamide) and ROS were used. Exposure to 4

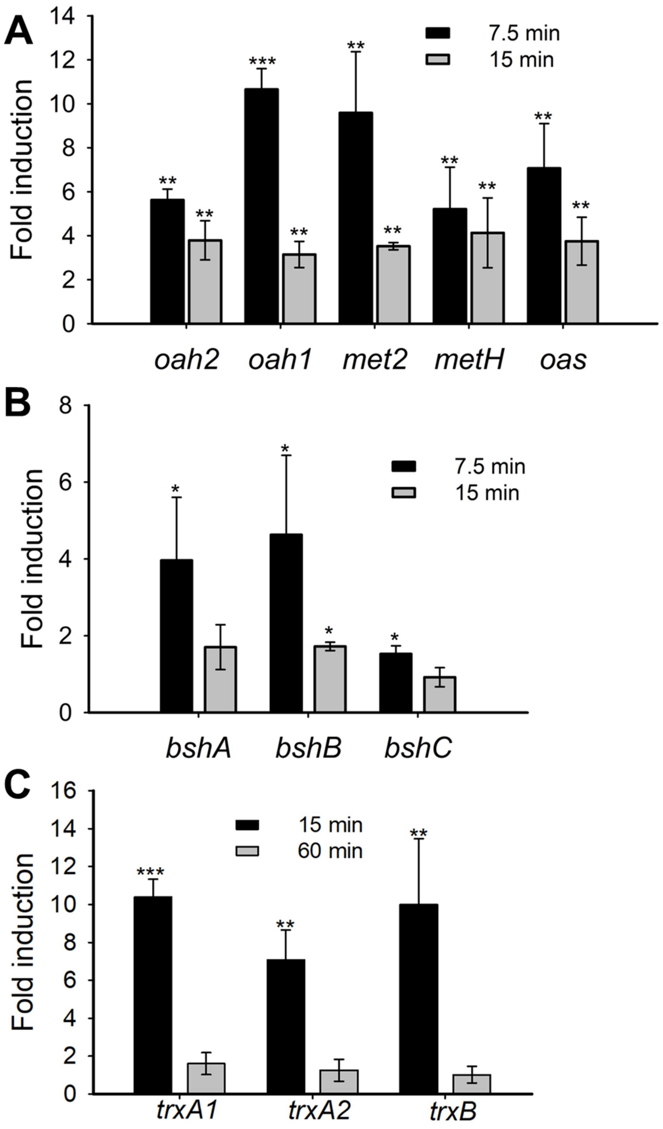

Figure 2.2. Thiol systems are induced by Hg(II). Abundance of mRNA transcripts involved in (A) methionine and cysteine biosynthesis, (B) BSH biosynthesis, and (C) thioredoxin system, were measured in the WT strain after 7.5, 15 or 60 minutes of exposure to 1 μM Hg(II). Gene expression was normalized to the abundance of the *gyrA* transcript and graphed as fold induction relative to the control (ΔΔCt method). Averages and standard deviations represent triplicate samples from three independent trials.

Statistical analysis was conducted using a two-tailed t-test; *P<0.05, **P <0.03 and ***P <0.001.

mM diamide (thiol-oxidizing agent), 160 μM paraquat (superoxide generator), or 1 mM hydrogen peroxide for 7.5 min did not induce *oah1*, *oah2*, *oas,* or *bshA* transcript levels in WT cells (Figure 2.S1). However, exposures induced expression of control genes for each stressor agent. Addition of diamide increased transcript levels of *trxA1* (Figure 2.S1, control gene), suggesting that increase in thioredoxin transcripts by Hg(II) could be an effect of disulfide stress. On the other hand, paraquat and hydrogen peroxide did increase SOD transcript levels (Figure 2.S1, control gene). These results suggest that induction of LMW thiol biosynthesis genes was likely directly triggered by Hg(II), rather than indirectly by disulfide stress (diamide) or accumulation of ROS (superoxide or hydrogen peroxide). Furthermore, the fast induction of LMW thiol genes caused by Hg(II) (7.5 minutes past exposure) suggests that this effect is not a consequence of unrelated Hg(II)-triggered responses that would likely require longer incubation times to be manifested. However, induction of protein-thiols system like thioredoxins (Figure 2.2C), might be related to Hg(II)-induced disulfide stress.

To evaluate if Hg(II) induction of thiol-related genes was unique to *Thermus*, the induction of homologous systems (thioredoxin, glutathione, cysteine and methionine biosynthesis) was tested in *Escherichia coli* strain K12, which lacks a *mer* system. When cells were exposed to 2 μM Hg(II) for 7.5 or 30 min, no increase in transcript levels of any of the tested thiol genes was observed when *ssrA* gene (Figure 2.S2) or *rrsB* (not shown) were used as reference genes (Onnis-Hayden *et al.*, 2009). There was no increase in transcript levels of genes involved in the biosynthesis of glutathione (*gshA* and *gshB*), cysteine/homocysteine (c*ysK*, *cysM* or *malY*), or in protein thiol systems like glutathione reductase (*gor*) or thioredoxin reductase (*trxB*) (Figure 2.S2). It has been previously shown that *zntA* is induced by Hg(II) in *E.coli* (Babai & Ron, 1998) and, as expected, Hg(II) exposure resulted in a 12-fold induction of transcript level of this gene (Figure 2.S2).

In summary, exposure to Hg(II) elicited two distinct, but complementary responses in *T. thermophilus*, but not in *E. coli*. First, LMW thiol biosynthesis genes showed rapid increase in transcript levels followed by a rapid decline. Second, the thioredoxin system appears to be induced more slowly than LMW biosynthesis genes possibly as a consequence of disulfide stress that results of Hg exposure.

Thiol genes are involved in Hg(II)-resistance.

A role for Oah and BSH in Hg(II)-resistance has not been described. Thioredoxins are known to be oxidized by Hg(II) (Carvalho *et al.*, 2008, Wang *et al.*, 2013) but little is known about their physiological role modulating Hg(II) toxicity in bacteria. To begin examining their roles in Hg(II)-resistance, thiol-related genes were individually replaced with the thermostable kanamycin-resistance gene (HTK gene) (Hoseki *et al.*, 1999) in the WT HB27 background. These included two genes for the biosynthesis of methionine/homocysteine (*oah1* and *oah2*), two genes involved in the biosynthesis of BSH (*bshA and bshC*), and two thioredoxin genes (*trxA1* and *trxA2*).

When the role of methionine/homocysteine biosynthesis pathway in Hg(II) resistance was evaluated in complex medium, the Δ*oah2* and Δ*oah1* strains were as resistant to Hg(II) as the WT (Figure 2.S3A). For reasons that are not currently understood, these mutant strains are unable to grow with sulfate as a sole sulfur source (data not shown), and therefore, growth and Hg(II) resistance was analyzed in a chemically defined medium supplemented with 10 µM homocysteine. As illustrated in Figure 2.3A, the Hg(II) IC_{50} values for the Δ*oah1* and Δ*oah2* strains was ~2 µM and the IC_{50} for the WT strain was ~4.5 µM. These results suggest that the cell's ability to synthesize homocysteine/methionine affects its Hg(II) resistance in defined medium. *Thermus* is found in hot springs were the sulfur sources is mostly sulfide or sulfate (Henley, 1996, Wang *et al.*, 2015, Geesey *et al.*, 2016), indicating that these genes may have an environmental relevancy to Hg(II) resistance.

oah2 is part of the *mer* operon in *T. thermophilus* (Wang *et al.*, 2009) (Figure 2.1A); therefore, the difference in Hg(II) resistance between Δ*oah2* and the WT strain could be due to a polar effect on *merA* expression. To test this possibility, MerA activities were measured in crude cell extracts of the WT, Δ*oah,* and Δ*merA* strains. MerA activity was statistically indistinguishable between the WT and Δ*oah2* strains in presence of Hg(II), while a Δ*merA* strain displayed negligible activity (Figure 2.S4).

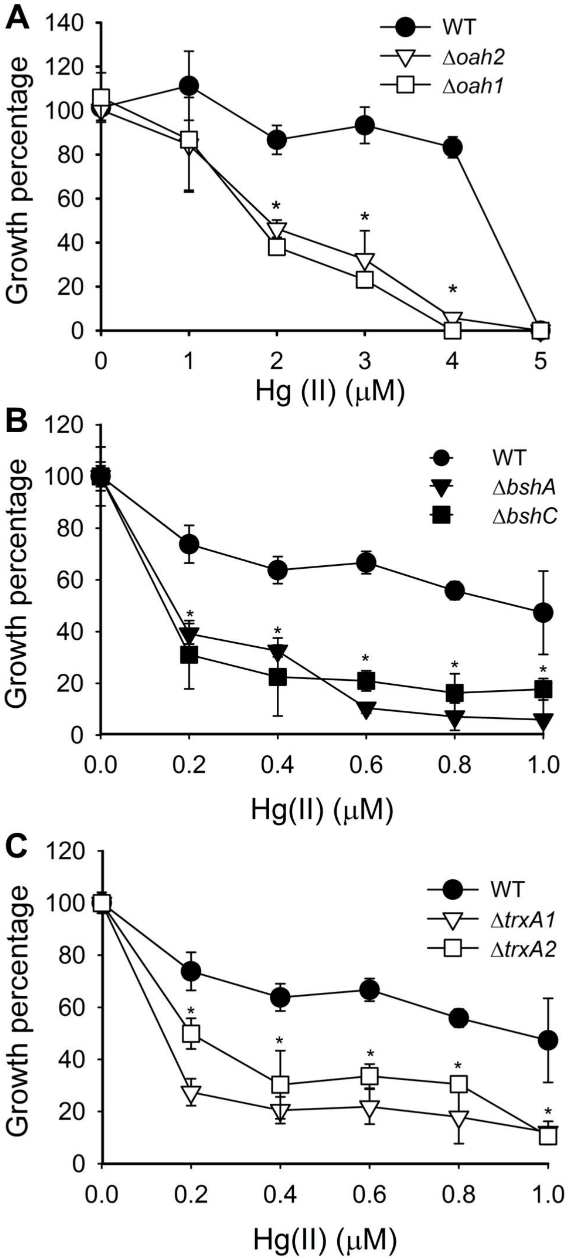

Figure 2.3. Sensitivity to Hg(II) increased in mutant strains lacking LMW thiol synthesis genes or thiol homeostasis systems. Effect of Hg(II) on growth in defined medium supplemented with (A) 10 μM homocysteine after 24 hours or (B and C) 5.2 mM sulfate after 20 hours of growth. Each point represents the average of three independent experiments and standard deviations are shown. Statistical analysis was conducted using a one way ANOVA, followed by a Tukey test; *P <0.001.

The BSH mutant strains were slightly more sensitive to Hg(II) when grown in complex medium as compared to the WT (Figure 2.S3B) and this difference was enhanced when grown in defined medium containing sulfate as the sulfur source. The Hg(II) IC_{50} for the Δ*bshA* and Δ*bshC* mutants was ~0.2 µM, whereas WT had an IC_{50} of ~1 µM (Figure 2.3B). The lower Hg(II) resistance of the strains in defined medium, as compared to complex media, is likely due to a decrease in exogenous Hg(II) ligands, which affect Hg(II) bioavailability (Farrell *et al.*, 1993). Furthermore, the higher sensitivity of the WT to Hg(II) in the defined medium supplemented with sulfate (Figure 2.3B and C) as compared to the one supplemented with homocysteine (Figure 2.3A) (1.6 times more sensitive), could be due to the fact that homocysteine can bind Hg(II) (Valko *et al.*, 2005, Jan *et al.*, 2011).

For the thioredoxin system, Δ*trxA1* and Δ*trxA2* strains were constructed. Similar to the Δ*bsh* strains, the Δ*trxA* strains were slightly more susceptible to Hg(II) than the WT strain in complex medium (Figure 2.S3C). In defined medium, the Δ*trxA* mutants were significantly more sensitive to Hg(II) than the WT. The Hg(II) IC_{50} was < 0.2 µM for the Δ*trxA1* and Δ*trxA2* mutants and ~1 µM for the WT (Figure 2.3C).

Taken together, the results in Figures 2.3 and 2.S3 clearly show that LMW thiols and thioredoxins enhance Hg(II) resistance in *T. thermophilus* HB27. It is environmentally significant that these genes have a higher impact on Hg(II) toxicity when sulfate is used as a sulfur source. In natural springs *Thermus* spp. do not have access to complex sulfur sources to use as substrates (Henley, 1996, Wang *et al.*, 2015, Geesey *et al.*, 2016).

Oxidation state of BSH and alternate LMW thiols is affected by Hg(II)

Due to the higher sensitivity of LMW thiol biosynthesis mutants to Hg(II), we examined how Hg(II) affected intracellular LMW thiol pools. The intracellular concentrations of LMW thiols were measured utilizing the fluorescent probe monobromobimane (mBrB) (Rethmeier *et al.*, 1997, Rao *et al.*, 2014) and products were identified and quantified by HPLC analysis coupled with a fluorescence detector. mBrB reacts with free thiols (reduced thiols) to produce a fluorescent derivative, which is detected in the elute. Thus, this assay only detects reduced thiols.

The main redox buffer detected in *T. thermophilus* was BSH, which was present at 27.1 ± 8.5 nmol per gram of cellular dry weight (Figure 2.4A, Table 2.S3, Figure 2.S5A and B). Two other LMW thiols were detected: cysteine (6.1 ± 3.1 nmol/g) and a large pool of sulfide (324.1 ± 88.4 nmol/g) (Figure 2.4A, Figure 2.S5 and 2.S3). The molar ratio for sulfide:BSH:Cys in the WT strain was ~ 12:1:0.2 (Figure 2.S5A and Table 2.S3). As expected, BSH was not detected in the LMW thiol pools from the Δ*bshA* and Δ*bshC* strains (Figure 2.4A and Table 2.S3), confirming the role for both genes in the BSH biosynthetic pathway.

We next examined whether the LMW thiol pool is affected by exposure to Hg(II). Cells were incubated with Hg(II) for 1 hour prior to determining the concentrations of free (reduced) LWM thiols. The addition of Hg(II) decreased free thiol pools in the WT strain (Figure 2.4B, Table 2.S3 and Figure 2.S5B) and Δ*merA* strain (Table 2.S3). Upon exposure to 1 μM Hg(II), cysteine was undetected and only 2% of reduced BSH remained in the WT strain (Figure 2.4B and Table 2.S3). BSH was undetected upon exposure to 3 μM Hg(II) (Figure 2.4B, Table 2.S3 and Figure 2.S5B). On the other hand,

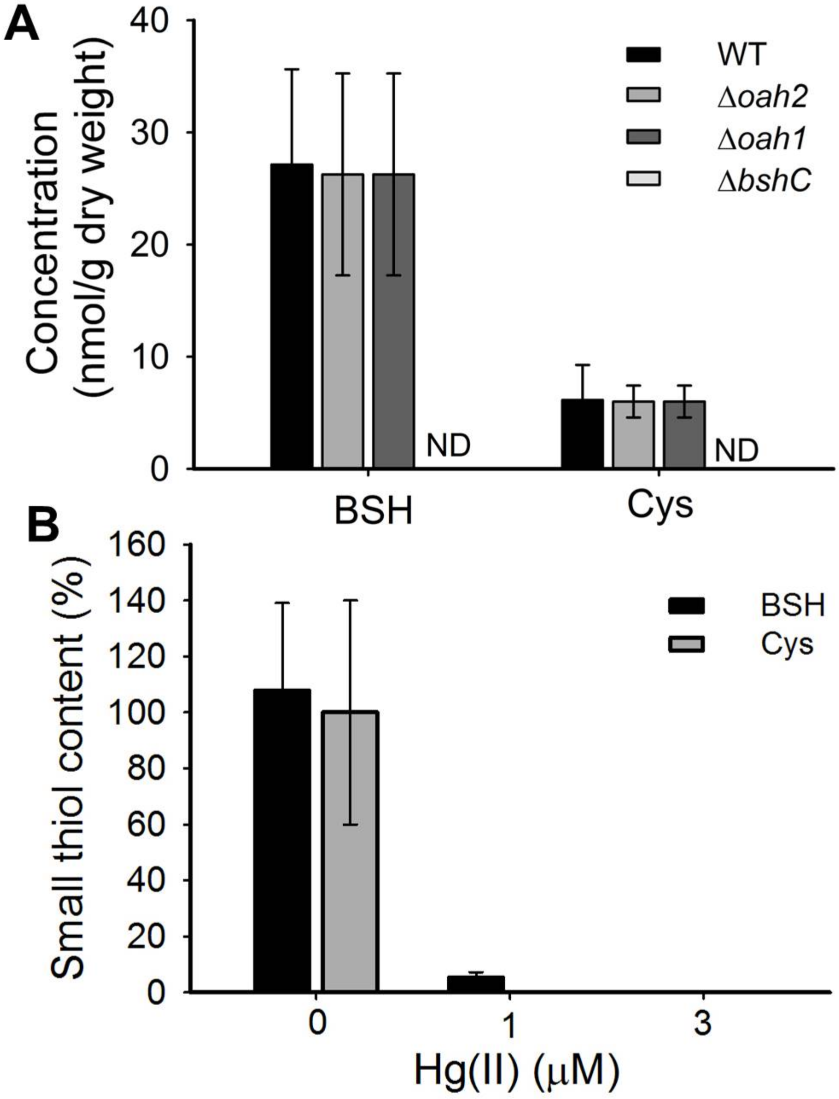

Figure 2.4. BSH is the primary LMW thiol in *T. thermophilus* and LMW thiols are responsive to Hg(II). (A) Cultures were grown in complex medium to O.D.600 ~0.4 and LMW thiols were quantified in WT, Δ*oah1*, Δ*oah2* and Δ*bshC* strains. (B) The WT strain was grown in complex medium to O.D.600 ~0.4, cells were exposed to different Hg(II) concentrations for 60 minutes, and small-thiols were quantified. Thiol concentration in cultures not exposed to Hg(II) were considered 100%. Averages and standard deviations represent triplicate samples from at least three independent trials. ND: not detected.

BSH and Cys were undetected when Δ*merA* was exposed to 1 μM Hg(II) (Table 2.S3), suggesting that Hg(II) removal by MerA in the WT strain alleviates the Hg(II)-induced disulfide stress.

These results suggest that LMW thiols scavenge Hg(II). In *T. thermophilus* BSH is the primary Hg(II) buffer, although cysteine, present at much lower concentration, also acts as Hg(II) buffer. The sequestration of Hg(II) by intracellular thiols is consistent with the hypothesis that induction of LMW thiol biosynthesis genes upon Hg(II) exposure (Figure 2.2A and B) may serve to increase the concentration of thiol ligands as a primary response to Hg(II) toxicity. Expression of thioredoxins (Figure 2.2C) may help to regenerate LMW thiol pools (Grant, 2001) that are sequestering Hg(II).

Cellular redox state modulates Hg resistance

The depletion of LMW thiols by Hg(II) and the importance of thioredoxins in Hg(II) resistance led us to hypothesize that a disturbance in the balance of reduced/oxidized thiols, would affect Hg(II) resistance. Diamide is a thiol-oxidizing agent that produces disulfide stress (Jan *et al.*, 2011) by interfering with thiol-dependent processes in the cell. In presence of diamide, at either 1 mM (Figure 2.S6) or 2 mM (Figure 2.5A), the WT, Δ*oah2*, and Δ*merA* strains were more sensitive to Hg(II). Resistance to Hg(II), as measured by IC_{50}, decreased with increasing diamide concentrations in both the WT and the Δ*merA* strains. As expected, the WT strain was more resistant than Δ*merA* at all diamide concentrations (Figure 2.5A and 2.S6). The addition of diamide had the same effect as growth under sulfur limiting conditions (Figure 2.3A) in the Δ*oah2* strain, Δ*oah2* was more sensitive to Hg(II) than the WT strain (Figure 2.5A and 2.S6).

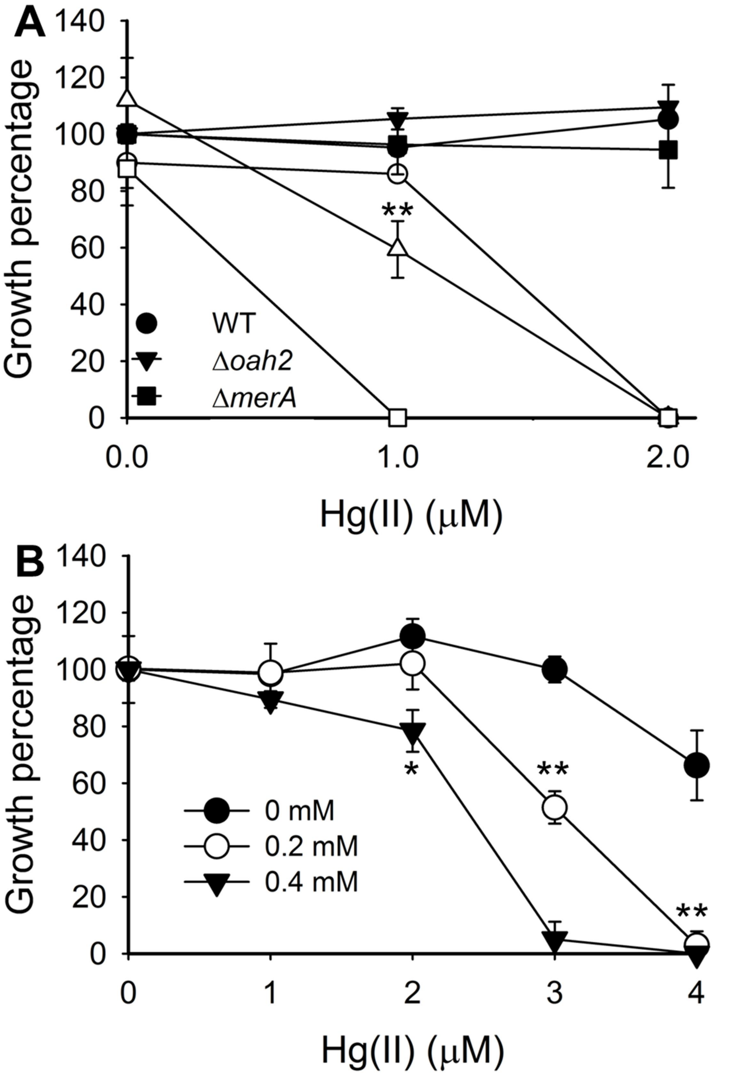

Figure 2.5. Decreased thiol availability enhances Hg(II) toxicity. (A) The effect of diamide on Hg(II) toxicity was evaluated in presence (2 mM; empty symbols) or absence (filled symbols) of diamide after 16 hrs of growth in WT (circle), Δ*oah2* (triangle) or Δ*merA* (square) strains. (B) Effects of the thiol alkaylating agent NEM on Hg(II) toxicity was evaluated after 24 hours of growth in the WT strain. Culture optical densities (A_{600}) at 0 μM of Hg(II) in complex medium was considered 100% growth. Averages and standard deviations are from at least 5 independent trials. Statistical analysis was conducted using a two-tailed t-test; * P <0.035,** P <0.001.

N-ethylmaleimide (NEM) is a thiol blocking agent that irreversibly binds to free thiols. When cells were exposed to 0.2 or 0.4 mM of NEM, no difference was detected in growth when compared with unexposed cells (not shown) indicating that NEM did not affect growth in the absence of Hg(II). When cells were co-exposed to Hg(II) and NEM they were more susceptible to Hg(II) than NEM-unexposed cells (Figure 2.5B). The Hg(II) IC_{50} for 0.2 mM and 0.4 mM NEM-exposed cells were ~3 and ~2.5 μM Hg(II), respectively, but more than 4 μM Hg(II) for NEM-unexposed cells. Taken together, these findings clearly indicated that the intracellular redox state and thiol availability greatly affect Hg(II) toxicity.

Evolutionary aspects of thiol genes and mercury

The presence of a gene related to the biosynthesis of thiol compounds has not been reported in other *mer* operons, as we reported for *oah2* in *T. thermophilus*'s *mer* operon. To examine how general this phenomenon is, genomes from organisms belonging to the Deinococcus-Thermus phylum were searched for the presence of *oah2* homologs or other thiol-related genes in the *mer* operons. Of the 75 Deinococcus-Thermus genomes available in June 2017, 32 belonged to Deinococcales and 43 to Thermales. Of the Thermales, 30 genomes were *Thermus* spp. and nine of them had *mer* operons (Table 2.S4). All the *Thermus* spp. *mer* operons had the *oah2* gene, or as annotated *O*-acetylhomoserine (thiol)-lyase. Only four other Thermales genomes, all belonging to the Thermaceae family, had *mer* operons, but none of them included the *oah2* gene. Only one Deinococcales had a *mer* operon lacking *oah2*. Thus, *oah2* is exclusive and always present in *mer* operons of *Thermus* spp. In all of these operons, *oah2* is located upstream to *merR* and *merA*. As in HB27, the genomes of all *mer*-containing *Thermus* spp. also had *oah1*. A phylogenetic analysis, performed with Oah1 and Oah2 sequences, shows a clear separation of the two proteins to two unique clades (Figure 2.6 and 2.S7), suggesting that these two genes are evolving independently of each other.

In a survey of 272 *mer* operons available in data bases in Dec. of 2011 (Boyd & Barkay, 2012), the only taxon containing a thiol-related gene, aside from *T. thermophilus,* was the Alphaproteobacteria (T. Barkay, unpublished), where 8 out of 25 operons had an ORF annotated as *gor*, which encodes for glutathione reductase (GR). The main LMW redox buffer in Alphaproteobacteria is GSH and GR keeps GSH reduced using NADPH as electron donor (Ritz & Beckwith, 2001). In Apr. 2017, there were 505 finished and assembled alphaproteobacterial genomes, when searched for the presence of MerA 40 additional *mer* operons were found, 5 of which included GR. From the 65 alphaproteobacterial genomes that had a *mer* operon only 13 genomes had GR present in the *mer* operon (Table 2.S5). With one exception, GR was always located downstream from *mer* transport genes. Another commonality between Alphaproteobacteria and *Thermus* spp. is the presence of a GR paralogous gene elsewhere in the genome. As designated for *Thermus*, GRs present in the *mer* operons were named GR2 and the non-*mer* operon GRs were designated as GR1. Similar to the Oah proteins, the GR2 proteins appear to be evolving independently from GR1, as suggested by the clustering pattern of the alphaproteobacterial GR phylogeny (Figure 2.S8).

This data indicates that the presence of a thiol gene in a *mer* operon is not unique to *Thermus* spp. The role of the GR system in Hg(II) resistance in Alphaproteobacteria remains to be studied.

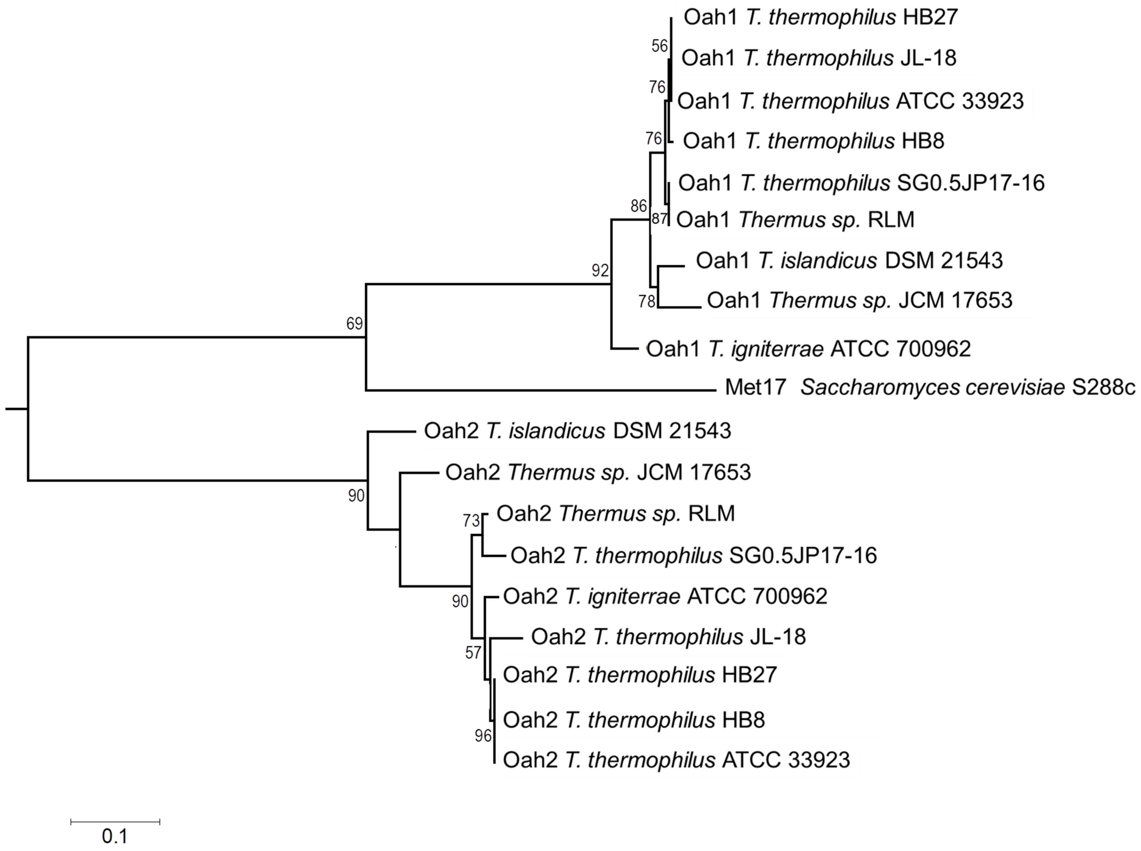
Oah1 *T. thermophilus* HB27
56
Oah1 *T. thermophilus* JL-18
76
Oah1 *T. thermophilus* ATCC 33923
76
Oah1 *T. thermophilus* HB8
Oah1 *T. thermophilus* SG0.5JP17-16
86
87
Oah1 *Thermus sp.* RLM
92
Oah1 *T. islandicus* DSM 21543
78
Oah1 *Thermus sp.* JCM 17653
69
Oah1 *T. igniterrae* ATCC 700962
Met17 *Saccharomyces cerevisiae* S288c
Oah2 *T. islandicus* DSM 21543
Oah2 *Thermus sp.* JCM 17653
90
73
Oah2 *Thermus sp.* RLM
Oah2 *T. thermophilus* SG0.5JP17-16
90
Oah2 *T. igniterrae* ATCC 700962
57
Oah2 *T. thermophilus* JL-18
Oah2 *T. thermophilus* HB27
Oah2 *T. thermophilus* HB8
96
Oah2 *T. thermophilus* ATCC 33923
0.1

Figure 2.6. Molecular phylogenetic analysis of Oah proteins in *Thermus* spp. by the Maximum Likelihood method. The Oah proteins encoded in the *Thermus* spp. genomes were *mer*-operons (Oah2) or met-operons (Oah1) associated. This is an enlargement of the original tree (Fig S7) presented to highlight diversification of Oah homologs. Oas (CysK) protein sequences used as an outgroup. The phylogeny with the highest log likelihood (-3752.97) is shown. The tree was drawn to scale, with branch lengths measured in the number of substitutions per site. Numbers at bifurcation points indicate bootstrap values. Protein IDs or locus tags are provided in table S6.

Discussion

The prior observation that in *T. thermophilus* HB27 *oah2* is co-transcribed with the *mer* genes in response to Hg(II) (Wang *et al.*, 2009), has led us to discover that in this bacterium: (i) expression of LMW and protein thiols genes are induced by Hg(II), (ii) BSH is the primary redox buffer, and (iii) BSH, along with other LMW thiols and thioredoxins, increase cellular resistance to Hg(II). Together, these results highlight a role of LMW and protein thiols in mitigating Hg(II) toxicity, supporting their integration into the paradigm of cellular defense against this highly toxic heavy metal.

The interaction of thiols with metals is one of life's foundations; this interactions control functional and structural attributes of molecules and cells. In fact, sequestration of soft metals by thiol compounds, such as metallothioneins and phytochelatins, is a well-established mechanism of metal resistance where the biosynthesis of the sequestering molecules is induced by exposure to the metals (Lemire *et al.*, 2013). The central paradigm for microbial resistance to Hg(II) is transformation to Hg(0) (Barkay *et al.*, 2003), although the role of GSH in Hg(II) resistance is known (Latinwo *et al.*, 1998, Rodríguez-Rojas *et al.*, 2016) not much information is available about other thiol genes. The *Thermus* system combines MerA-dependent reduction (Barkay *et al.*, 2003) with thiol-based sequestration (this study). Upon Hg exposure, the induction of genes encoding for LMW and protein thiol systems along with *merA* suggests a role for both in Hg(II) detoxification. Note that mercury-dependent induction of thiol biosynthesis genes did not occur in *E. coli* (Figure 2.S2), consistent with a previous study in which Hg(II) exposure did not induce expression of the glutathione transferase gene (Onnis-Hayden *et al.*, 2009).

This study shows induction of various LMW thiol biosynthesis genes by Hg(II). Moreover, knock-out mutants of all thiol biosynthesis genes were more susceptible to Hg(II) than the WT, connecting these genes and their Hg(II)-induced expression with a role in resistance to Hg(II). We propose the following model (Figure 2.7) to explain how Hg(II) sequestration by thiols and reduction work together. In Hg(II) exposed cells, the expression of thiol biosynthesis and *mer* genes is induced. LMW thiols bind Hg(II) and prevent Hg(II) from damaging sensitive targets in the cell. Oah synthesizes homocysteine that can be used as a precursor in cysteine biosynthesis (Figure 2.7, broken arrows); homocysteine may also bind Hg(II) with its free thiol (not shown). Cysteine availability is ensured by Hg(II)-induced overexpression of *oas* and this cysteine can be used by BshC to finalize the biosynthesis of BSH. In addition, thioredoxins might directly reduce or sequester Hg(II), the resulting thioredoxin-Hg complex can be resolved by NADPH-dependent thioredoxin reductase leading to Hg detoxification. The expression of *merA* results in the reduction of Hg(II) to Hg(0), leading to removal of the metal. This model accounts for the two cellular lines of defense against Hg(II) toxicity; sequestration by thiol-based redox buffers, and a *mer*-based detoxification system. The role of LMW thiol agents, including BSH, in Hg(II) resistance among prokaryotes warrants additional study.

The important question raised by this model is how thiol agents interact with MerA in Hg detoxification. One possibility is suggested by the fact that in *Thermus* MerA lacks NmerA, the N-terminal extension of 70 amino acids (Ledwidge *et al.*, 2005). In the proteobacterial MerA, NmerA delivers Hg(II) to the catalytic core of the enzyme; when absent, Hg(II) can be transferred, less efficiently, by thioredoxins and GSH (Ledwidge *et al.*, 2005). Generally, taxa carrying the core MerA exhibit mM concentra-

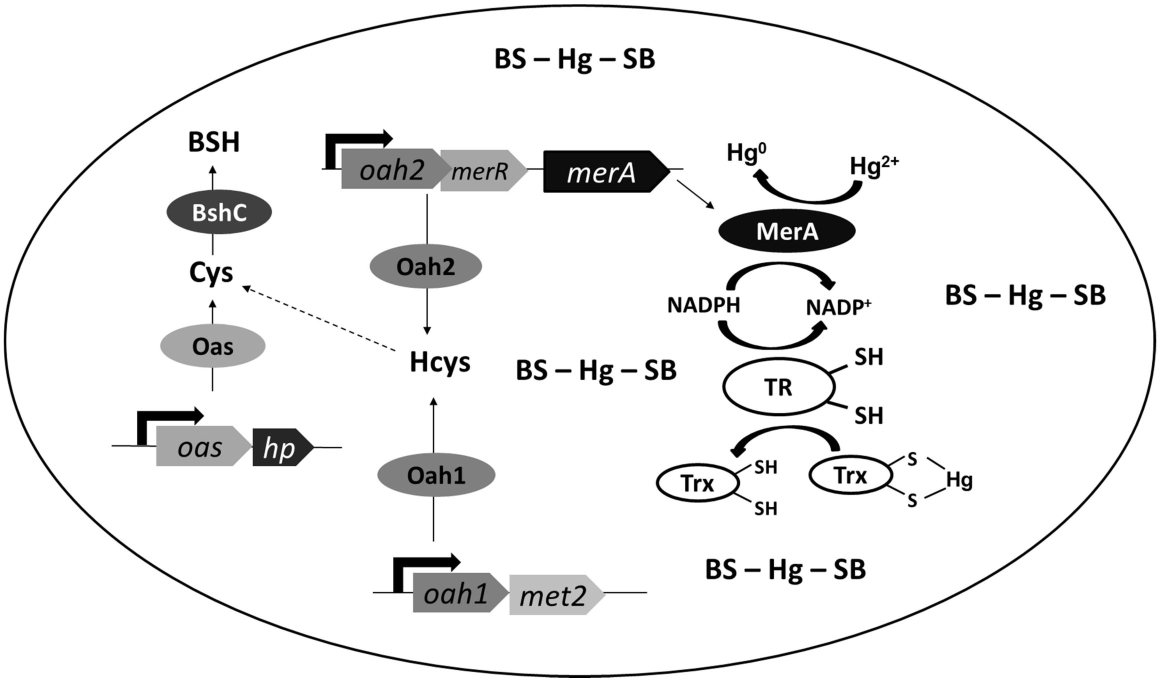
BS – Hg – SB
BSH
BshC
Cys
Oas
oas
hp
oah2
merR
merA
Oah2
Hcys
BS – Hg – SB
Oah1
oah1
met2
Hg^0
Hg^{2+}
MerA
NADPH
NADP$^+$
BS – Hg – SB
TR
SH
SH
Trx
SH
SH
Trx
S
S
Hg
BS – Hg – SB

Figure 2.7. Proposed model for a two-tiered response to Hg(II) toxicity in *T. thermophilus*. Hg(II) exposure (black arrows) induces expression of mer, LMW thiols, and thioredoxin systems. The latter two aid in sequestering Hg(II) until reduction of Hg(II) to the less toxic Hg(0) by MerA. Abbreviations: bacillithiol: BSH; homocysteine: Hcys; cysteine: Cys; hp: hypothetical protein; TR: thioredoxin reductase; Trx: thioredoxin.

tions of LMW thiols, but those carrying full length MerA (i.e., including NmerA) exhibit lower concentrations of LMW thiols (Barkay *et al.*, 2010). The lack of the NmerA domain in *Thermus* spp. might suggest that in addition to their role in intracellular sequestration of Hg(II), thioredoxins and/or BSH may play a role in tolerance by delivering Hg(II) to the enzyme.

Our results demonstrate a role for the thioredoxin/thioredoxin reductase system in Hg(II) resistance. Most studies on thioredoxin systems and Hg(II) have been performed in eukaryotic cells. These studies found that Hg(II) induced *trx* expression

(Branco *et al.*, 2014) but not enzymatic activities (Carvalho *et al.*, 2008, Branco *et al.*, 2014), likely due to inhibition of these proteins by Hg(II) (Carvalho *et al.*, 2008). Bacterial thioredoxin systems are different from those of mammalian cells. The little that is known about bacterial thioredoxin systems under Hg(II) stress indicate that bacterial thioredoxin, unlike the human enzyme, does not dimerize in presence of Hg(II) (Carvalho *et al.*, 2008). Moreover, Hg(II) oxidizes thioredoxin in *Geobacter sulfurreducens*, but not in *Shewanella oneidensis* (Wang et al., 2013), and Hg(II) exposure increases the amount of thioredoxin reductase in *Corynebacterium glutamicum* (Fanous *et al.*, 2008). Whereas our study adds new information on the role of the thioredoxin system in response to Hg(II) in a thermophilic bacterium, additional studies are needed to better understand the role of thioredoxin interactions with toxic metals considering the diversity of redox homeostasis systems among prokaryotes (Fahey, 2013).

Identification of BSH as a major LMW thiol agent in *Thermus* is another new finding of our research. Whereas this was expected because BSH was reported as the main LMW thiol agent in the related taxon *Deinococcus* (Newton *et al.*, 2009), we show that Δ*bsh* mutants are more susceptible to Hg(II) than the WT. We also determined that, similar to what has been reported in *Bacillus subtilis* (Ma et al., 2014), *T. thermophilus* BSH mutants were more sensitive to Zn(II) than the WT strain (data not shown). This information suggests that BSH has a general role in metal ion tolerance and/or buffering (Rosario-Cruz & Boyd, 2015). *Thermus mer* operons are not the only ones that contain thiol-related genes; some Alphaproteobacteria *mer* operons include *gor*, a glutathione reductase gene. Although studies have reported Hg resistance in environmental alphaproteobacterial isolates (Rasmussen *et al.*, 2008, Moller *et al.*, 2011) and the presence of alphaproteobacterial *merA* in soil metagenomes (Oregaard & Sorensen, 2007), the role of *gor* and that of the *mer* operons in managing Alphaproteobacterial Hg(II) stress have received little attention. Nevertheless, the presence of the *gor* gene (Figure 2.S8 and Table 2.S5) clearly suggests that the *mer* operon of *T. thermophilus* may not be the only example for the integration of genes involved in thiol systems. Possibly, in some Alphaproteobacteria the supply of reduced glutathione is increased upon Hg(II) exposure, a proposition that remains to be tested. Interestingly, *Thermus* spp. and Alphaproteobacterial genomes carry a second copy of the thiol related gene in their genome and in both the two paralogs appear to be evolving independently of each other (Figure 2.6 and 2.S8), suggesting evolution in response to different selective pressure. If so, the *mer*-associated thiol gene might have a unique function that is not shared with the chromosomally located gene.

In our prior research on the evolution of *mer* operons (Boyd & Barkay, 2012), we suggested a gradual evolution from simple constitutively expressed operons (*merA* and a possible transporter gene) in early thermophilic lineages to a highly efficient and more complex detoxification system in the Proteobacteria. Possibly, LMW and protein thiols are another line of defense against Hg toxicity in at least one early bacterial lineage. We have previously argued that the *mer* system originated among thermophilic bacteria from geothermal environments (Barkay *et al.*, 2010, Boyd & Barkay, 2012) with high Hg levels of geological origin (Geesey *et al.*, 2016). The discovery of LMW thiol-based defense against Hg toxicity in *Thermus* may suggest that the thiol-dependent cellular defense strategy originated early in the evolution of microbial life as well.

CHAPTER 3

SUPEROXIDE DISMUTASE AND PSEUDOCATALASE PROMOTE HG(II) RESISTANCE IN *THERMUS THERMOPHILUS* HB27 BY MAINTAINING THE REDUCED BACILLITHIOL POOL.

Abstract

Mercury (Hg) is a widely distributed heavy metal with no known cellular role. Mercury toxicity has been linked to the production of reactive oxygen species (ROS). Mercury does not directly perform redox chemistry with oxygen and how Hg(II) exposure increases ROS titers is unclear. We tested the hypothesis that Hg(II) exposure leads to ROS accumulation by oxidizing bacillithiol (BSH), which is the primary redox buffer in *Thermus thermophilus*. Exposure of *T. thermophilus* to Hg(II) triggered ROS accumulation and increased transcription and activities of superoxide dismutase (SOD) and pseudocatalase (Pcat). Hg(II) also decreased the activities of SOD and Pcat *in vitro*. Strains lacking SOD or Pcat had oxidized BSH pools and were more sensitive to Hg(II). Treatment of *T. thermophilus* with Hg(II) decreased aconitase activity and increased intracellular concentrations of free Fe. These phenotypes were exacerbated in Δ*sod* and Δ*pcat* strains. Treatment with Hg(II) also resulted in increased DNA damage. We conclude that sequestration of the redox buffering thiols by Hg(II) in conjunction with inactivating ROS scavenging enzymes directly impairs the ability of *T. thermophilus* to effectively metabolize ROS generated as a normal consequence of growth in aerobic environments.

Introduction

All aerobes face oxidative stress. Oxidative stress occurs when there is an imbalance between pro-oxidants and antioxidants, shifting the balance towards pro-oxidants, like reactive oxygen species (ROS). ROS are produced by reduction of dioxygen by intracellular flavoproteins (Imlay, 2013). A one electron transfer to oxygen produces superoxide (O_2^-), while a two electron transfer produces hydrogen peroxide (H_2O_2) (Imlay, 2008, Imlay, 2014). These reactive species can damage methionine, cysteine and iron-sulfur (Fe-S) clusters (Imlay, 2008, Imlay, 2014). A three-electron transfer can be catalyzed by redox active divalent transition metals such as copper and iron (Fe) via Fenton and Haber-Weiss reactions to produce hydroxyl radicals ($HO^{\bullet}$). These radicals rapidly react with multiple cellular constituents (Imlay, 2008, Imlay, 2014).

Mercury (Hg) does not perform redox chemistry under biological conditions, but in animal models Hg(II) exposure results in oxidative stress (Lund *et al.*, 1991, Miller *et al.*, 1991, Ariza *et al.*, 1998, Ariza & Williams, 1999, Valko *et al.*, 2005). Increased ROS upon Hg(II) exposure is thought to result from depletion of the main cellular redox buffer (Lund *et al.*, 1991, Ercal *et al.*, 2001, Valko *et al.*, 2005) or inhibition of the electron transport chain (Lund *et al.*, 1991, Miller *et al.*, 1991, Nath *et al.*, 1996). In bacteria, Hg-triggered ROS has been linked to the release of Fe^{2+} from solvent exposed iron sulfur (Fe-S) clusters accelerating Fenton reactions (Xu & Imlay, 2012). There is not a clearly established connection between Hg(II) and ROS in microbes and even less is known about physiologically diverse microbes with utilize alternate redox buffers.

Most studies that have examined Hg(II) detoxification and the physiological effects of Hg(II) exposure have been conducted in model organisms and Eukarya. *T.*

thermophilus is a deep-branching thermophilic organism that responds differently to Hg(II) exposure than *Escherichia coli* (Norambuena *et al.*, 2018). It also possesses a different arsenal of enzymes to detoxify ROS and it uses bacillithiol, instead of glutathione, as the primary low molecular weight thiol (LMW). Mercury has a high affinity for cellular thiols (Oram *et al.*, 1996, Helbig *et al.*, 2008, Jan *et al.*, 2011, LaVoie *et al.*, 2015, Norambuena *et al.*, 2018). We previously showed that Hg(II) exposure decreases the concentration of reduced BSH (Norambuena *et al.*, 2018). The disturbance of thiol-containing redox buffers, which normally quench ROS generated during respiration, can lead to ROS accumulation (Murphy, 2009).

In this study we tested the hypothesis that upon Hg(II) exposure of *T. thermophilus* ROS will accumulate, due to decreased in the reduced BSH pool and activities of ROS metabolizing enzymes. Data presented herein shows that Hg(II) exposure allows ROS accumulation because it quenches the LMW thiol buffer. Moreover, strains lacking ROS metabolizing enzymes have low levels of reduced BSH, the lack in BSH buffering capacity would likely increases “free” Hg(II) which can facilitate the release of Fe^{2+} from Fe-S clusters (LaVoie *et al.*, 2015). This effect is most likely perpetuated by ROS oxidation of FeS clusters perpetuating Fenton’s reaction and cellular damage. Results consistent with this model and indicate that an enzymatic capacity to detoxify ROS is key to maintaining an adequate thiol pool to mitigate Hg(II) toxicity in *T. thermophilus*.

Methods

Chemicals and bacterial growth conditions

Thermus thermophilus HB27 (DSMZ 7039) and its mutants were cultured at 65°C in 461 Castenholz TYE medium (complex medium, CM) as previously described (Wang *et al.*, 2009). When cultured in liquid media, cells were grown in 3 mL of medium in 13 mL test tubes shaken at 200 rpm. Solid culture media was supplemented with 1.5% agar. When present, kanamycin (Kan) was supplemented at 25 μg/ml and 40 μg/ml Hygromycin B. Unless otherwise stated, *T. thermophilus* overnight (ON) cultures were diluted in fresh medium to optical density $(OD)_{600}$ of 0.1 and further grown to OD_{600} reached of ~0.3 before challenge. Test tubes were used to grow cells for ROS, RNA extraction resistance assays and AP sites quantification. Flasks (2:5 ratio) were used for protein extracts, zymograms, thiol content and intracellular iron concentration. $HgCl_2$ was used for all assays. Unless stated otherwise, all chemicals were purchased from Sigma-Aldrich.

Mutant construction

Construction of the Δ*merA* (Wang *et al.*, 2009) and Δ*bshA* strains (Norambuena *et al.*, 2018) were previously described. The in-frame deletions for *sod* (WP_011172643.1) and *pcat* (WP_011174225.1) were performed as previously described (Norambuena *et al.*, 2018). DNA primers utilized are listed in Table 3.S1. In-frame gene replacements were confirmed by DNA sequencing. For genetic complementation the 16S rRNA gene (*rrsB* locus, TT_C3024), was replaced with the complementing gene constructs. It was previously reported that *T. thermophilus* HB27 is capable of surviving with a single copy of its two *rrs* genes (Gregory & Dahlberg, 2009). All stains used the native gene promoter to express resistance cassettes or genes.

Monitoring reactive oxygen species

ROS was monitored utilizing the fluorophore 2',7'-dichlorodihydrofluorescein diacetate (H_2DCDA) (Wang & Joseph, 1999, Myhre *et al.*, 2003, Rosario-Cruz *et al.*, 2015). Cell were incubated for 30 or 60 minutes in the presence and absence of Hg(II). One mL of cells was spun down, washed with phosphate buffered saline (PBS), resuspended in 500 µL of 10 µM H_2DCFDA in PBS, and incubated for 30 min at 37°C. After incubation, cells were washed with PBS and lysed by sonication. Fluorescence was measured using 485 nm as excitation and 535 nm as emission wavelengths (Perkin Elmer HTS 7000 Plus Bio Assay Reader). Data was normalized to protein concentration. Protein concentration was determined using Bradford reagent (Bio-Rad Laboratories Inc., Hercules, CA).

RNA extraction, cDNA synthesis and qPCR

Cells were exposed to 1 µM $HgCl_2$ for 15 or 30 min. Three mL aliquots were removed and mixed with RNA protect (QIAGEN). RNA extraction and cDNA synthesis were performed as previously described (Norambuena *et al.*, 2018). Transcripts were quantified by qPCR (iCycler iQ, Bio-Rad Laboratories Inc., Hercules, CA) as previously described (Norambuena *et al.*, 2018). DNA primers and cycling temperatures used for each gene are indicated in Table 3.S2.

Enzymatic assays

Cells were co-cultured with Hg(II) for 30 minutes. Cultures (25 mL) were centrifuged, washed in PBS buffer and cell pellets were frozen until further use. Crude cell extracts were prepared as previously described (Vetriani *et al.*, 2005). All enzyme assays were performed at 50°C. When crude cell extracts were directly exposed to Hg(II), Hg(II) was added at the indicated concentrations and incubated for 5 min before measuring the enzymatic activity. For the superoxide dismutase (SOD) activity the assay was performed as described by Spitz and Oberley (1989) using 30 µg of crude extract. One unit was defined as the amount of enzyme needed to reduce by 50% the reference rate. Measurements were carried out using an AVIV, biomedical spectrophotometer, model 14 UV-VI. Catalase activity was performed as described by Beers and Siezer (1952) using 0.6 mg of protein extract. One unit was defined as the amount of enzyme needed to degrade 1 µmole of H_2O_2 per min, using $\mathcal{E}= 43.6\ M^{-1}cm^{-1}$ for H_2O_2. For aconitase activity, cell lysis was performed under anaerobic conditions, enzymatic assay was performed as described by Kennedy *et al*. (1983) using 20 µg of protein extract in assay buffer (50 mM Tris, 150 mM NaCl pH 7.4). One unit was defined as the amount of enzyme needed to degrade 1 µmole of DL-isocitrate per sec, using $\mathcal{E}= 3.6\ mM^{-1}cm^{-1}$ for cis-aconitate. Catalase and aconitase activities were carried out using UVmini-1240 spectrophotometer (Shimadzu).

Resistance assays

ON cultures were diluted to $O.D_{600}$ 0.1 in fresh CM and a varying concentrations of toxicant (fosfomycin, paraquat, or $HgCl_2$) was added to individual 12 mL test tubes at different concentration ranges. Growth was followed at OD_{600}. Resistance was assessed as the percentage of growth observed at the indicated times (from 18-22 hours) relative to control that was unexposed to the toxicant (100% of growth). Soft agar assays were used to asses H_2O_2 sensitivity. Cells were grown as for liquid assays and 1% of the culture was added to 3 mL of CM soft agar (0.8%), then poured over a 25 mm petri dish with CM agar. Ten µL of 10 mM H_2O_2 was added to the center of the plate. Plates were incubated for 24 hours before the halo of inhibition was measured.

Zymograms

Native gels were prepared as described by Weydert and Cullen (2010). SOD and catalase (for Pcat) in-gel activities were performed and revealed as described by Weydert and Cullen (2010). For SOD and Pcat activities, 25 µg and 50 µg, respectively, of total protein extracts were loaded on the gels. Protein extracts were prepared as described for enzymatic assays.

Thiol concentration determination

Extraction and quantification of low molecular weight thiols was performed as previously described (Norambuena *et al.*, 2018). For total BSH determinations, cells were exposed to 10 mM DTT for 30 min prior to thiol extraction.

Intracellular iron quantification

Cells were co-cultured (100 mL) with Hg(II) for 30 min. Cells were then pelleted by centrifugation and resuspended in 5 mL of PBS with 10 mM diethylene triamine pentaacetic acid (DTPA) and 20 mM deferoxamine mesylate salt (DF), shaken at 37 °C for 15 min at 180 rpm, and cells were pelleted at 4°C (LaVoie *et al.*, 2015). Cell pellet was washed once with ice-cold 20 mM Tris–HCl (pH 7.4) and resuspended in the same buffer supplemented with 15% glycerol buffer. Cells were stored at -80 °C. The assay followed the description of LaVoie *et al.* (LaVoie *et al.*, 2015). For EPR analysis, cell suspensions were thawed on ice and 200 µL aliquots were loaded into 4-mm OD quartz EPR tubes and frozen in liquid nitrogen. Continuous-wave (CW) EPR experiments were performed with an X-band Bruker EPR spectrometer (Elexsys580) equipped with an Oxford helium-flow cryostat (ESR900) and an Oxford temperature controller (ITC503). EPR parameters used in our experiments were: microwave frequency, 9.474 GHz; microwave power, 20 mW; modulation amplitude, 2 mT; and sample temperature, 25°K. The Fe(III):DF concentration of each sample was determined by comparing the peak-to-trough height of EPR signal at g = 4.3 against the standard sample with a known Fe(III):DF concentration (50 µM $FeCl_3$ and 20 mM DF in 20 mM Tris–HCl at pH 7.4 with 15% glycerol).

AP sites

Cells were exposed to different Hg(II) concentrations for 60 min. 3 mL of cells were spun down and washed with PBS prior to DNA extraction using QIAamp DNA kit (QIAGEN). AP sites were quantified using the Oxiselect™ Oxidative DNA Damage Quantification Kit (Cell Biolabs) as instructed by the manufacturer.

Statistical analysis

One-way ANOVA followed by a Dunnet test analysis was performed for multiple group comparison to a control. For two group comparisons (controls vs treatment), student's t-tests were performed. All analyses were conducted with Sigmaplot 11.

Results

Mercury exposure results in ROS accumulation and deactivates ROS-scavenging enzymes.

We tested the hypothesis that Hg(II) exposure would increase ROS accumulation in *T. thermophilus*. After exposure to Hg(II), total ROS levels were qualitatively measured using the fluorescent probe DCFDA. There was no significant increase in ROS after 30 min of exposure to 2-8 M Hg(II) (Figure 3.1A). However, after 60 minutes of exposure to 4 or 8 µM Hg(II), a significant increase in ROS accumulation was observed.

We examined if Hg(II) exposure increased transcription of gene encoding ROS metabolizing enzymes. The genome of *T. thermophilus* encodes one Mn-SOD (*sod*) to detoxify superoxide. It does not possess catalase, but instead, encodes a nonheme catalase, or pseudocatalase (*pcat*), that utilizes an active site Mn instead of heme (Hidalgo *et al.*, 2004). It also possesses 2 types of peroxiredoxins: osmotically inducible protein (*osmC*) and bacterioferritin comigratory protein (*bcp*). These are members of the thiol peroxidase family, which catalyze the reduction of hydroperoxides (Clarke *et al.*, 2010, Flohe *et al.*, 2011). OsmC has the ability to reduce alkyl and organic hydroperoxides (Lesniak *et al.*, 2002, Lesniak *et al.*, 2003, Saikolappan *et al.*, 2015) and BCP can reduce H_2O_2 and organic hydroperoxides (Jeong *et al.*, 2000, Reeves *et al.*, 2011). There is also a thioredoxin-related protein, thiol:disulfide interchange protein (*tlpA*), which is periplasmic protein involved in oxidative stress responses (Achard *et al.*, 2009). Exposure of *T. thermophilus* to 1 µM Hg(II) increased transcript levels of *sod, pcat*, *osmC*, and *tlpA* (Figure 3.1B); while *bcp* transcript level was unchanged. This induction was noted after 7.5 minutes (not shown) and sustained for at least 30 minutes after Hg(II) exposure (Figure 3.1B). The strongest induction was observed for *pcat*,

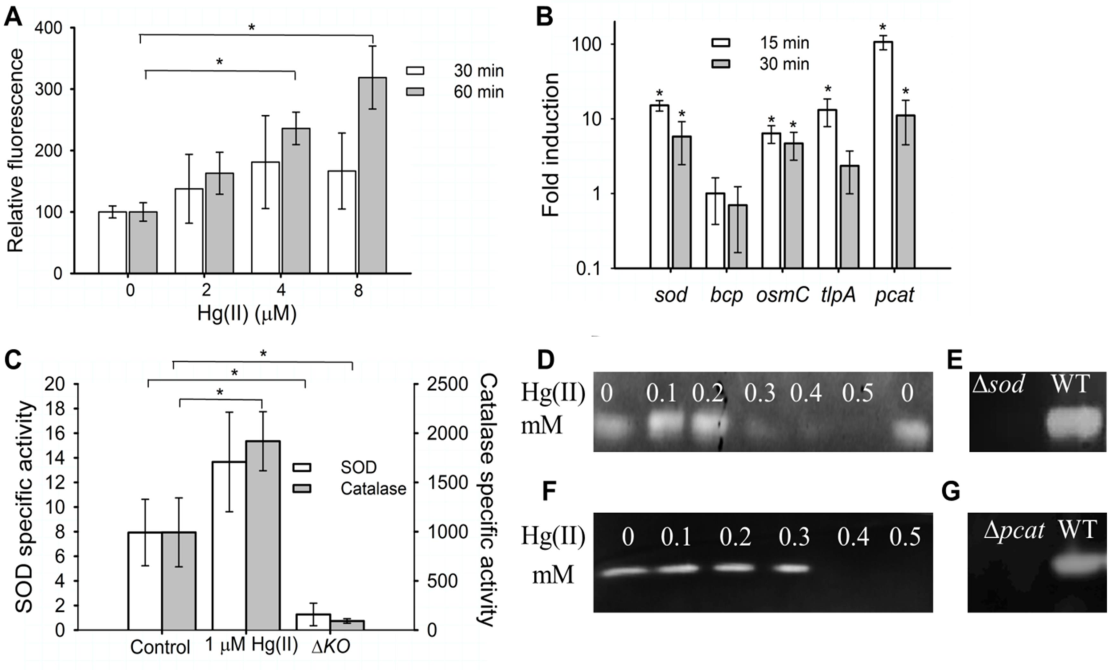

Figure 3.1. Mercury exposure induces ROS and increased SOD and Pcat expresion. (A) Cultures were grown to OD_{600} of 0.3 and exposed to varying concentrations of Hg(II) for 30 (white) or 60 minutes (grey) in the WT strain before total ROS was measured using DCFDA. (B) Transcript levels of superoxide dismutase (*sod*), bacterioferritin comigratory protein (*bcp*), organic hydroperoxide reductase (*osmC*), thiol peroxidase (*tlpA*) and pseudocatalase (*pcat*), were measured in the WT strain after 15 or 30 minutes of exposure to 1 μM of Hg(II). (C) WT cells were exposed to 0 or 1 μM of Hg(II) for 30 minutes and SOD (white) or catalase (grey) activities were measured. Each activity was compared to their respective mutant strain (Δ*sod* or Δ*pcat*) not exposed to Hg(II). (D and F) Crude protein extracts of the WT strain where incubated with different Hg(II) concentrations and then loaded on the gels. Zymograms where revealed for (D and E) SOD activity or (F and G) catalase activity. Cell extracts of the (E) WT and Δ*sod* strains or (G) WT and Δ*pcat* are also shown. For panels A, B, and C, each point represents the

average of at least three independent experiments and standard deviations are shown. Student's t-tests were performed on the data in panels A and C, and * indicates P≤ 0.5. A Mann-Whitney Rank Sum Test was performed on the data in panel B against the control and * P≤0.29**.**

reaching about 107±23 -fold induction after 15 min of Hg(II) exposure. The data are consistent with the hypothesis that Hg(II) exposure induces transcription of genes necessary to detoxify ROS.

We tested the hypothesis that Hg(II) exposure results in increased SOD and Pcat expression. Cells were exposed to Hg(II) for 30 min and H_2O_2 and superoxide scavenging activities were measured in cell-free lysates. Hg(II) exposure significantly increased H_2O_2 consumption by approximately 2-fold. A Δ*pcat* mutant strain lost 90% of the H_2O_2 consumption activity (92 ± 23 U vs. 992 ± 350 U for the unexposed WT) verifying that Pcat functions in H_2O_2 metabolism (Figure 3.1C). Superoxide consumption increased in cell lysates, but the increase was not statistically significant (Figure 3.1C). A Δ*sod* strain displayed 8-fold lower superoxide scavenging activity than the Hg(II)-unexposed parent (0.2 ± 0.9 U vs. 7.9 ± 3.0 U of the WT strain), correlating superoxide consumption with *sod*.

Hg(II) exposure resulted in greatly increased *sod* and *pcat* mRNAs, which did not correlate with large increases in SOD and Pcat activities. We tested the hypothesis that Hg(II) exposure damaged these enzymes. Cell-free *T. thermophilus* extracts were exposed to Hg(II) before measuring SOD and Pcat activities. Hg(II) exposure resulted in decreased activities for both SOD and Pcat (Figures 3.1D and F). Gel-localized activities were verified using the Δ*sod* and Δ*pcat* strains (Figures 3.1E and G). Moreover, Δ*sod* and Δ*pcat* strains were more sensitive to paraquat and H_2O_2, respectively (Figure 3.S1). Taken together, these findings show that Hg(II) exposure triggers ROS accumulation and induces transcription and expression of ROS-metabolism genes *in vivo*. Hg(II) exposure also decreased SOD and Pcat activities *in vitro*.

Strains lacking superoxide or H_2O_2 *scavenging activities are more sensitive to Hg(II).*

We tested the hypothesis that SOD and Pcat have roles in preventing Hg(II) toxicity. When compared to the WT, the Δ*sod* and Δ*pcat* mutants had increased sensitivity to Hg(II) with 50% inhibitory concentrations (IC_{50}) of 2.5 µM and 3 µM, respectively (Figures 3.2A and B). The WT IC_{50} was 4.5 µM Hg(II). The Δ*sod* strain was as sensitive to Hg(II) as the Δ*merA* strain, indicating that SOD plays a fundamental role in Hg(II) resistance to the same extent as MerA. Genetic complementation of the Δ*sod* (Figures 3.S2A and C) and Δ*pcat* (Figures 3.S2B and D) strains verified that the lack of SOD or Pcat was resulting in the witnessed phenotypes.

We tested the hypothesis that Hg(II) sensitivity in strains lacking SOD or Pcat was the result of altered MerA function. To this end, we compared the Hg(II) sensitivities of the Δ*sod* Δ*merA,* Δ*pcat* Δ*merA* double mutants to that of the Δ*merA* mutant. The Δ*sod* Δ*merA* and Δ*pcat* Δ*merA* double mutants were more sensitive to Hg(II) than the Δ*merA* strain (Figure 3.2C) suggesting that the roles of SOD, Pcat and MerA in Hg(II) resistance are independent and complementary.

Finally, we tested the hypothesis that ROS accumulation would occur at lower Hg(II) concentrations in the Δ*sod* and Δ*pcat* strains compared to the WT strain. When

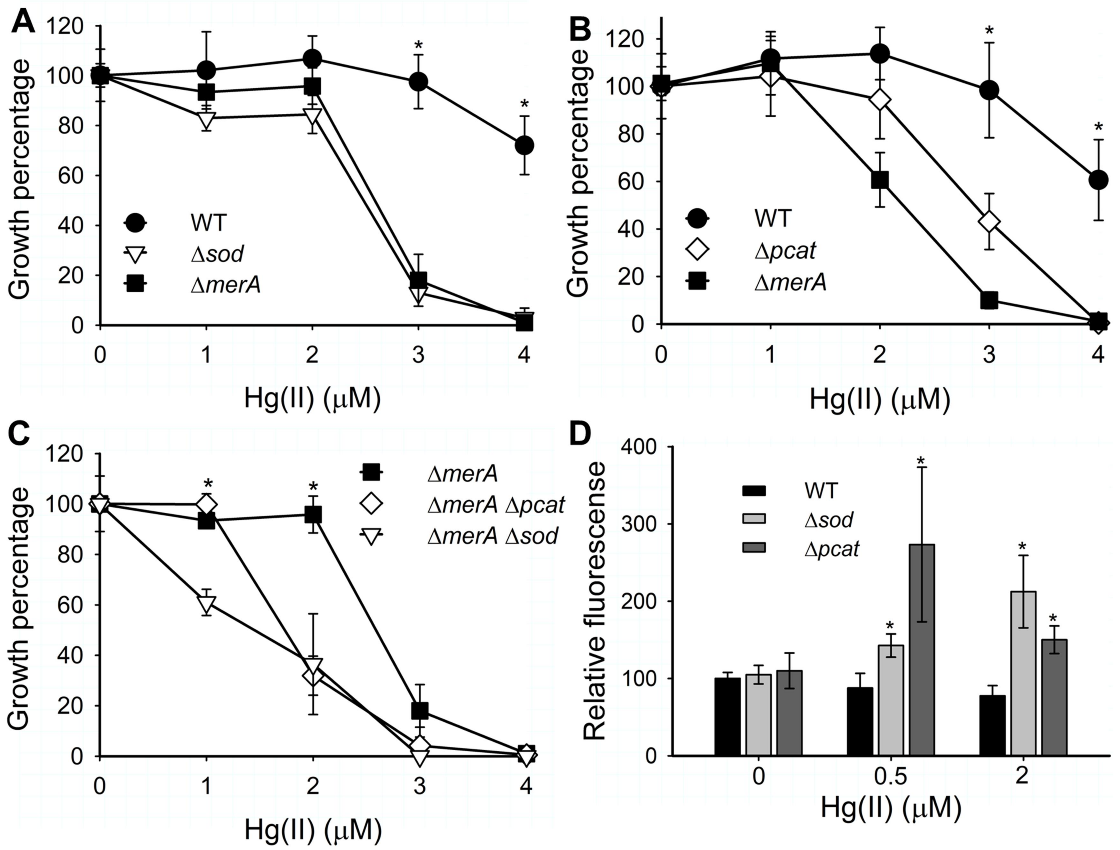

Figure 3.2. ROS mutants are more sensitive to Hg(II) and have increased ROS levels upon Hg(II) exposure. Culture optical densities were determined after (A and C) 21 hours or (B) 18 hours of growth (C). Growth in the unexposed control was considered 100% of growth. (D) Cultures were grown to OD_{600} of 0.3 and one-half were exposed to Hg(II) for 60 minutes. The fluorescence obtained for the unexposed WT strain was considered 100% fluorescence. Each point represents the average of three independent cultures and standard deviations are shown. Student's t-tests were performed and * indicates a $P \leq 0.049$.

grown in absence of Hg(II), the mutant strains did not accumulate more ROS than the WT strain (Figure 3.2D). ROS accumulation was noted in the Δ*sod* and Δ*pcat* strains upon exposure to 0.5 and 2 μM Hg(II), whereas no change in ROS levels were noted in the WT strain. These results led us to conclude that SOD and Pcat mitigate Hg(II) toxicity by preventing ROS accumulation.

Quenching of BSH by Hg(II) results in ROS accumulation.

We next examined the mechanism(s) of ROS accumulation upon Hg(II) exposure. We have previously shown that BSH plays a fundamental role in Hg(II) resistance in *T. thermophilus* and upon exposure to 3 μM Hg(II) BSH was undetectable (Norambuena *et al.*, 2018). We tested the overarching hypothesis that Hg(II) lowers the levels of reduced BSH available to aid in ROS metabolism, resulting in increased ROS accumulation.

We tested the hypothesis that BSH has a role(s) in metabolizing ROS or the byproducts of ROS damage. We quantified the BSH pools in the Δ*sod* and Δ*pcat* strains. Reduced BSH was undetectable in the Δ*sod* mutant. While, the WT and Δ*pcat* strains had 33.2± 10.2 and 7.2± 6.7 nmol/g dry weight of reduced BSH, respectively (Figure 3.3A). Importantly, all strains had approximately same intracellular concentration of BSH (Figure 3.3A). Reduced BSH is required to detoxify fosfomycin (Gaballa *et al.*, 2010). The Δ*sod* and Δ*pcat* strains were more sensitive to fosfomycin than the WT and had similar sensitivity to fosfomycin than of the Δ*bshA* strain (Figure 3.3B), which cannot synthesize BSH (Norambuena *et al.*, 2018).

ROS scavenging deficient strains were constructed in the Δ*bshA* background to test if there was further impairment in Hg(II) resistance in the Δ*pcat* and Δ*sod* strains when BSH was not produced. The Hg(II) sensitivity phenotypes corresponding to the Δ*bshA* and Δ*pcat* mutations were not additive (Figure 3.3C). However, the Δ*sod* strain

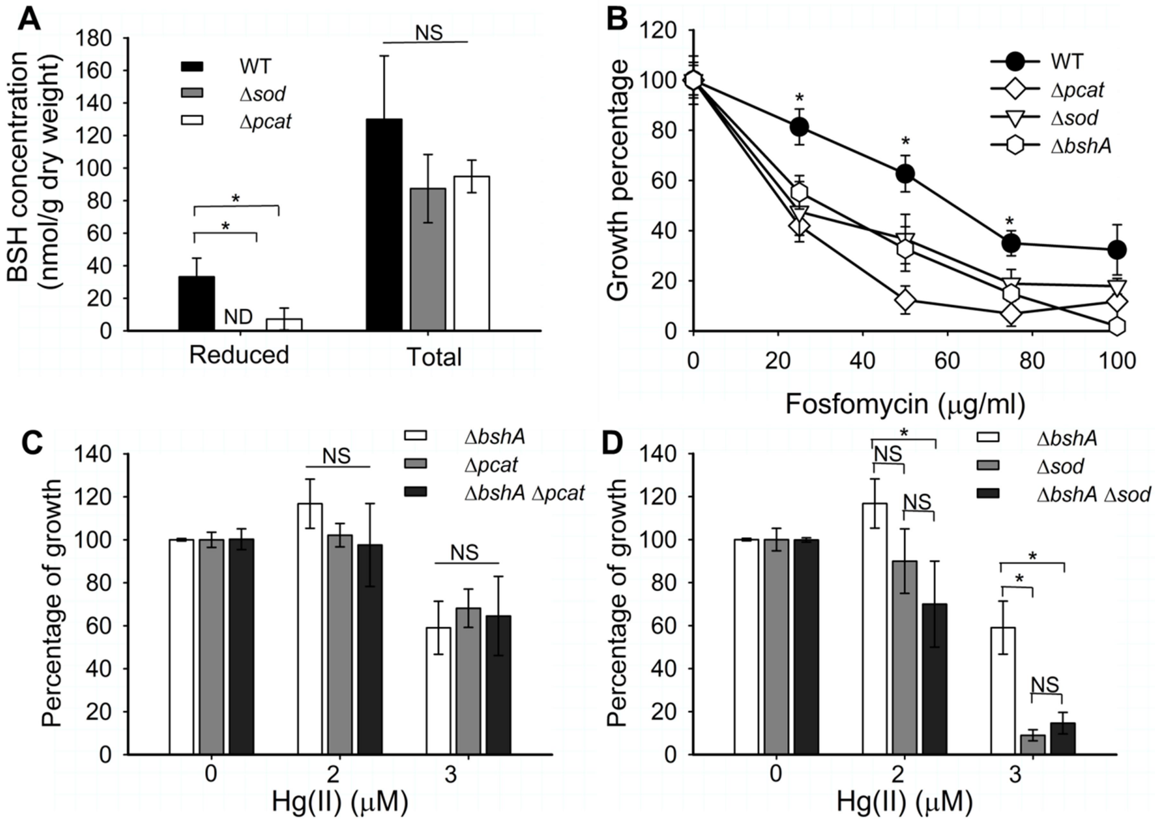

Figure 3.3. *T. thermophilus* strains lacking SOD or Pcat have decreased reduced BSH. (A) Cultures were grown to OD_{600} of 0.3 and exposed or not to 10 mM of DTT for 30 min, and LMW thiols were quantified with mBrB. DTT treated cells were used to measure total BSH. (B) Final culture optical densities were recorded after 20 hours of growth in cultures exposed to various concentration of fosfomycin. Effect of Hg(II) on cell growth was evaluated after 20 hours of growth in (C) the Δ*pcat*, Δ*bshA*, and Δ*pcat* Δ*bshA* mutant strains and (D) in the Δ*sod*, Δ*bshA*, and Δ*sod* Δ*bshA* mutant strains. Unexposed controls were considered 100% of growth. Each point represents the average of three independent cultures and standard deviations are shown. ND: no signal detected. Student's t-tests were performed on the data and * indicates a $P \leq 0.033$.

was more sensitive to Hg(II) than the Δ*bshA* strain (Figure 3.3D). These results suggested that SOD has a role in preventing Hg(II) toxicity in addition to preventing the oxidation of BSH pool. The Hg(II) sensitivity of the Δ*pcat* strain may be, in part, the result of a decreased titer of reduced BSH.

Hg(II) exposure results in decreased aconitase activity and an increase in non-chelated cytosolic Fe.

The Δ*sod* and Δ*pcat* strains had a decreased concentration of reduced BSH. We hypothesized that there would be more non-chelated Hg(II) (not BSH bound) in the cytoplasms of the Δ*sod* and Δ*pcat* strains when challenged with Hg(II). Prior work in *E. coli* found that Hg(II) can displace Fe^{2+} from solvent exposed Fe-S clusters inactivating the enzyme (Xu & Imlay, 2012, LaVoie *et al.*, 2015). Aconitase (AcnA) requires a solvent exposed Fe-S cluster that can also be damaged by ROS (Flint *et al.*, 1993, Varghese *et al.*, 2003, Djaman *et al.*, 2004). When *T. thermophilus* was exposed to 1 µM Hg(II) for 30 minutes, AcnA activity was decreased 2-fold (Figure 3.4A). The non-challenged Δ*pcat* and Δ*sod* strains had 12 and 16% of the AcnA of the WT strain, respectively (Figure 3.4A). Upon exposure to Hg(II), AcnA activity was 30-fold lower in the Δ*sod* strain and 4.5-fold lower in the Δ*pcat* (Figure 3.4A inset). Next, we examined the hypothesis that Hg(II) inactivated AcnA *in vitro*. To this end, we added Hg(II) to cell free lysates previous to measurement of AcnA activity. AcnA activity decreased as a function of Hg(II) added and was nearly undetectable after exposure to 100 µM Hg(II) (Figure 3.4B).

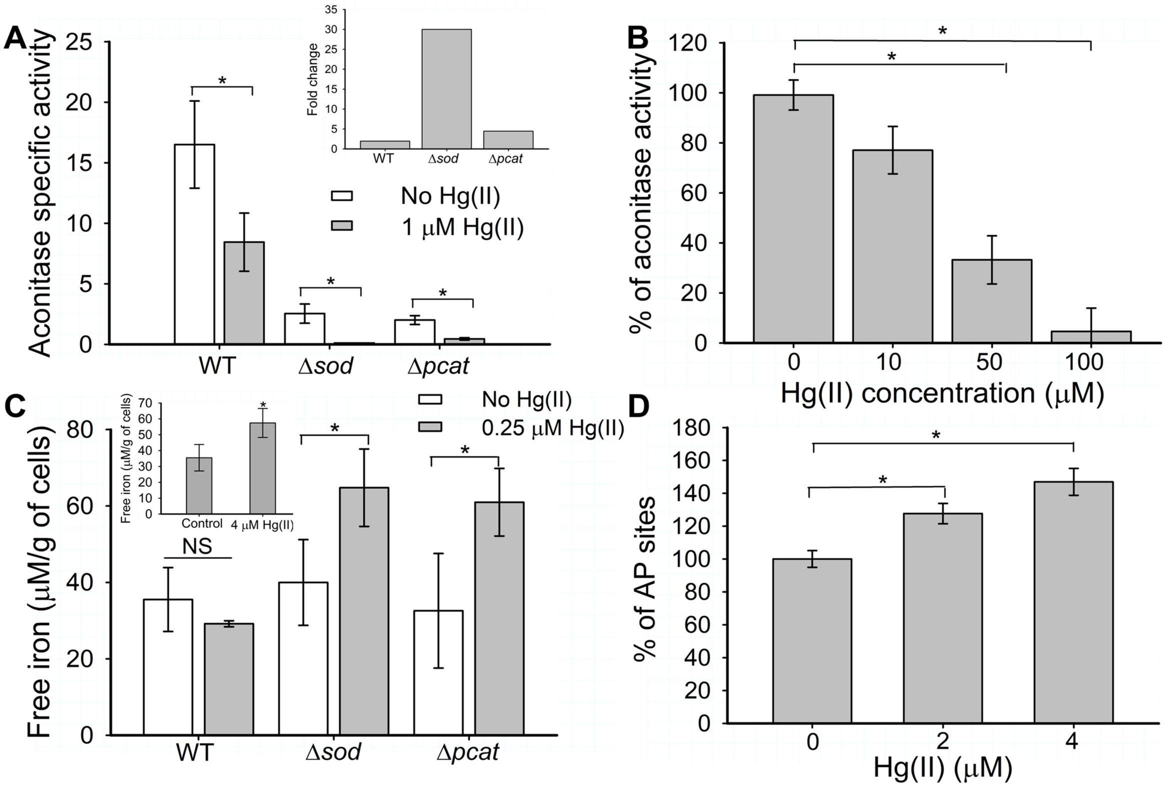

Figure 3.4. Mercury stress results in aconitase inactivation and increased intracellular free iron. (A) Aconitase activity was monitored in cell free lysates after cells had been exposed or not to 1μM Hg(II) for 30 minutes. (B) Cell-free lysates from the WT strain were exposed to 0-100 μM Hg(II) before aconitase activity was determined. (C) The concentration of free Fe was quantified after exposure to 0.25 μM of Hg(II) or 4 μM (inset) for 30 minutes on the different strains. (D) DNA damage was determined by quantifying the number of apurinic/apyrimidinic sites (AP sites) in the WT strain (cells unexposed to Hg(II) had an average of 8.38± 0.77 AP sites per 100,000 base-pairs of DNA). Each point represents the average of at least three independent cultures and standard deviations are shown. Where shown, student's t-tests were conducted on the data and * indicates $P \leq 0.044$.

Next, we tested the hypothesis that Hg(II)-exposure would increase the size of the cytosolic free Fe pool. *T. thermophilus* was exposed to 4 μM Hg(II) or not for 30 min and intracellular free Fe was quantified using electron paramagnetic resonance (EPR) spectroscopy (LaVoie *et al.*, 2015). Exposure to Hg(II) almost doubled the amount of free Fe (Figure 3.4C inset). We next exposed the WT, Δ*sod*, and Δ*pcat* strains to 0.25 μM Hg(II) and measured free Fe. At this Hg(II) concentration, the WT free Fe pool was unaltered; however, it was increased 1.5-2-fold in the Δ*sod* and Δ*pcat* strains (Figure 3.4C). Thus, treatment with a lower concentration of Hg(II) was capable of disrupting the Fe pool in the Δ*sod* and Δ*pcat* strains. These strains had similar free Fe levels when cultured in the absence of Hg(II) (35.5 ± 8.4 μM/g WT cells, 39.9 ± 11.2 μM/g Δ*sod* cells*,* and 32.6 ± 4.7 μM/g Δ*pcat* cells) (Figure 3.4A).

Free Fe^{2+} can catalyze Fenton chemistry to produce $HO^{\bullet}$ (Imlay, 2008), which can damage DNA by producing apurinic/apyrimidinic (AP) sites (Morita *et al.*, 2010). We hypothesized that Hg(II) exposure would result in increased DNA damage. After exposure to either 2 and 4 μM Hg(II) there is an increase in AP sites (Figure 3.4D). An increase in AP sites requires base excision repair systems and in *T. thermophilus* this system depends on the Nfo endonuclease IV (Morita *et al.*, 2010). We found that a Δ*nfo* mutant was more sensitive to Hg(II) than the WT strain (Figure 3.S3).

Taken together these data are consistent with a model wherein Hg(II) exposure decreases the activity of Fe-S enzymes and increases intracellular free Fe. This Fe likely increases DNA damage and its repair Nfo-dependent. By inference, these results suggest increased hydroxyl radical concentrations by exposure to Hg(II). Release of Fe was higher in the Δ*sod* and Δ*pcat* suggesting that the increased Hg(II) sensitivity can be linked to Fe-dependent ROS formation, this increase in Hg(II) sensitivity is due to lack of reduced BSH that can buffer this metal.

Discussion

The mechanisms by which metals exert toxicity are not fully understood. A large majority of studies examining these phenomena were conducted in model organisms and relative few in physiologically diverse organisms. In this study, we examined the effect of Hg(II) exposure on the deeply branching thermophilic bacterium to expand our knowledge of Hg(II) toxicity and resistance in phylogenetically and physiologically diverse microbes. Data presented herein and from our previous study (Norambuena *et al.*, 2018) have led to a working model (Figure 3.5) wherein exposure of *T. thermophilus* to Hg(II) results in the inactivation of two ROS detoxifying enzymes (SOD and Pcat) and ROS accumulation. SOD and Pcat strains have increased levels of BSH oxidation, BSH is necessary to prevent Hg(II) intoxication. Hg(II) accumulation inactivates enzymes, such as aconitase, with solvent exposed Fe-S clusters and increases intracellular free Fe. Free Fe^{2+} participates in Fenton chemistry producing hydroxyl radicals, which damage DNA.

T. thermophilus displays a distinct gene expression pattern upon Hg(II) exposure relative to *E. coli*. In *T. thermophilus*, *sod*, *pcat*, *osmC* and *tlpA* transcripts were induced in response to Hg(II), but not *bcp* (Figure 3.1A). In *E. coli*, Hg(II) induces the expression of *sodB* and the peroxiredoxin *ahpC*, but not the catalase genes *katG* and *katE* (Onnis-Hayden *et al.*, 2009). The *T. thermophilus sod* is an ortholog of *sodA* that was repressed by short term Hg(II) exposure in *E. coli*. Similarly, the *T. thermophilus bcp* gene encodes

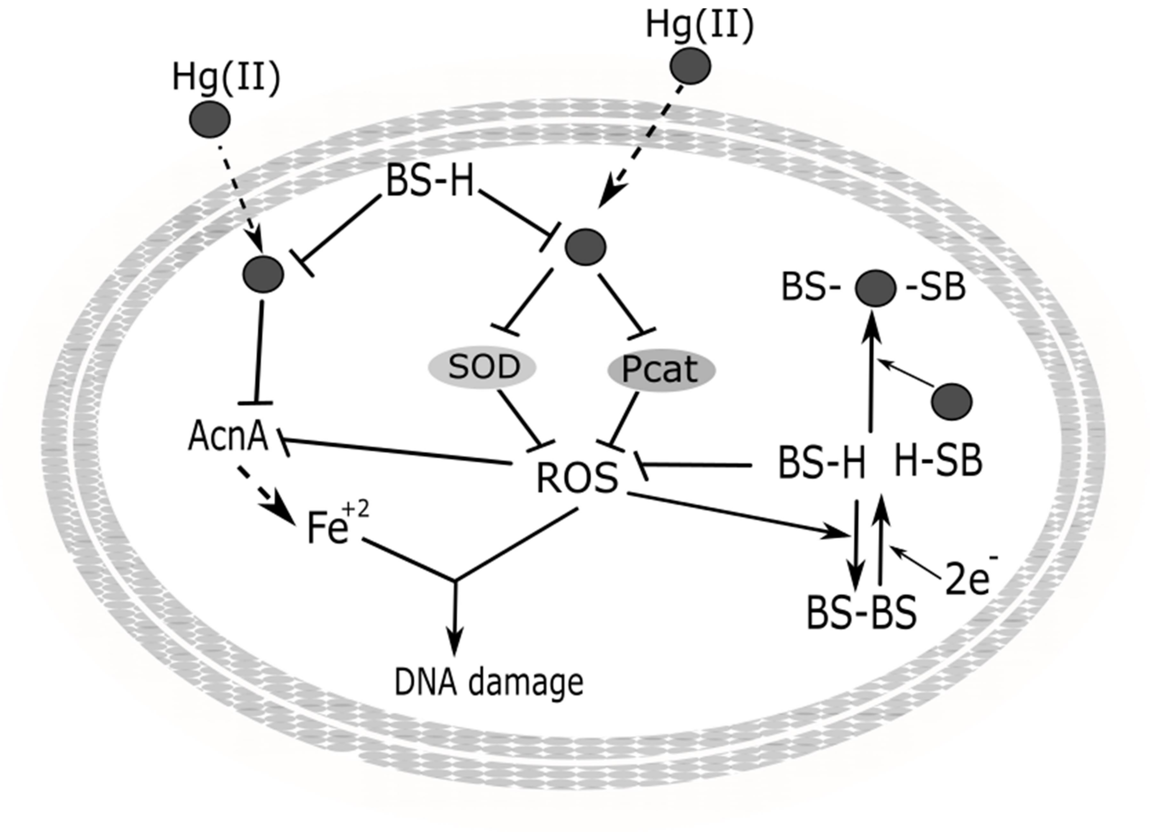

Figure 3.5. Working model for ROS generation by Hg(II). Exposure of *T. thermophilus* to Hg(II) results in the inactivation of two ROS detoxifying (SOD and Pcat) enzymes and ROS accumulation. Hg(II) decreases bioavailable reduced BSH, which is necessary to prevent Hg(II) intoxication. Strains lacking either Sod or Pcat have increased levels of oxidized BSH. Hg(II) accumulation inactivates enzymes, such as aconitase, with solvent exposed Fe-S clusters and increases intracellular free Fe. The free Fe^{2+} participates in Fenton and Haber-Weiss chemistry producing hydroxyl radicals and increasing total ROS, which damage DNA.

a homolog of *E. coli ahpC*, which is upregulated in *E. coli* while in *T. thermophilus bcp* is not responsive to Hg(II). This suggest that Hg(II) triggers different responses in these organisms suggesting diversity of responses to the oxidative stress that is elicited by exposure.

Hg(II) exposure quickly decreases the concentration of reduced BSH present in *T. thermophilus* (Norambuena *et al.*, 2018). We found that the Δ*sod* and Δ*pcat* strains had lower levels of reduced BSH (Figure 3.3A). Primary roles of LMW thiols are to maintain a reduced cytoplasm and detoxifying ROS or repairing proteins damaged by ROS. BSH is oxidized during these processes (Gaballa *et al.*, 2010, Loi *et al.*, 2015). This can explain why there is no difference in ROS between the ROS scavenging deficient strains and the WT strain under growth in absence of Hg(II), the excess of ROS in ROS scavenging deficient strains is buffered by BSH, oxidizing it resulting in lower pools of free BSH (Figure 3.3A). Free thiols are also critical in metal homeostasis and we contend that the effects of Hg(II) in *T. thermophilus* are largely due to disruption of metal, particularly Fe, homeostasis. Here we found that Hg(II) exposure increases free intracellular Fe in *T. thermophilus* (Figure 3.4C) as it does in *E. coli* (LaVoie *et al.*, 2015). Hg(II) exposure also decreased AcnA activity in vivo and in cell lysates (Figures 3.4A and B). Work by others found that Hg(II) inactivated fumarase A, a member of the same family than AcnA (Xu & Imlay, 2012). Any Fe that is released upon AcnA activation can then generate ROS which causes further Fe-S cluster damage (Lund *et al.*, 1991, Miller *et al.*, 1991, Ariza *et al.*, 1998, Ariza & Williams, 1999, Valko *et al.*, 2005) perpetuating AcnA damage. In *E. coli*, GSH is the main buffer for the Fe labile pool (Thorgersen & Downs, 2008, Hider & Kong, 2011). Here, we interpret our data to conclude that BSH may acts as Fe buffer in *T. thermophilus*. This is consistent with proposed *Staphylococcus aureus* where BSH has a role in the maturation of Fe-S proteins (Rosario-Cruz *et al.*, 2015).

This study reports on the effects of Hg(II) on *T. thermophilus*, which is part of the earliest aerobic bacterial lineages. We found that ROS detoxification is important for resistance to Hg(II); therefore, in *T. thermophilus*, resistance to Hg(II) is achieved through both *mer*-based detoxification (Wang *et al.*, 2009, Norambuena *et al.*, 2018) and the oxidative stress response. We previously argued that the *mer* system evolved in response to Earth oxygenation due to the increased availability of oxidized Hg species (Barkay *et al.*, 2010); likely, these same environmental changes led to the evolution by the oxidative stress response. While numerous reports have documented metal-induced oxidative stress (reviewed in Nies, 1999, Ercal *et al*., 2001, Hobman & Crossman, 2015), few examined how responses to this stress alleviate metal toxicity among prokaryotes. Our findings in *T. thermophilus* alert us to these hitherto little-studies aspect of metal homeostasis.

CONCLUDING REMARKS

Mercury, a highly toxic heavy metal, is widely spread in the environment. Microorganisms have developed ways to detoxify this metal, one among them is mediated by the functions of the *mer* operon. How this system is regulated has been well studied in the most evolved bacterial lineages like the proteobacteria, but not much information is available for early lineages like *Thermus*.

The *mer* operon and its regulation

In this study I found that *T. thermophilus* HB27 has an unusual *mer* operon, which includes a LMW thiol biosynthetic gene (*oah2*), as well as *merR* (regulator), a hypothetical protein, and *merA* (mercury reductase) genes. This operon has two promoters which are differentially regulated. The first promoter (P_{oah2}) is able to transcribe the whole operon in absence of Hg(II), but it does not transcribe much of *hp* and *merA* as it does of *oah2* and *merR* (Figure 4.1, shows only the expression of the first two genes, as they are the preferentially transcribed genes from this promoter). This is due to the second promoter, P_{mer}, which is located in *merR*, to which MerR can bind and repress the transcription of the *hp* and *merA* genes, allowing very low basal expression of these genes. When Hg(II) is present, MerR acts as an activator of transcription from P_{mer}, favoring transcription of *merA* from this promoter, allowing MerA expression and Hg(II) detoxification (Figure 4.1). The proximity of P_{mer} to *merA* might favor an efficient production of MerA; if transcription was only initiated from P_{oah2}, three other genes would have to be transcribed first. Thus, P_{mer} allows for a fast (7.5 min) expression of *merA* and a high fold induction. The presence of *oah2* in this operon favors the synthesis

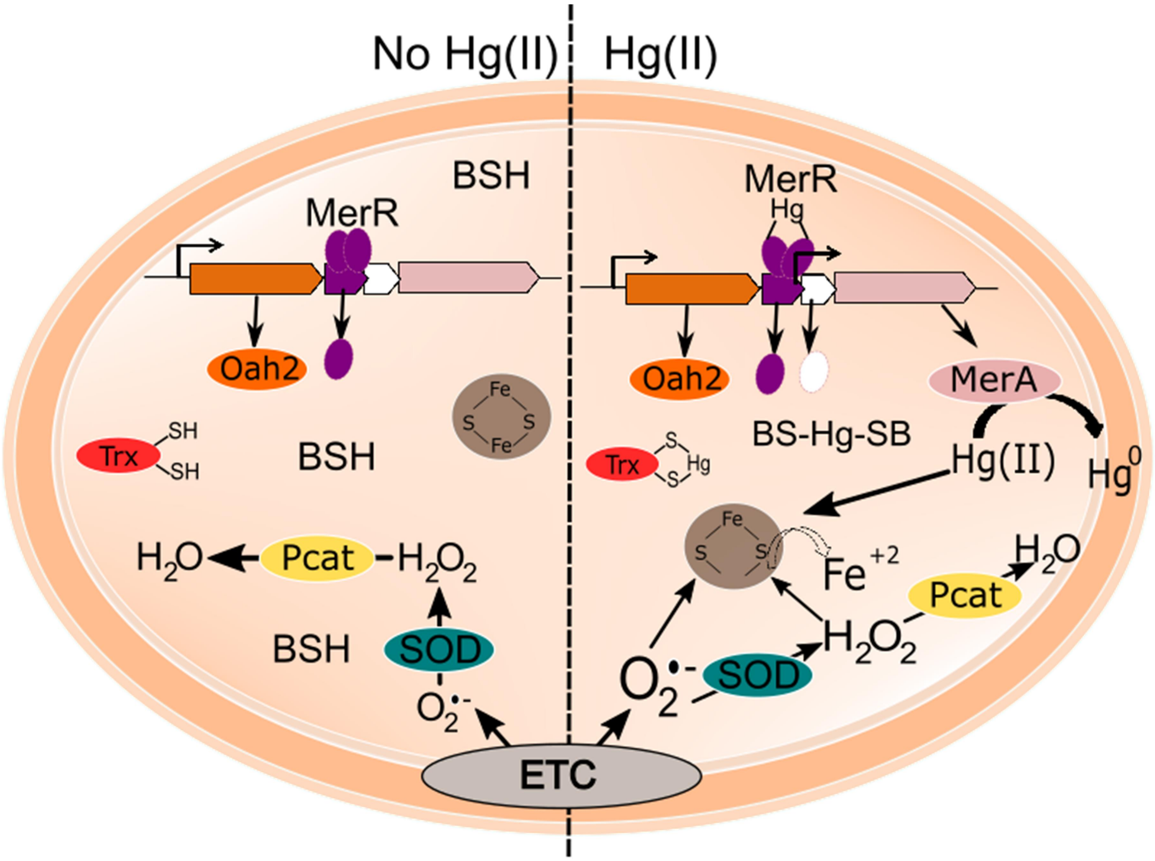
No Hg(II)
Hg(II)
BSH
MerR
Oah2
Fe
S
S
Fe
Trx
SH
SH
BSH
H_2O
Pcat
H_2O_2
BSH
SOD
$O_2^{\bullet-}$
ETC
MerR
Hg
Oah2
MerA
Trx
S
Hg
S
BS-Hg-SB
Hg(II)
Hg^0
Fe
S
S
Fe^{+2}
H_2O
Pcat
H_2O_2
$O_2^{\bullet-}$
SOD

Figure 4.1. Proposed mechanism of Hg(II) toxicity and detoxification in *T. thermophilus*. In absence of Hg(II) the *mer* operon partially produces Oah2 (orange) and MerR (purple) from the P_{oah2} promoter, MerR binds to the P_{mer} and represses the transcription of the hypothetical protein and *merA* (pink). Reactive oxygen species (ROS) are normally produced in the electron transport chain (ETC) and are quenched by bacillithiol (BSH), thioredoxins (not shown) or ROS-detoxifying enzymes like superoxide dismutase (SOD, green) or pseudocatalase (Pcat, yellow). When Hg(II) is present, it quickly oxidizes BSH; the depletion in reduced BSH, causes the accumulation of endogenous ROS, possibly damaging Fe-S containing proteins. The Hg(II) that is not buffered may release Fe from Fe-S clusters to damage Pcat and SOD (not shown), which helps to increase ROS. Mercury detoxification occurs following transcription of *merA* from P_{mer}.

of LMW-thiols that can act as a secondary Hg(II) buffer, helping the main LMW thiol, BSH.

It would be interesting to understand how P_{oah2} is regulated upon mercury exposure and other stresses. I observed that *oah2* and *merR* are fast induced and briefly present upon Hg(II) exposure. I propose that this is due to the Hg-induced transcription from P_{mer}, which causes the stabilization of the short transcript (*oah2-merR*) from P_{oah2}, decreasing the among of long transcripts from P_{oah2} (*oah2-merA*). It is also worth considering that P_{oah2} could possibly be subjected to regulation by levels of homocysteine, methionine or/and cysteine, due to its involvement in biosynthesis of thiol amino acids. This regulation might interfere with the expression of *merA* if the cell has high levels of methionine. If this is the case, P_{mer} ensures transcription of *merA* independent from the thiol amino acid content in the cell. How P_{oah2} is repressed by methionine it is not known, so understanding of this regulation could be of interest to further understand this peculiar *mer* operon.

The LMW thiols in Hg(II) resistance

In this work we also showed the importance of LMW-thiols biosynthesis systems, including those of BSH, cysteine and homocysteine, in alleviating Hg(II) toxicity. All of these LMW-thiol biosynthesis genes, except for *bshC*, were upregulated by Hg(II) exposure, which did not occur in *E. coli* cells. The Hg(II) dependent upregulation of these genes in *T. thermophilus* HB27 is an interesting mechanism to deal with Hg(II) toxicity; it provides the cell a higher capacity to buffer Hg(II), that may limit cellular damage until *merA* is expressed and Hg(II) is detoxified. As shown for other LMW-thiol redox buffer

(Latinwo *et al.*, 1998, Wang *et al.*, 2013), BSH is oxidized upon Hg(II) exposure (Figure 4.1), generalizing a role in Hg(II) by diverse LMW-thiol buffers. These data also provide an interesting insight to cellular responses triggered by metals in diverse organisms, making highlighting the need to understand toxic metal-microbe interactions in microbes that represent all branches of the prokaryotes. Such efforts can improve bioremediation techniques when organisms that are not *E. coli* are used.

ROS and Hg(II) resistance

One of the most interesting findings of this work is the high sensitivity of Δ*sod* strain to Hg(II). This is the first work to my knowledge that has shown such a strong dependence of Hg(II) resistance on the response to ROS. The Δ*sod* strain was as sensitive to Hg(II) as the Δ*merA* strain, where reduction of Hg(II) was abolished. The increase in ROS by Hg(II) can be triggered by different mechanisms like: direct inhibition of SOD and Pcat activities, increased release of Fe from Fe-S clusters containing proteins (Xu & Imlay, 2012) and ATPase damage (Wang & Horisberger, 1996, Omotayo *et al.*, 2011). Here I showed, by the double (Δ*bshA* Δ*pcat* or Δ*bshA* Δ*sod*) knock out strains that the main mechanism is the oxidation/quenching of BSH by Hg(II), leading to reduced BSH depletion (Figure 4.1). The low pool of reduced BSH likely increases accumulation of ROS, this ROS can led to Fe release from Fe-S clusters (Imlay, 2008). Thus, an amplification loop is caused by the released Fe which can catalyze ROS accumulation via Haber-Weiss reaction. This aspect of Hg(II) toxicity that has been known but not well understood for some time. This work provides another perspective to Hg(II), a none ROS-active metal, toxicity. When approaching bioremediation of Hg(II), ROS triggered by it should be taken into account and the engineering of strains with strong ROS detoxifying systems as well as efficient *mer* systems should be employed. In general, I propose that the study of metal toxicity and detoxification should be more holistic, rather than being focused on only one mechanism.

Finally, I think it is very interesting that ROS-related genes are upregulated upon short Hg(II) exposure (7.5 min). It was shown, only after 60 minutes of Hg(II) exposure ROS are produced; so, how are this genes upregulated so fast?. I propose that Hg(II) affects the regulators of genes involved in ROS; SoxR and OxyR are an Fe-S cluster and a thiol-base regulators, respectively. Mercury may activate OxyR by oxidizing its thiols and affect the state of SoxR's Fe-S clusters. Future research could focus on how Hg(II) affects transcription, an unexplored phenomenon that might answer and explain a how this metal affect microbial systems.

This dissertation provides a comprehensive study upon Hg(II) triggered responses in an early evolved lineage. Here the *mer* operon provides a direct link between LMW thiols and Hg(II) resistance genes, this LMW thiols, as protein thiols, are very important in Hg(II) resistance. BSH showed to be mainly responsible for the decrease in Hg(II) resistance in strains defective on ROS-detoxification mechanisms, integrating the Hg(II) responses in *T. thermophilus*.

APPENDIX A

Supplementary Material for Chapter 1

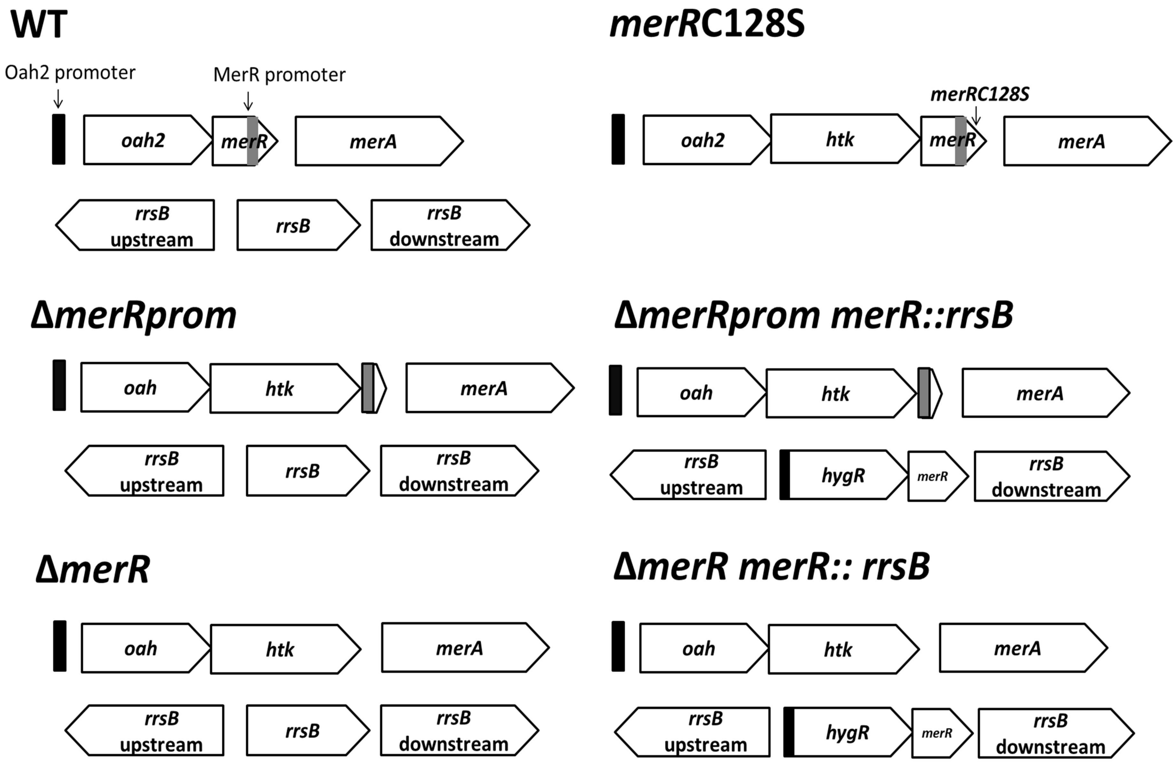
WT
Oah2 promoter
MerR promoter
oah2
merR
merA
rrsB upstream
rrsB
rrsB downstream
merRC128S
merRC128S
oah2
htk
merR
merA
ΔmerRprom
oah
htk
merA
rrsB upstream
rrsB
rrsB downstream
ΔmerRprom merR::rrsB
oah
htk
merA
rrsB upstream
hygR
merR
rrsB downstream
ΔmerR
oah
htk
merA
rrsB upstream
rrsB
rrsB downstream
ΔmerR merR:: rrsB
oah
htk
merA
rrsB upstream
hygR
merR
rrsB downstream

Figure 1.S1. Schematics of the *mer* operons and *rrsB* loci of the different strains used on Chapter 1. P_{oah2} is shown in black and P_{mer} is shown in grey. The WT is shown as reference for the 2 genomic regions used to construct the strains used in this work. The *merR*C128S strain has the same gene organization as the WT strain, except that the HTK resistance cassette was added to select the transformed strain. Δ*merRprom* strain conserved the P_{mer} but lacked the N-terminus of *merR*. The Δ*merR* strain lacks *merR*, including P_{mer}. The complemented strains (*merR::rrsB*) had *merR* expressed from its native promoter (P_{oah2}) cloned downstream from *hygR*, replacing *rrsB*. The hypothetical gene located between *merR* and *merA* (Fig. 1A) was omitted from the operon for simplification proposes.

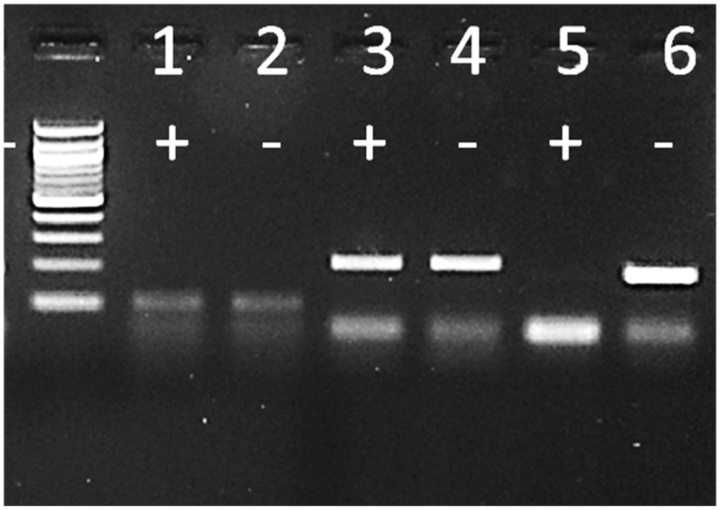

Figure 1.S2. Differential expression of *mer* operon's genes in response to Hg(II) exposure. Cells were exposed (+) or not (-) to 1 μM Hg(II) for 15 min before RNA extraction and cDNA synthesis. cDNA was synthesized using only the coding strand (reverse) primer (Table S1) for *oah2* (lines 1 and 2, PCR product of 104 bp), *merR* (lines 3 and 4, PCR product of 211 bp) and *merA* (lines 5 and 6, PCR product of 186 bp). cDNA was used as PCR template and PCR products were visualized in a 2 % agarose gel and 100bp ladder was used.

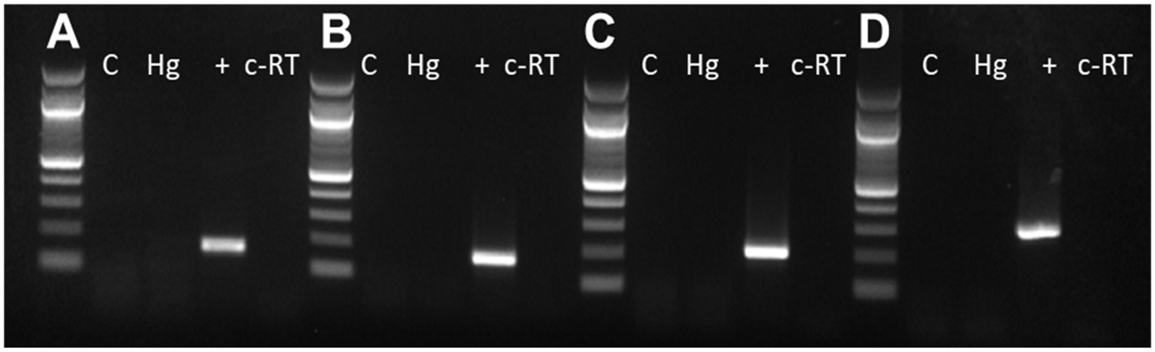

Figure 1.S3. Control reactions for gene junction PCR. Control reactions with primer sets targeting the junction between (A) *oah2* and *merR*, (B) *merR* and *hp*, (C) *merR* and *merA*, and (D) *hp* and *merA* (see Fig. 3B). RNA extracted from cells exposed (Hg) or not (C) to 1 μM Hg(II) for 15 min was used. + positive control (DNA from *T. thermophilus*); c-RT correspond to all components of the cDNA kit withouth RNA template. PCR products were visualized in a 2 % agarose gel and 100bp ladder was used.

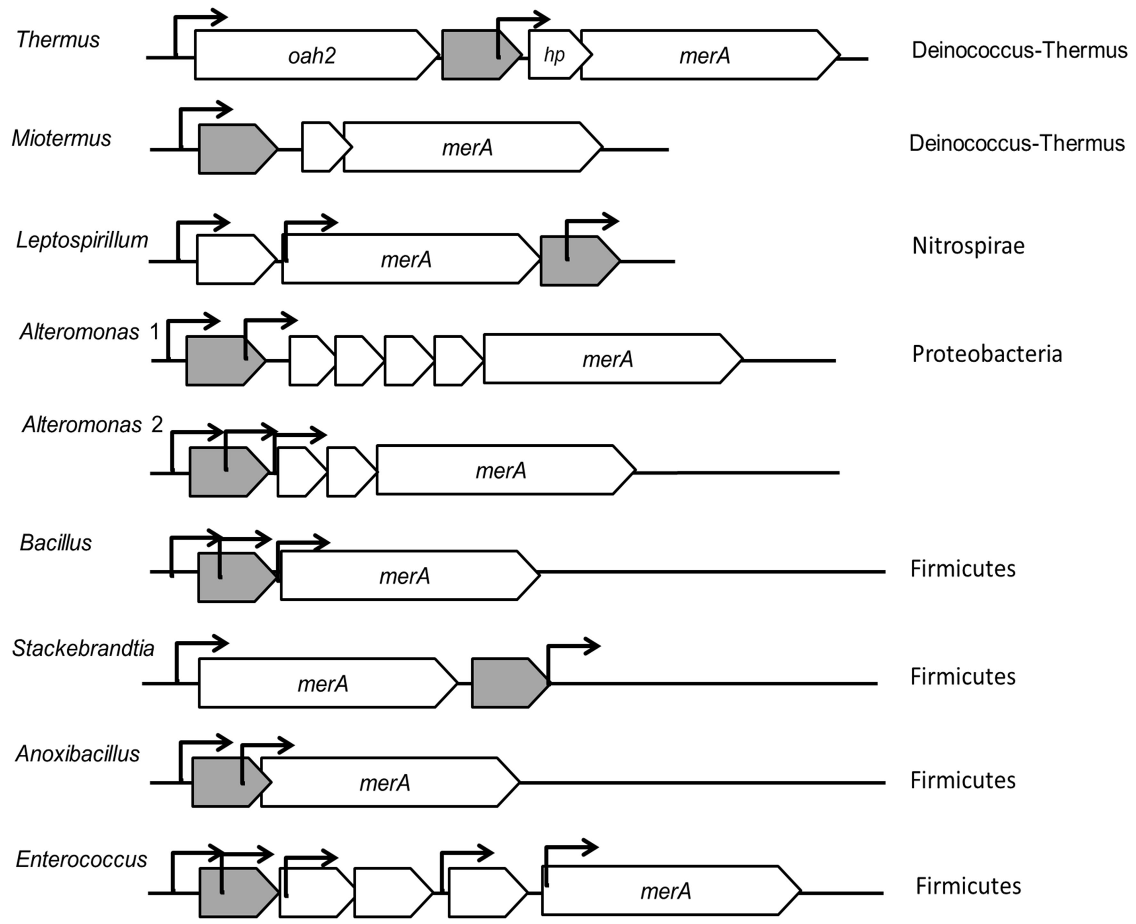
Thermus
oah2
hp
merA
Deinococcus-Thermus
Miotermus
merA
Deinococcus-Thermus
Leptospirillum
merA
Nitrospirae
Alteromonas 1
merA
Proteobacteria
Alteromonas 2
merA
Bacillus
merA
Firmicutes
Stackebrandtia
merA
Firmicutes
Anoxibacillus
merA
Firmicutes
Enterococcus
merA
Firmicutes

Figure 1.S4. Convergent *mer* operons possess multiple promoters. *mer* operons with convergent *merR*s were search in the JGI database. Genera are indicated on the left and phylum on the right. In grey *merR* is shown, frames that are found in white represent genes other than *merA*, arrows indicate possible promoter determined by BPROM.

Table 1.S1 Primers used on Chapter 1

Primer	Sequence	T (°C)	Source
gyrase-F	GGGCGAGGTCATGGGC	61	Norambuena et al
gyrase-R	CGCCGTCTATGGAGCCG		
oah2-F3	GAGCTCTGGCGGAACTAC	56	Norambuena et al
oah2-R3	AAGGTGCGGACCCTTTC		
merR4-F	AGCTTGAGGACATCGCCTGGAT	61	Norambuena et al
merR4-R	TCCAAATAGACGCAGCGGTCCC		
merA for	GCCTTCAAGATCGTGGTGGACGAAGAG	62	Wang et al.
merA rev	CCTGGGCCACGAGCCTTATCC		
oah2 seq rev 5’ RACE outer	CTCCTCCTTGAGGCGGCTG	58	This study
oah2 seq rev 5’ RACE inner	GTGGCGAAGCGCTCCTGGC	58	This study
merA seq rev 5’ RACE outer	ACCTCCTGGTACTTCTCCTTCCTGAGG	58	This study
merA seq rev 5’ RACE inner	GAGCCCACGATGAGGAGGTCGTAG	60	This study
5' RACE Adapter	GCUGAUGGCGAUGAAUGAACACUGCGUUUGCUGGCUUUGAUGAAA	-	FirstChoice® RLM-RACE Kit
5' RACE inner primer	GAACACTGCGTTTGCTGGCTTTGATG	-	FirstChoice® RLM-RACE Kit
5' RACE outer primer	GCTGATGGCGATGAATGAACACTG	-	FirstChoice® RLM-RACE Kit
3' RACE Adapter	GCGAGCACAGAATTAATACGACTCACTATAGGTTTTTTTTTTTTVN	-	FirstChoice® RLM-RACE Kit
3' RACE Outer Primer	GCGAGCACAGAATTAATACGACT	-	FirstChoice® RLM-RACE Kit
3' RACE Inner Primer	CGCGGATCCGAATTAATACGACTCACTATAGG	-	FirstChoice®

			RLM-RACE Kit
Oah2 1216 for	GTGACCCCGGGGCTCGTGC	60	This study
merR 1406 rev	TTCGTAGTAGCGGAGGGCATCAGGA	60	This study
Hp 1859 for	GAGAAGGCGTGGATGGGCTACC	60	This study
Hp 1881 rev	GGTAGCCCATCCACGCCTTCTC	60	This study
merR 1712 for	GACCGCTGCGTCTATTTGGACCCC	60	This study
merA 1923 rev	GAGCCCACGATGAGGAGGTCGTAG	60	This study
merA 2193 rev	ACCTCCTGGTACTTCTCCTTCCTGAGG	60	This study

Table 1.S2 Primers used for knockout construction on Chapter 1

Strain	Primer	Sequence[1]	Target
Δ*merR*	1 PstI mer 1915F	CTGAGGGTTCTGCAGATGAGCGAGACCG	*merR* upstream
	mer 2331R	CGATGGTGTAGGGCATCTAGACCGCCT	
	A htk merR F	CGTCGACTAGTCTAGATGAAAGGAC	HTK
	B HTK merR rev	CAATTATTAGAGGTGCATGCTCAAAATGGTATGC	
	F mer 2717F	GACCCTGGAGCACGCTCCGCATGCTAGCCTGGGGGCAT	*merR* *d*ownstream
	4 EcoRI mer 3026R	GGAGGTACTTGGAATTCACGCACCCCACGTTGACG	
Δ*merRprom*	A oah2 htk for	CTGGAGGCGGTCTAGATGAAAGGACCAAT	HTK
	B merR prom	TCAAGGGGGTCCTCAAAATGGTATGCGT	
	1 oah2 ecoR1 for	GCTTCCCCGAATTCG TCC GCA	*merR prom* upstream
	E HTK oah2 rev	ATTGGTCCTTTCATCTAGACCGCCTCCAG	
	F2 merR prom	ACGCATACCATTTTGAGGACCCCCTTGACCCTGGA	*merR prom* downstream
	4.2 hindIII merRpheS	GTCCAGGAAGCTTGCCCTCC	
*merR*C128S	A HTK merR FLAG	GAGGCGGTCTAGATGAAAGGACCAATAATAATGAC	HTK
	B HTK merR FLAG	GATGGTGTAGGGCATTCAAAATGGTATGCGTTTTGACACATC	
	F2 HTK merR FLAG	GCATACCATTTTGAATGCCCTACACCATCGG	*merR*C128
	C128S rev	GTCCAAATAGACGCTGCGGTCC	
	C128S for	GACCGCAGCGTCTATTTGGACC	*merR*C128 - *merA*
	4 HTK merR FLAG	CCGGTGGAATTCGTCGG	
	P1 pstI oah2	CCAGTTTCTGCAGCCCGACC	*oah2*
	E merRflag HTK	ATTGGTCCTTTCATCTAGACCGCCTCCAGG	
	A hygB for	GACTAGGGGGTATGAAAAAGCCTGAACTCACC	HygB
	B hygB rev	GGTGTAGGGCATCTATTCCTTTGCCCTCG	
	merR prom for D	CATCTTGaGCGGCAAGGATCAGCTTC	*merR* promoter

merR::rrsB	merR prom rev C	GGCTTTTTCATACCCCCTAGTCTAGCGAAAAAC	
	merR for 7	GCAAAGGAATAGATGCCCTACACCATCGGC	*merR*
	merR rev 8.2	CGCGGCCTCTCTAGACCCTGGAGCGTGCT	
	1.2 ecori Hp 16S for	GTCCGGGGGGAATTCGAGGAGC	*16S* upstream
	E.2 16S rev	ATCCTTGCCGCtCAAGATGGGGGCATGGAC	
	p4 pyrF Pst1rev	CACCCGGCTGCAGGGACCCTC	*16S* downstream
	F 16S downstream for	TCCAGGGTCTAGAGAGGCCGCGCAC	

[1] Underlined sequences indicate restriction enzyme cutting sites.

APPENDIX B

Supplementary Material for Chapter 2

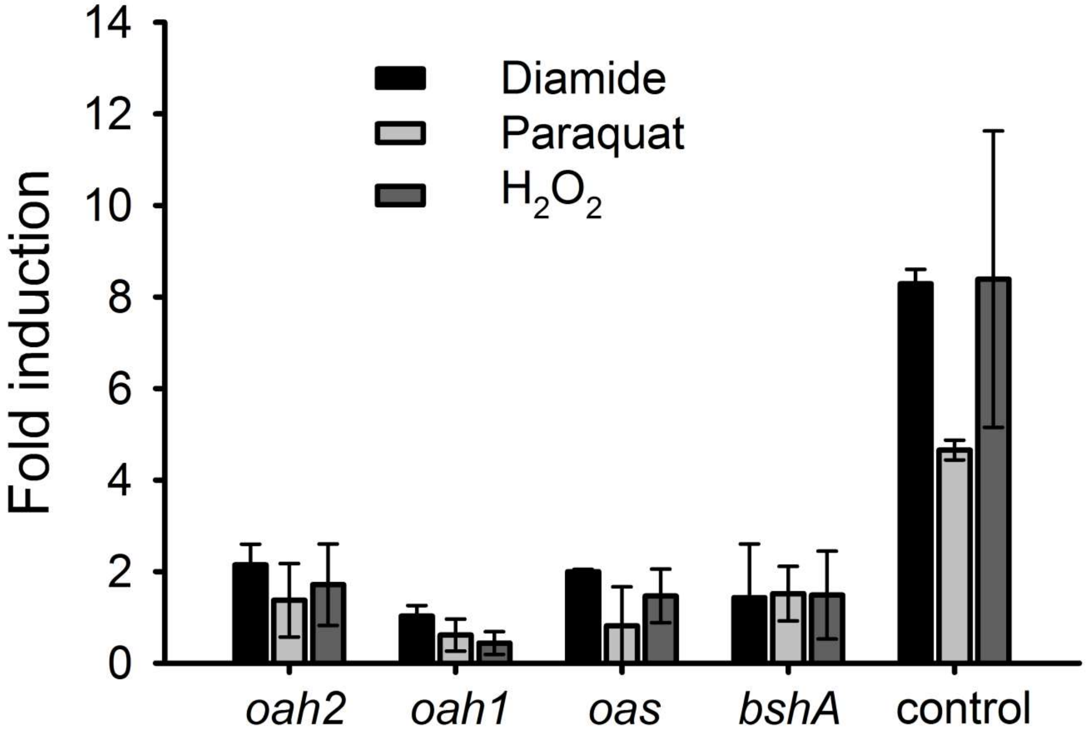

Figure 2.S1. LMW thiol biosynthesis genes are not induced by ROS or disulfide stress. Gene expression of different LMW thiol biosynthesis genes were evaluated in WT at 7.5 minutes after exposure to either 4 mM diamide, 160 µM paraquat, or 1 mM hydrogen peroxide (H_2O_2). Transcript abundance was normalized to *gyrA*. Thioredoxin A1 was included as a control for diamide treatment and superoxide dismutase (TT_RS00960) was used as a positive control for paraquat and hydrogen peroxide stress. Averages and standard deviations represent triplicate samples from three independent trials.

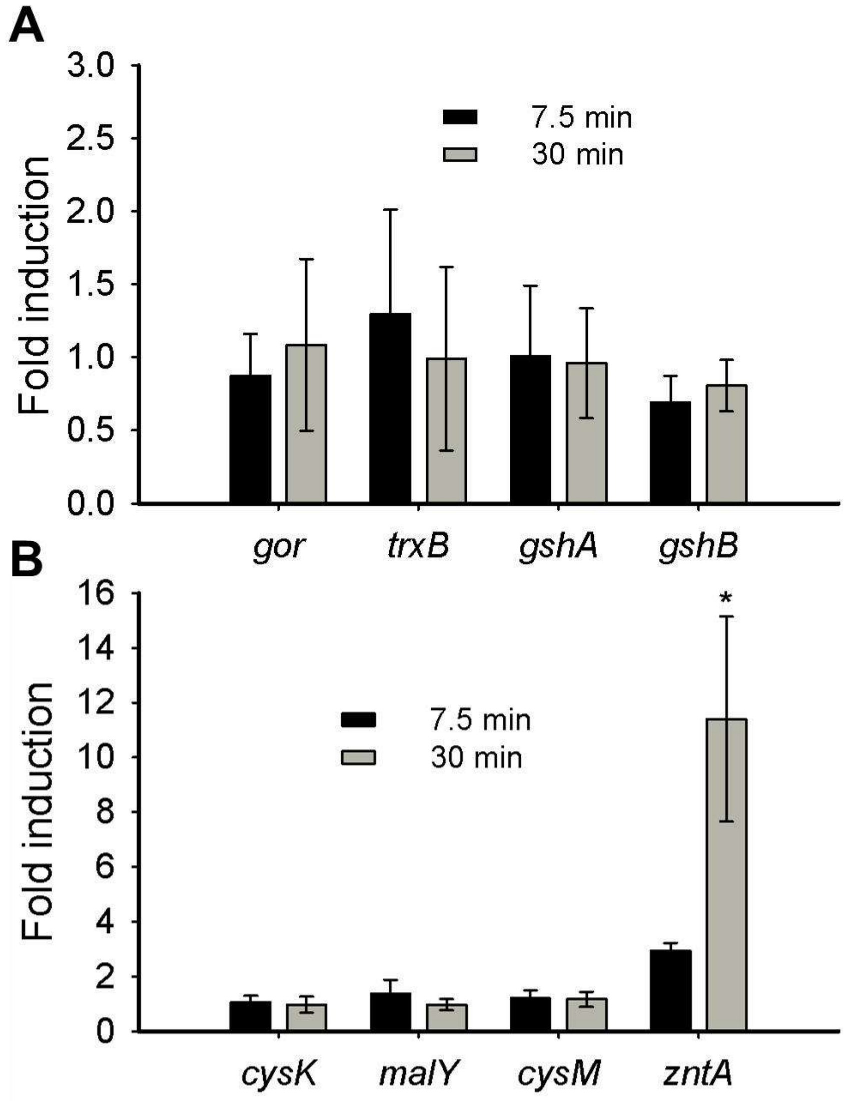

Figure 2.S2. Thiol related genes are not induced by Hg(II) in *E. coli*. Gene expression of (A) thioredoxin and glutathione systems and (B) cysteine and homocysteine biosynthesis genes were evaluated in *E. coli* at 7.5 or 30 minutes after exposure to 2 μM Hg(II). RNA abundance was normalized to *ssrA* transcripts (Onnis-Hayden *et al.*, 2009). *zntA* (Ga0175964_11254) was used as positive control (Babai and Ron, 1998). Averages and standard deviations represent triplicate samples from three independent trials. t-test * P<0.009.

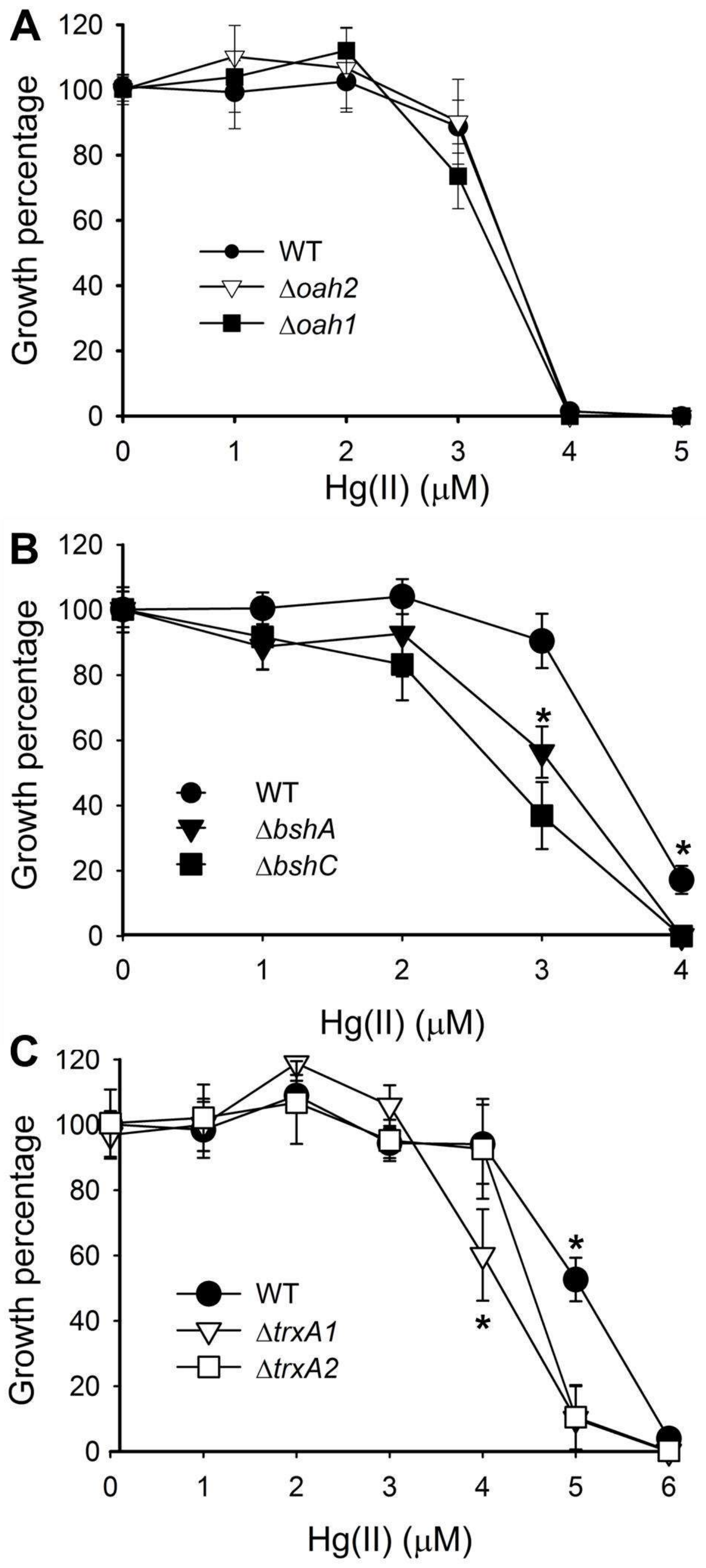

Figure 2.S3. Resistance to Hg(II) in complex medium. Mercury tolerance was compared to that of the wild type strain after 18 hours of growth for (A) *oah* mutants and (B) *bsh* mutants, and after 20 hours of growth for (C) *trx* mutants. The culture optical density (A_{600}) at 0 μM of Hg(II) was considered 100% growth. Averages and standard deviations are from three independent trials. One way ANOVA, followed by a Tukey test, *P <0.001.

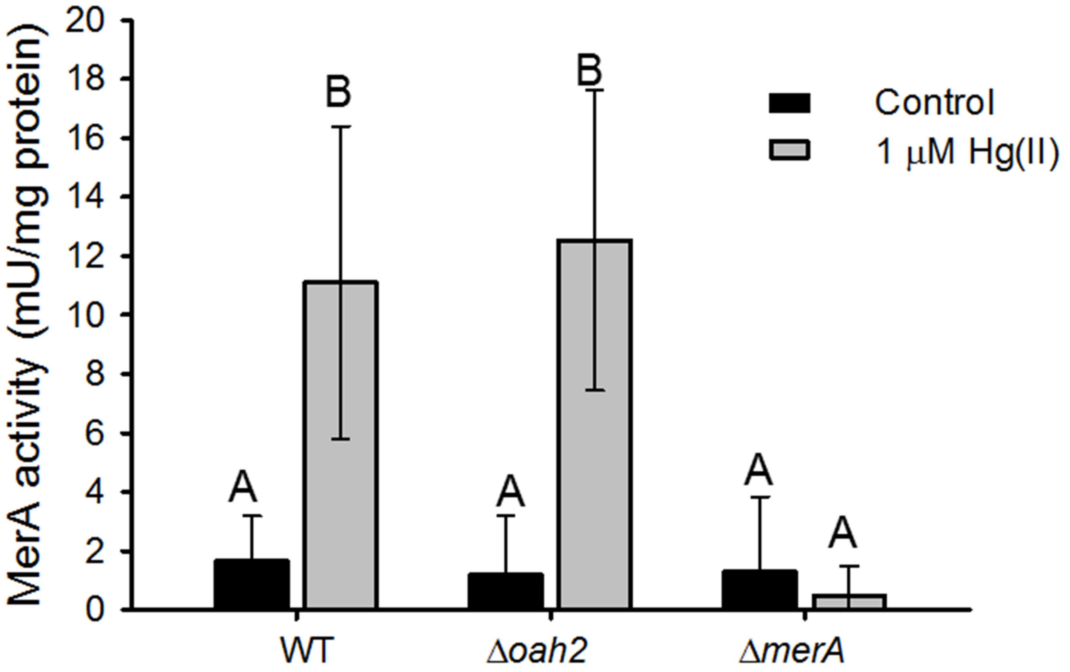

Figure 2.S4. MerA activity is not affected by exposure to Hg(II) in the Δ*oah2* strain. MerA activity was monitored in crude cell extracts of various strains after exposure to 1 μM Hg(II) (gray) or not (black) for 30 minutes in complex medium. One unit of MerA activity was defined as the Hg-dependent oxidation of 1 μmol of NADH per minute. One-way ANOVA followed by a Tukey test analysis was performed on the data; letters indicate statistical differences between groups ($P<0.05$). Averages and standard deviations represent triplicate samples from three independent trials.

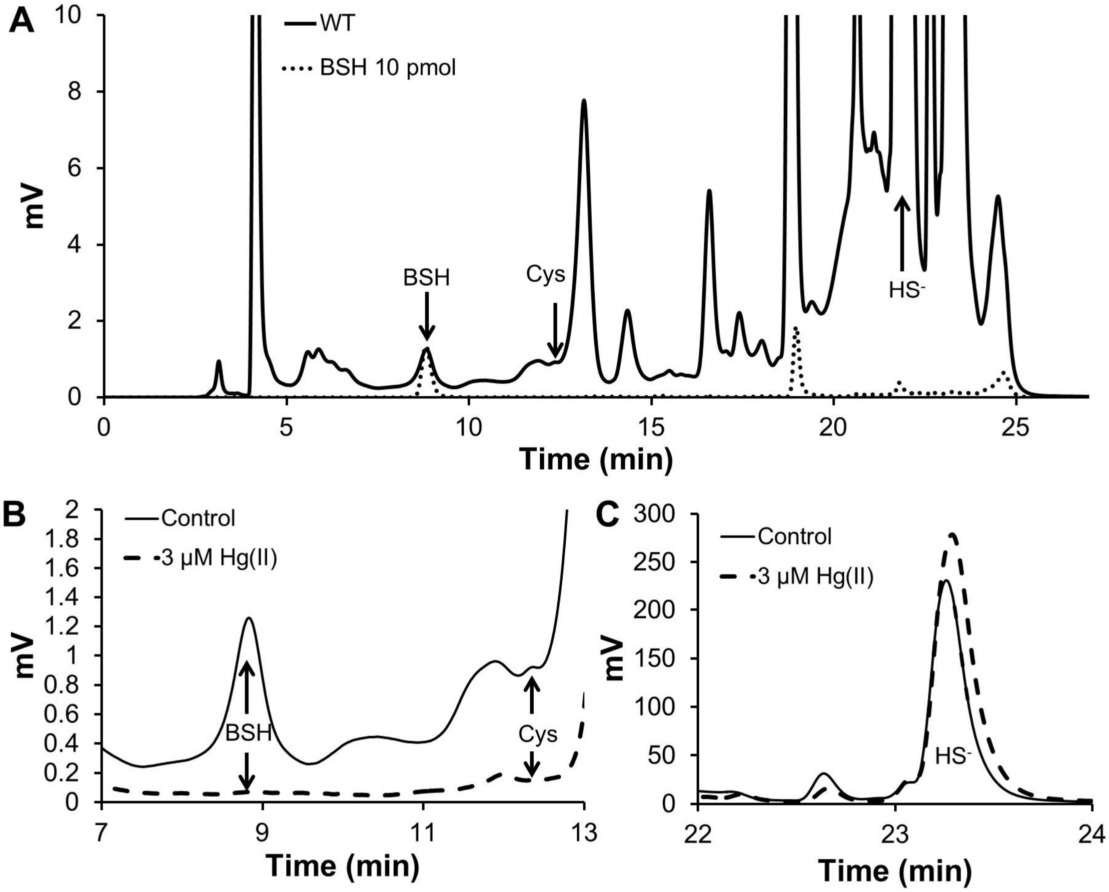

Figure 2.S5. HPLC chromatograms of small thiol pools in *T. thermophilus*. (A) Extended HPLC chromatogram of *T. thermophilus's* thiol-pool (filled line) and BSH standard (dotted line). Thiol pools of interest are indicated by arrows. Magnifications of the (B) BSH and Cys pools and (C) sulfide pool are shown in cultures exposed (broken lines) or not (filled line) to 3 μM Hg(II). The WT strain was grown to optical density (A_{600}) of 0.4 and then exposed to Hg(II) for one hour. Concentrations of small-thiols were measured by the mBrB method and thiols were quantified by HPLC analysis. One representative chromatogram of all experiments is shown.

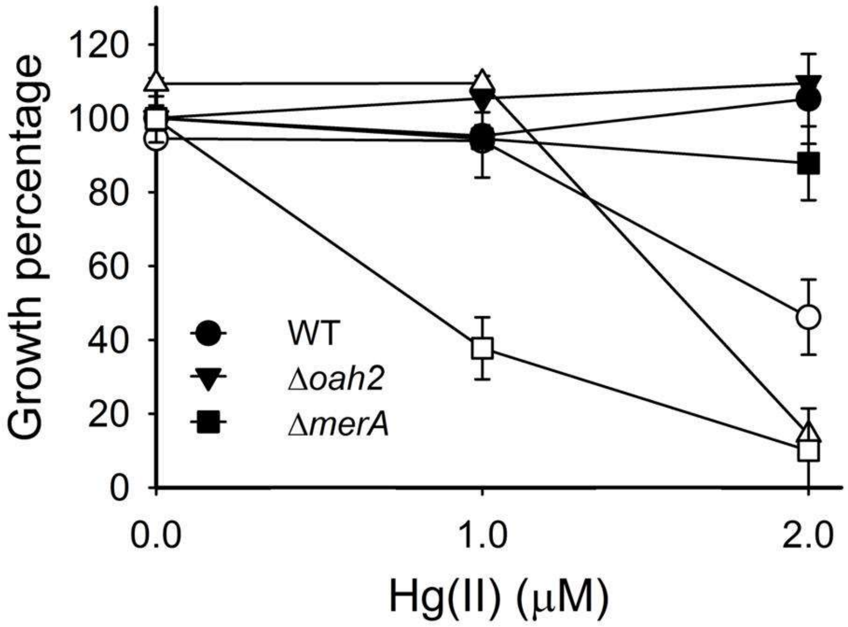

Figure 2.S6. Effect of diamide on Hg(II) toxicity. Cells were exposed (empty symbols) or not (filled symbols) to 1 mM diamide. Growth was evaluated after 16 hours. Culture optical densities (A_{600}) at 0 μM of Hg(II) in complex medium was considered 100% growth. Averages and standard deviations are from at least 5 independent trials.

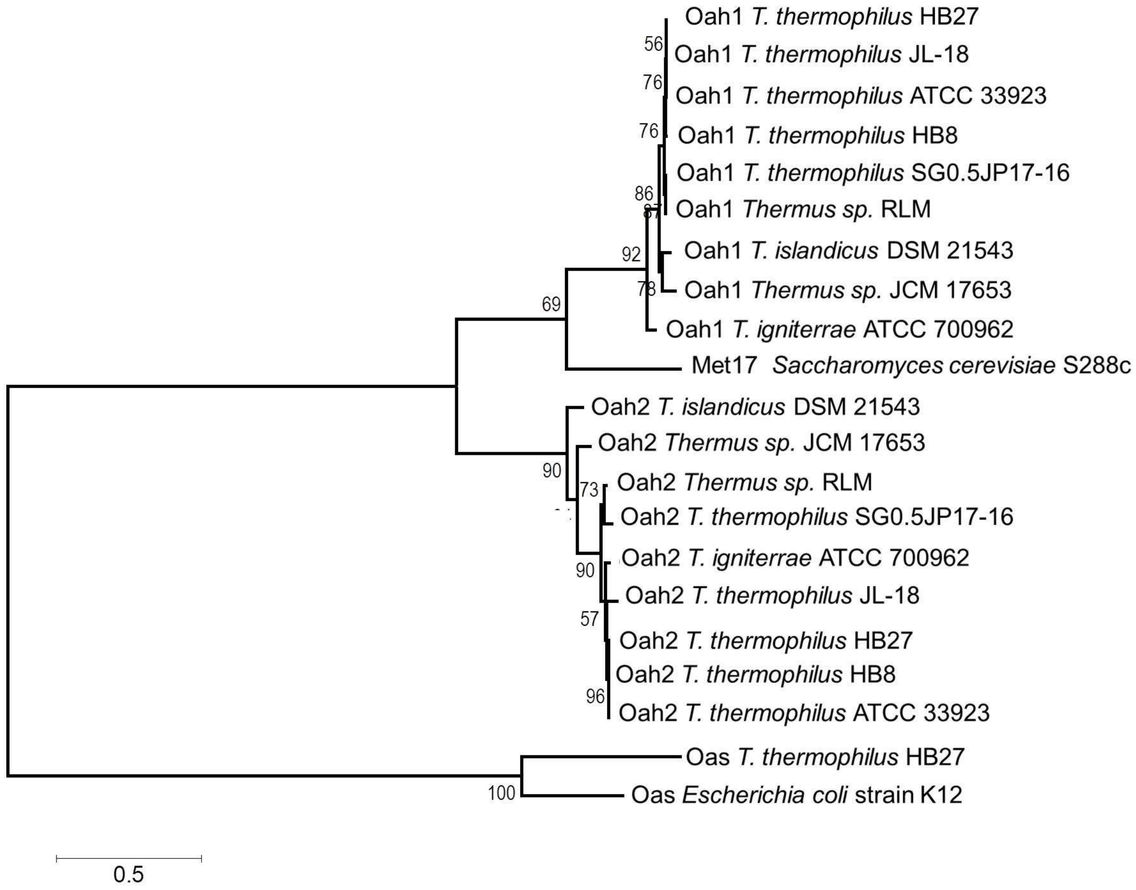
Oah1 T. thermophilus HB27
56
Oah1 T. thermophilus JL-18
76
Oah1 T. thermophilus ATCC 33923
76
Oah1 T. thermophilus HB8
Oah1 T. thermophilus SG0.5JP17-16
86
87
Oah1 Thermus sp. RLM
92
Oah1 T. islandicus DSM 21543
78
Oah1 Thermus sp. JCM 17653
69
Oah1 T. igniterrae ATCC 700962
Met17 Saccharomyces cerevisiae S288c
Oah2 T. islandicus DSM 21543
Oah2 Thermus sp. JCM 17653
90
73
Oah2 Thermus sp. RLM
Oah2 T. thermophilus SG0.5JP17-16
90
Oah2 T. igniterrae ATCC 700962
Oah2 T. thermophilus JL-18
57
Oah2 T. thermophilus HB27
Oah2 T. thermophilus HB8
96
Oah2 T. thermophilus ATCC 33923
Oas T. thermophilus HB27
100
Oas Escherichia coli strain K12
0.5

Figure 2.S7. Molecular Phylogeny of Oah proteins in different *Thermus* spp. by the Maximum Likelihood method. The tree was constructed with Oah2 encoded in the *mer* operon and Oah1 encoded in the *met* operon of *Thermus* spp. The outgroup used was the Oas (CysK) protein. The tree with the highest log likelihood (-3752.97) is shown. The tree is drawn to scale, with branch lengths measured as the number of substitutions per site. Numbers next to bifurcation points indicate bootstrapping values. Oah protein IDs or locus tags are found in table S6. Other proteins locus tags: *T. thermophilus* Oas (WP_011174005), *E. coli* Oas (WP_053885459) and *S. cerevisiae* Met17 (NP_013406).

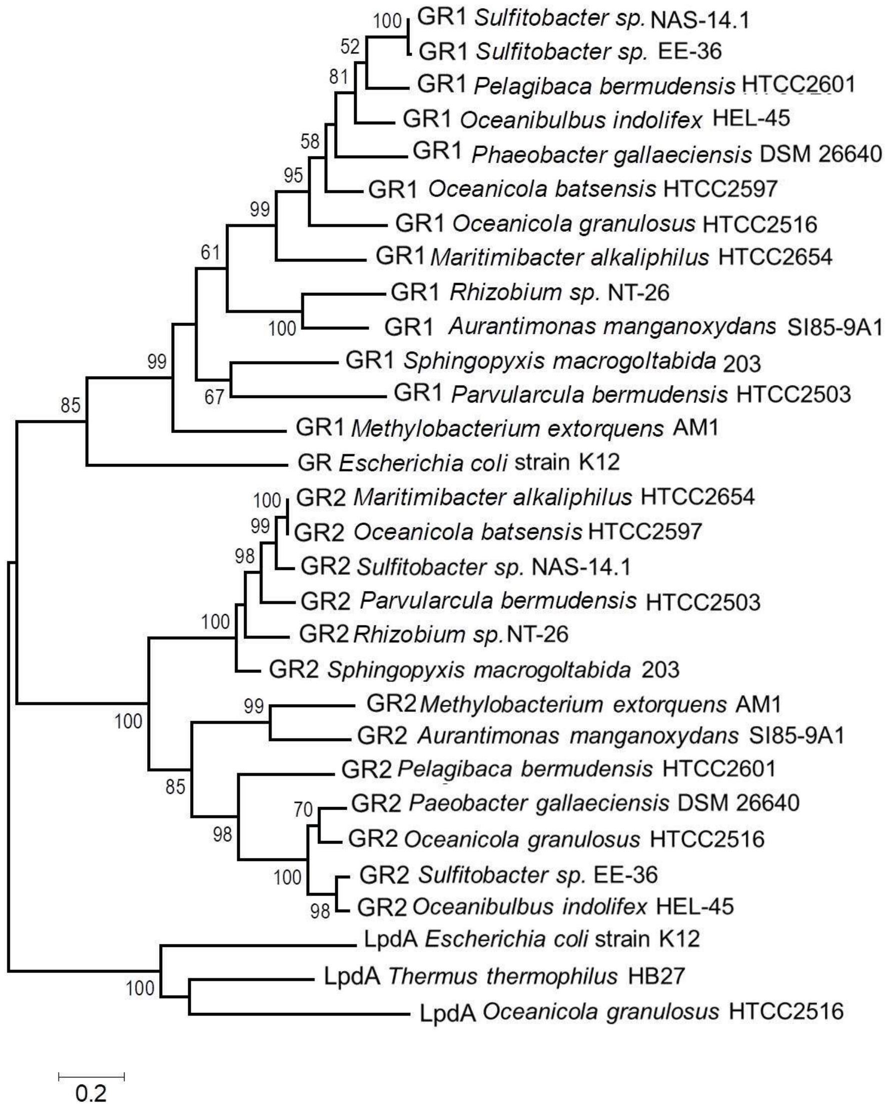
100
GR1 Sulfitobacter sp. NAS-14.1
52
GR1 Sulfitobacter sp. EE-36
81
GR1 Pelagibaca bermudensis HTCC2601
GR1 Oceanibulbus indolifex HEL-45
58
GR1 Phaeobacter gallaeciensis DSM 26640
95
GR1 Oceanicola batsensis HTCC2597
99
GR1 Oceanicola granulosus HTCC2516
61
GR1 Maritimibacter alkaliphilus HTCC2654
GR1 Rhizobium sp. NT-26
100
GR1 Aurantimonas manganoxydans SI85-9A1
99
GR1 Sphingopyxis macrogoltabida 203
67
GR1 Parvularcula bermudensis HTCC2503
85
GR1 Methylobacterium extorquens AM1
GR Escherichia coli strain K12
100
GR2 Maritimibacter alkaliphilus HTCC2654
99
GR2 Oceanicola batsensis HTCC2597
98
GR2 Sulfitobacter sp. NAS-14.1
GR2 Parvularcula bermudensis HTCC2503
100
GR2 Rhizobium sp. NT-26
GR2 Sphingopyxis macrogoltabida 203
99
GR2 Methylobacterium extorquens AM1
100
GR2 Aurantimonas manganoxydans SI85-9A1
GR2 Pelagibaca bermudensis HTCC2601
85
70
GR2 Paeobacter gallaeciensis DSM 26640
98
GR2 Oceanicola granulosus HTCC2516
100
GR2 Sulfitobacter sp. EE-36
98
GR2 Oceanibulbus indolifex HEL-45
LpdA Escherichia coli strain K12
LpdA Thermus thermophilus HB27
100
LpdA Oceanicola granulosus HTCC2516
0.2

Figure 2.S8. Molecular phylogeny of GR proteins from Alphaproteobacteria obtained by the Maximum Likelihood method. The GR proteins encoded in the Alphaprotobacteria genomes were *mer*-operons associated (GR2) or non-*mer*-related (GR1). The tree with the highest log likelihood (-12590.30) is shown. Numbers at bifurcation points indicate bootstrapping. For protein IDs go to table S7. Outgroups protein IDs: *E. coli* LpdA (P0A9P0.2), *O. granulosus* LpdA (ZP_01155676), *T. thermophilus* LpdA (YP_005722) and *E. coli* GR (P06715).

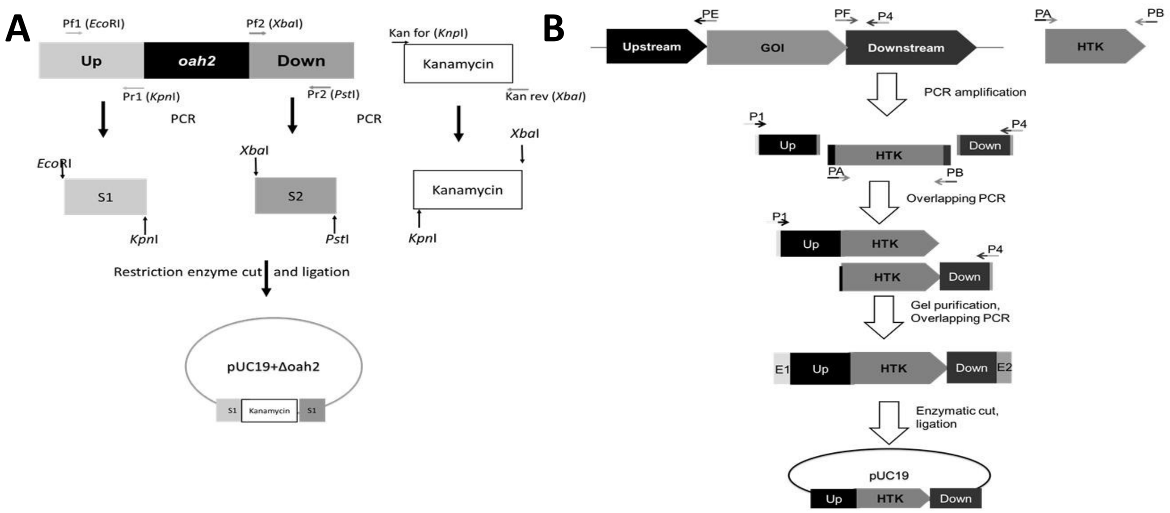
A
Pf1 (EcoRI)
Pf2 (XbaI)
Up
oah2
Down
Pr1 (KpnI)
Pr2 (PstI)
PCR
PCR
EcoRI
XbaI
S1
S2
KpnI
PstI
Kan for (KnpI)
Kanamycin
Kan rev (XbaI)
XbaI
Kanamycin
KpnI
Restriction enzyme cut and ligation
pUC19+Δoah2
S1
Kanamycin
S1
B
PE
PF
P4
PA
PB
Upstream
GOI
Downstream
HTK
PCR amplification
P1
P4
Up
HTK
Down
PA
PB
Overlapping PCR
P1
Up
HTK
P4
HTK
Down
Gel purification, Overlapping PCR
E1
Up
HTK
Down
E2
Enzymatic cut, ligation
pUC19
Up
HTK
Down

Figure 2.S9. Construction of HB27 knockout strains. (A) The Δ*oah2* strain was constructed by ligation of 3 digested PCR products (upstream flanking region, kanamycin resistance cassette [HTK] and downstream flanking region) into pUC19. (B) Fusion PCR strategy was used to construct all other knockout strains. Three PCR products were amplified (upstream flanking region, HTK cassette and downstream flanking region), primers A, B, E and F contained sequences homologous to those adjacent to the gene of interest (GOI); these homologous regions were used for the fusion PCR. Then, two consecutive PCR reactions were performed to fuse the flanking sequences of the GOI to the HTK gene; the upstream region was fused using primers P1 and PB, and the downstream region with primers PA and P4 (See table 1 for primer sequences). These two fusion fragments 1B and A4, were then fused in a final PCR, gel purified and digested with specific restriction enzymes (E1 and E2). Finally, the fused PCR product (fragment 14) was ligated into pUC19. The recombinant pUC19-derived plasmids were used to transform the HB27 WT to create knockout mutants (see main text).

Table 2.S1. *gyrA* Ct values obtained in qPCR experiments for the WT strain of *T. thermophilus* HB27

Sample[1]	Avg Ct	Time
Control 1	23.6	7.5 min
Control 2	24.3	
Control 3	25.7	
Control 4	24.3	
Hg 1	25.6	
Hg 2	24.9	
Hg 3	24.3	
Hg 4	25.4	
Control 1	24.9	15 min
Control 2	27.4	
Control 3	26	
Control 4	25.7	
Hg 1	25.2	
Hg 2	25.3	
Hg 3	26.1	
Hg 4	26.7	
Control 1	21.2	30 min
Control 2	22.9	
Control 3	24.9	
Control 4	23.9	
Hg 1	22	
Hg 2	23.7	
Hg 3	22.9	
Hg 4	22.0	

[1] Control: No Hg(II) exposure; Hg: exposure to 1 μM Hg(II) for the time indicated in the third column. The number following the sample name refers to the individual library examined.

Table 2.S2. Fold induction of *trx* genes in *T. thermophilus* HB27 at different times after exposure to 1 μM Hg(II).

Gene	**Time post exposure**	
	7.5 min	30 min
trxA1	14.5± 2.9	11.1± 3.0
trxA2	4.9± 0.8	6.2± 2.0
TrxB	7.5± 2.6	6.9± 1.2

Table 2.S3. Concentrations of LMW thiols and effect of exposure to Hg(II) in *T. thermophilus* HB27 and in some of its mutants[1].

	BSH	**Cysteine**	**sulfide-major**
	(nmol/g cell dry weight)		
WT	27.1 ± 8.5	6.1 ± 3.1	324 ± 88
WT 1 μM Hg(II)	0.6 ± 1	N.D.	230 ± 151
WT 3 μM Hg(II)	N.D.	N.D.	251 ± 61
Δ*merA*	56.7 ± 2	8.6 ± 0.3	111± 19
Δ*merA* 1 μM Hg(II)	N.D.	N.D.	251 ± 28
Δ*oah2*	26.2 ± 9	6.1 ± 1.4	337 ± 73
Δ*oah1*	27.0 ± 1.5	4.8± 2.7	410 ± 73
Δ*bshA*	N.D.	N.D.	473 ± 60
Δ*bshC*	N.D.	N.D.	440 ± 107

[1] Cells were exposed to the indicated concentrations of Hg(II) for 60 minutes.

N.D. signifies not detected.

Table 2.S4. Structure of *mer* operons in Deinococcus-Thermus.

Organism	***mer* operon structure**[1]
Thermus thermophilus JL-18	***oah2***,R,H,A
Thermus parvatiensis RLM	***oah2***,R,H,A
Thermus igniterrae ATCC 700962	***oah2***,R,H,A
Thermus thermophilus ATCC 33923	***oah2***,R,H,A
Thermus sp. JCM 17653	***oah2***,R,H,*copZ*[2],A
Thermus thermophilus HB8	***oah2***,R,H,A
Thermus islandicus DSM 21543	***oah2***,R,*copZ*,A
Thermus thermophilus SG0.5JP17-16	***oah2***,R,H,A
Marinithermus hydrothermalis T1, DSM 14884	R,*copZ*,A
Meiothermus silvanus VI-R2, DSM 9946	R,*copZ*,A
Meiothermus chliarophilus ALT-8, DSM 9957	(2H),R,A
Oceanithermus profundus 506, DSM 14977	H,R,A
Deinococcus sp. YIM 77859	R,*copZ*,A,B,B,E

[1] Letters relate to various *mer* genes with H indicating hypothetical genes. The order of genes represent their position in the *mer* operon. Identified ORF's other than *mer* genes are spelled out as annotated by https://img.jgi.doe.gov/cgi-bin/mer/main.cgi?section=FindGenesBlast&page=geneSearchBlast.

[2] *copZ* encodes for a copper transport and sequestration.

Table 2.S5. Alphaproteobacterial *mer* operons containing *gor*, the gene encoding for glutathione reductase (GR)

Organism	**Order**	***mer* operon structure**[1]
Phaeobacter gallaeciensis DSM 26640	Rhodobacterales	R(divergent),T,CopZ,F,A,H,**GR**
Maritimibacter alkaliphilus HTCC2654	Rhodobacterales	R(divergent),T,(3xH),**GR**,A
Oceanibulbus indolifex HEL-45	Rhodobacterales	R(Divergent),T,P,H,A,H,**GR**
Oceanicola batsensis HTCC2597	Rhodobacterales	R(divergent),T,P,(2xH), **GR**,A
Oceanicola granulosus HTCC2516	Rhodobacterales	R(divergent),T,(2xH),A,H,**GR**
Pelagibaca bermudensis HTCC2601	Rhodobacterales	R(divergent),T,P,transport,H,A,**GR,** EmrE[2]
Sulfitobacter sp. EE-36	Rhodobacterales	R(divergent),T,P,H,A,H,**GR**
Sulfitobacter sp. NAS-14.1	Rhodobacterales	R(divergent),T,P,H,**GR**,A
Parvularcula bermudensis HTCC2503	Parvularculales	R(divergent),T,P,F,**GR**,A
Methylobacterium extorquens AM1	Rhizobiales	**GR**(divergent)[3], R(divergent),virginiamycin B lyase,T,P,A
Rhizobium sp. NT-26	Rhizobiales	R(divergent),T,P,C,A,H,**GR**
Aurantimonas manganoxydans SI85-9A1	Rhizobiales	R(divergent),T,A,H,**GR**
Sphingopyxis macrogoltabida 203	Sphingomonadales	R(divergent),T,P,F,**GR**, A

[1] Letters relate to various *mer* genes as ordered in the operon. H - hypothetical genes, R(divergent) - *merR* located on the complementary DNA strand to other *mer* genes. Identified ORF's other than *mer* genes are spelled out as annotated by https://img.jgi.doe.gov/cgibin/mer/main.cgi?section=FindGenesBlast&page=geneSearchBlast.

[2] EmrE: Multidrug resistance efflux transporter

[3] ~700 nucleotides separate the end of *merR* from the beginning of *gor*.

Table 2.S6. Locus tags of the proteins used to construct *Thermus* phylogenies

Organism	Oah1	MerA	Oah2
Thermus thermophilus JL-18	TtJL18_129	TtJL18_0903	TtJL18_0900
Thermus parvatiensis RLM	RLTM_05389	RLTM_07013	RLTM_07028
Thermus igniterrae ATCC 700962	B128DRAFT_00153	B128DRAFT_00187	B128DRAFT_00184
Thermus thermophilus ATCC 33923	K677DRAFT_02284	K677DRAFT_00627	K677DRAFT_00624
Thermus sp. JCM 17653	Ga0128324_13572	Ga0128324_102119	Ga0128324_102115
Thermus thermophilus HB8	TTHA0760	TTHA1153	TTHA1156
Thermus islandicus DSM 21543	H531DRAFT_01004	H531DRAFT_00268	H531DRAFT_00265
Thermus thermophilus SG0.5JP17-16	Ththe16_0767	Ththe16_1165	Ththe16_1168
Thermus thermophilus HB27	TTC0408	TTC0789	TTC0792

Table 2.S7 Locus tag used to construct alphaproteobacterial phylogenies

Organism	Protein ID GR1	MerA protein ID	Protein ID GR2
Phaeobacter gallaeciensis DSM 26640	Gal_01017	Gal_03997	Gal_03999
Maritimibacter alkaliphilus HTCC2654	RB2654_05742	RB2654_22733	RB2654_22738
Oceanibulbus indolifex HEL-45	OIHEL45_10798	OIHEL45_14005	OIHEL45_14015
Oceanicola batsensis HTCC2597	OB2597_08744	OB2597_16362	OB2597_04905
Oceanicola granulosus HTCC2516	OG2516_15544	OG2516_01481	OG2516_01471
Pelagibaca bermudensis HTCC2601	R2601_08346	R2601_07528	R2601_07533
Sulfitobacter sp. EE-36	EE36_12388	EE36_00835	EE36_00845
Sulfitobacter sp. NAS-14.1	NAS141_17639	NAS141_02041	NAS141_02036
Parvularcula bermudensis HTCC2503	PB2503_08544	PB2503_12389	PB2503_12394
Methylobacterium extorquens AM1	MexAM1_META1p 2302	MexAM1_META1p 2635	MexAM1_META1p 2630
Rhizobium sp. NT-26	Ga0070469_121863	Ga0070469_1154	Ga0070469_1156
Aurantimonas manganoxydans SI85-9A1	Ga0112814_121107	Ga0112814_14154	Ga0112814_14152
Sphingopyxis macrogoltabida 203	Ga0100937_111557	Ga0100937_111201	Ga0100937_111202

APPENDIX C

Supplementary Material for Chapter 3

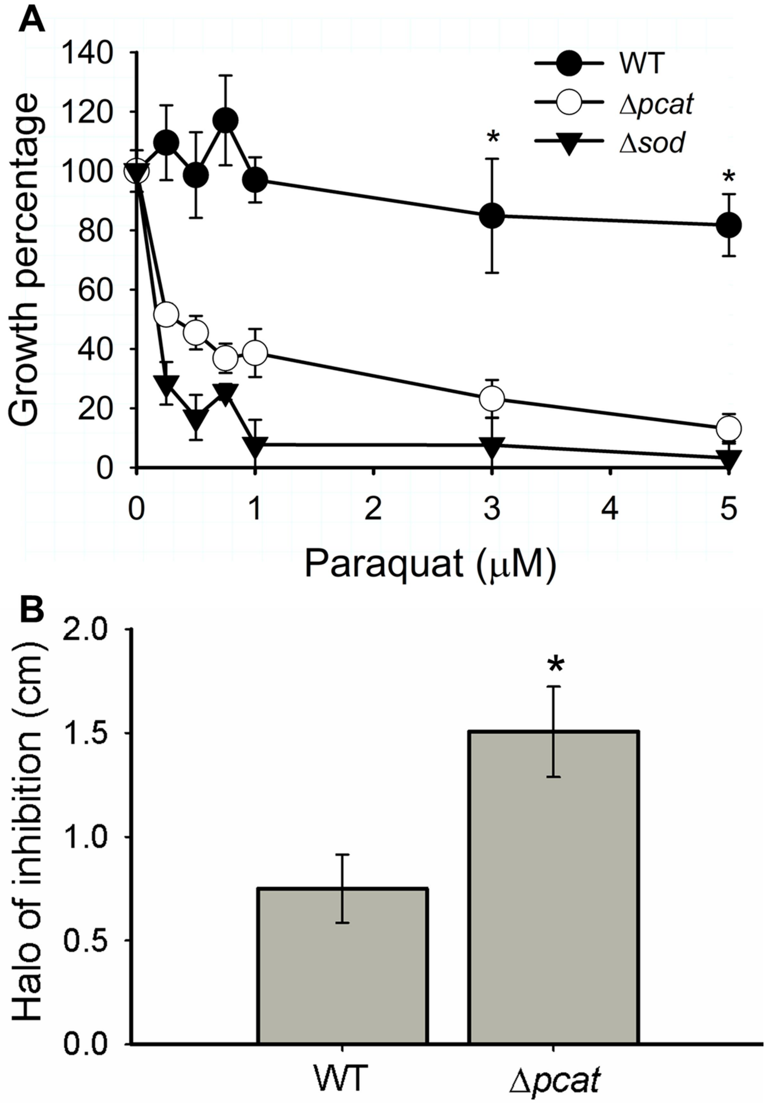

Fig 3.S1. Δ*sod* and Δ*pcat* strains are more sensitive to ROS than the WT strain. (A) The WT, Δ*sod*, and Δ*pcat* strains were grown with and without paraquat and culture optical densities after 18 hours of growth are shown. (B) The zone of clearing was monitored after exposure to 10 mM H_2O_2 was evaluated on soft agar plates. Each point represents the average of three independent cultures and standard deviations are shown. Student's t-tests were performed on the data and * indicates $P < 0.001$.

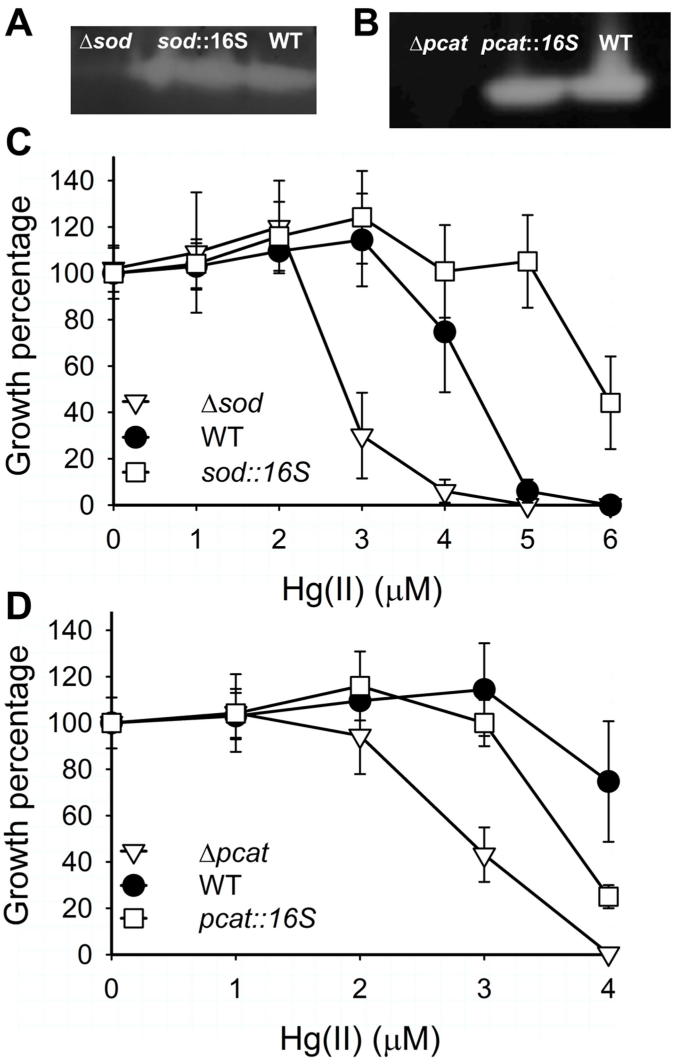

Fig 3.S2. Genetic complementation of Δ*sod* and Δ*pcat* strains. (A) Zymogram showing superoxide consumption activity in cell lysates from the WT, Δ*sod*, Δ*sod sod*::*16S* (*sod*::*16S* in the figure) strains. (B) Zymogram showing hydrogen peroxide comsuption activity of cell free lysates from the WT, Δ*pcat*, and Δ*pcat cat*::*16S* (*pcat*::*16S* in the figure) strains. Restored Hg(II) resistance for (C) *sod*::*16S* and (D) *pcat*::*16S*. Culture optical densities were determined after 21 hours of growth. Growth in the unexposed control was considered 100% of growth. Each point represents the average of three independent experiments and standard deviations are shown. Student's t-tests were performed on the data and * indicates P <0.01 when compared to the WT.

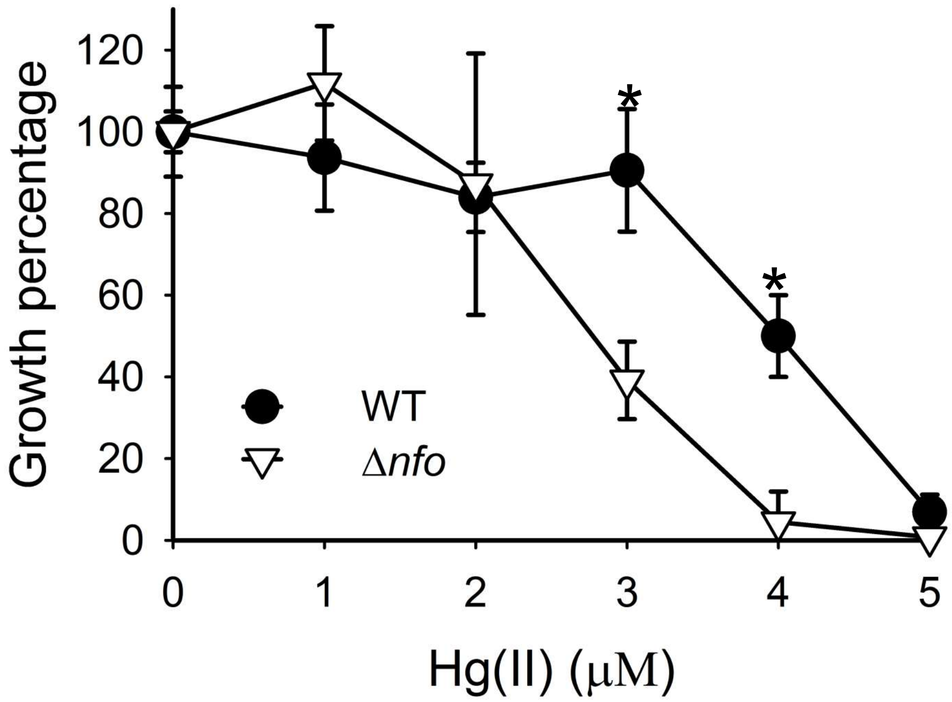

Figure 3.S3. A strain lacking Nfo is more sensitive to Hg(II). Strains were cultured with various concentrations of Hg(II) and final optical densities were measured after 20 hours. Growth in the unexposed control was considered 100% of growth. Each point represents the average of at least three independent cultures, and bars represent standard deviations. Student's t-tests were performed against the WT strain and * denotes $P < 0.001$.

Table 3.S1. Primers used to construct mutant strains for Chapter 3

Mutant strain	Primer	Sequence[1]
Δ*sod*	1 fum ecoRi for	TCGCGGGAATTCAGGGGAAC
	E HTK SOD rev	ATTGGTCCTTTCATACTTCACCTCCGC
	A sod HTK for	GGAAGCGGAGGTGAAGTATGAAAGGACCAATAATAA
	B sod htk rev	GCTATAAGGCTATGGGGATCAAAATGGTATGCGTT
	4 sod bamh1 rev	GGCGGATCCGGGCCTTA
	F HTK SOD for	GCATACCATTTTGATCCCCATAGCCTTATAGC
	5 fum upins for	GGAAGGTCAACCCCACCCAG
	6 sod downins rev	AAGGCCCTCCTCTTCGGC
Δ*pcat*	A cat	AAAGGAGGGAGAAGATGAAAGGACCAATAATAATG
	B cat	GCCAGGCTAAGGGTCAAAATGGTATGCGTTT
	NdeI 1 cat	GGGCCACATATGCCCAGAAG
	E cat	TTATTGGTCCTTTCATCTTCTCCCTCCTTTC
	F cat	TACCATTTTGACCCTTAGCCTGGCCCGTAG
	4.3 cat ecoR1	CCCAAGCCCGAATTCTTTCCC
	5 cat	ACCCAGGTGTCCTCGAGG
	6 cat	CTGGACCGGGTCTACCCC
Δ*pcat* *hygB*	NdeI 1 cat	GGGCCACATATGCCCAGAAG
	E cat hygB KO rev	AGGCTTTTTCATCTTCTCCCTCCTTTCG
	B cat hygB KO rev	AGGCTAAGGGCTATTCCTTTGCCCTC
	A cat hygB KO for	GAGGGAGAAGATGAAAAAGCCTGAACTCA
	4.3 cat eco R1	CCCAAGCCCGAATTCTTTCCC
	F cat hygB KO for	AAAGGAATAGCCCTTAGCCTGGCCC
Δ*sod* *hygB*	1 fum ecoRi for	TCGCGGGAATTCAGGGGAAC
	E sod hygB rev	TTCAGGCTTTTTCATACTTCACCTCCGCTTC
	A sod hygB for	CGGAGGTGAAGTATGAAAAAGCCTGAACTCAC
	B sod hygB rev	GCTATGGGGACTATTCCTTTGCCCTCG
	F sod hygB for	GCAAAGGAATAGTCCCCATAGCCTTATAGCC
	4 SOD HygB rev hindIII	GCCTGAAGCTTGCGGTGG

[1] Underlined sequences indicate restriction enzyme cutting sites.

Table 3.S2. Primers and parameters used for qPCR in Chapter 3

Primer	Sequence	C (µM)**	T_A (°C)	Size (bp)
gyrase-F	GGGCGAGGTCATGGGC	1	61	134
gyrase-R	CGCCGTCTATGGAGCCG	0.25		
SOD-F	CGTTCAAGCTTCCTGACCTAGG	1.25	59	117
SOD-R	CGTTGAGGTTCGTCACGTAGGC	1.25		
osmC-F	GATTGAGCTTCTGACCGAGGC	1.25	60	126
osmC-R	AGGACGATCTCCTTCACCCC	1.25		
bcp-F	GAAGTACGGCCTGAACTTTCC	1.25	58	132
bcp-R	TCTATGAGGAAGGTCTGGCG	1.25		
TplA-F	TGGCTTTGTCTTGGAGAACGC	1.25	60	141
TplA-R	CAGAGGTGTTTGGGCAAGGC	1.25		
pcat rev	CGCCACCAGCTCAATGT	1.25	57	105
pcat for	ATGTACCAGTCCTTCAACTTCC	1.25		

**C indicates final concentration of the primers

REFERENCES

Achard ME, Hamilton AJ, Dankowski T, Heras B, Schembri MS, Edwards JL, Jennings MP & McEwan AG (2009) A periplasmic thioredoxin-like protein plays a role in defense against oxidative stress in Neisseria gonorrhoeae. *Infection and immunity* **77**: 4934-4939.

Ansari AZ, Chael ML & O'Halloran TV (1992) Allosteric underwinding of DNA is a critical step in positive control of transcription by Hg-MerR. *Nature* **355**: 87-89.

Ariza ME & Williams MV (1999) Lead and mercury mutagenesis: Type of mutation dependent upon metal concentration. *Journal of Biochemical and Molecular Toxicology* **13**: 107-112.

Ariza ME, Bijur GN & Williams MV (1998) Lead and mercury mutagenesis: Role of H2O2, superoxide dismutase, and xanthine oxidase. *Environmental and Molecular Mutagenesis* **31**: 352-361.

Babai R & Ron EZ (1998) An Escherichia coli gene responsive to heavy metals. *FEMS microbiology letters* **167**: 107-111.

Barkay T, Miller SM & Summers AO (2003) Bacterial mercury resistance from atoms to ecosystems. *FEMS Microbiology Reviews* **27**: 355.

Barkay T, Kritee K, Boyd E & Geesey G (2010) A thermophilic bacterial origin and subsequent constraints by redox, light and salinity on the evolution of the microbial mercuric reductase. *Environ Microbiol* **12**: 2904-2917.

Beers RF, Jr. & Sizer IW (1952) A spectrophotometric method for measuring the breakdown of hydrogen peroxide by catalase. *J Biol Chem* **195**: 133-140.

Boyd ES & Barkay T (2012) The mercury resistance operon: from an origin in a geothermal environment to an efficient detoxification machine. *Front Microbiol* **3**: 349.

Branco V, Godinho-Santos A, Gonçalves J, Lu J, Holmgren A & Carvalho C (2014) Mitochondrial thioredoxin reductase inhibition, selenium status, and Nrf-2 activation are determinant factors modulating the toxicity of mercury compounds. *Free Radical Biology and Medicine* **73**: 95.

Brown NL, Stoyanov JV, Kidd SP & Hobman JL (2003) The MerR family of transcriptional regulators. *FEMS Microbiology Reviews* **27**: 145.

Brünker P, Rother D, Klein J, Mattes R, Altenbuchner J & Sedlmeier R (1996) Regulation of the operon responsible for broad-spectrum mercury resistance inStreptomyces lividans 1326. *Molecular and General Genetics MGG* **251**: 307-315.

Cappello T, Brandão F, Guilherme S, Santos MA, Maisano M, Mauceri A, Canário J, Pacheco M & Pereira P (2016) Insights into the mechanisms underlying mercury-induced oxidative stress in gills of wild fish (Liza aurata) combining 1H NMR metabolomics and conventional biochemical assays. *Science of The Total Environment* **548-549**: 13.

Carvalho CM, Chew EH, Hashemy SI, Lu J & Holmgren A (2008) Inhibition of the human thioredoxin system. A molecular mechanism of mercury toxicity. *J Biol Chem* **283**: 11913-11923.

Cassier-Chauvat C & Chauvat F (2014) Responses to Oxidative and Heavy Metal Stresses in Cyanobacteria: Recent Advances. *International Journal of Molecular Sciences* **16**: 871.

Chang CC, Lin LY, Zou XW, Huang CC & Chan NL (2015) Structural basis of the mercury(II)-mediated conformational switching of the dual-function transcriptional regulator MerR. *Nucleic acids research* **43**: 7612-7623.

Clarke DJ, Ortega XP, Mackay CL, Valvano MA, Govan JR, Campopiano DJ, Langridge-Smith P & Brown AR (2010) Subdivision of the bacterioferritin comigratory protein family of bacterial peroxiredoxins based on catalytic activity. *Biochemistry* **49**: 1319-1330.

Cusick KD, Fitzgerald LA, Cockrell AL & Biffinger JC (2015) Selection and Evaluation of Reference Genes for Reverse Transcription-Quantitative PCR Expression Studies in a Thermophilic Bacterium Grown under Different Culture Conditions. *PLoS One* **10**: e0131015.

Djaman O, Outten FW & Imlay JA (2004) Repair of oxidized iron-sulfur clusters in Escherichia coli. *J Biol Chem* **279**: 44590-44599.

Dopson M (2003) Growth in sulfidic mineral environments: metal resistance mechanisms in acidophilic micro-organisms. *Microbiology* **149**: 1959.

Dressaire C, Picard F, Redon E, Loubiere P, Queinnec I, Girbal L & Cocaign-Bousquet M (2013) *Role of mRNA Stability during Bacterial Adaptation*.

Ercal N, Gurer-Orhan H & Aykin-Burns N (2001) Toxic metals and oxidative stress part I: mechanisms involved in metal-induced oxidative damage. *Curr Top Med Chem* **1**: 529-539.

Fahey RC (2013) Glutathione analogs in prokaryotes. *Biochimica et Biophysica Acta (BBA) - General Subjects* **1830**: 3182-3198.

Fanous A, Weiss W, Gorg A, Jacob F & Parlar H (2008) A proteome analysis of the cadmium and mercury response in Corynebacterium glutamicum. *Proteomics* **8**: 4976-4986.

Farrell RE, Germida JJ & Huang PM (1993) Effects of chemical speciation in growth media on the toxicity of mercury(II). *Appl Environ Microbiol* **59**: 1507-1514.

Flint DH, Tuminello JF & Emptage MH (1993) The inactivation of Fe-S cluster containing hydro-lyases by superoxide. *J Biol Chem* **268**: 22369-22376.

Flohe L, Toppo S, Cozza G & Ursini F (2011) A comparison of thiol peroxidase mechanisms. *Antioxid Redox Signal* **15**: 763-780.

Freedman Z, Zhu C & Barkay T (2012) Mercury resistance and mercuric reductase activities and expression among chemotrophic thermophilic Aquificae. *Appl Environ Microbiol* **78**: 6568-6575.

Gaballa A, Newton GL, Antelmann H, Parsonage D, Upton H, Rawat M, Claiborne A, Fahey RC & Helmann JD (2010) Biosynthesis and functions of bacillithiol, a major low-molecular-weight thiol in Bacilli. *Proceedings of the National Academy of Sciences of the United States of America* **107**: 6482-6486.

Gambill BD & Summers AO (1992) Synthesis and degradation of the mRNA of the Tn21 mer operon. *J Mol Biol* **225**: 251-259.

Geesey GG, Barkay T & King S (2016) Microbes in mercury-enriched geothermal springs in western North America. *The Science of the total environment* **569-570**: 321-331.

Gleason FK & Holmgren A (1988) Thioredoxin and related proteins in procaryotes. *FEMS Microbiol Rev* **4**: 271-297.

Grant CM (2001) Role of the glutathione/glutaredoxin and thioredoxin systems in yeast growth and response to stress conditions. *Mol Microbiol* **39**: 533-541.

Gregory ST & Dahlberg AE (2009) Genetic and structural analysis of base substitutions in the central pseudoknot of Thermus thermophilus 16S ribosomal RNA. *RNA* **15**: 215-223.

Guo H-B, Johs A, Parks JM, Olliff L, Miller SM, Summers AO, Liang L & Smith JC (2010) Structure and conformational dynamics of the metalloregulator MerR upon binding of Hg(II). *Journal of molecular biology* **398**: 555-568.

Hartmann RK, Wolters J, Kröger B, Schultze S, Specht T & Erdmann VA (1989) Does Thermus Represent Another Deep Eubacterial Branching? *Systematic and Applied Microbiology* **11**: 243-249.

Helbig K, Bleuel C, Krauss GJ & Nies DH (2008) Glutathione and transition-metal homeostasis in Escherichia coli. *Journal of bacteriology* **190**: 5431-5438.

Heltzel A, Lee IW, Totis PA & Summers AO (1990) Activator-dependent preinduction binding of sigma-70 RNA polymerase at the metal-regulated mer promoter. *Biochemistry* **29**: 9572-9584.

Heltzel A, Gambill D, Jackson WJ, Totis PA & Summers AO (1987) Overexpression and DNA-binding properties of the mer-encoded regulatory protein from plasmid NR1 (Tn21). *J Bacteriol* **169**: 3379-3384.

Henley RW (1996) Chemical and physical context for life in terrestrial hydrothermal systems: chemical reactors for the early development of life and hydrothermal ecosystems. *Ciba Foundation symposium* **202**: 61-76; discussion 76-82.

Hidalgo A, Betancor L, Moreno R, Zafra O, Cava F, Fernandez-Lafuente R, Guisan JM & Berenguer J (2004) Thermus thermophilus as a cell factory for the production of a thermophilic Mn-dependent catalase which fails to be synthesized in an active form in Escherichia coli. *Appl Environ Microbiol* **70**: 3839-3844.

Hider RC & Kong XL (2011) Glutathione: a key component of the cytoplasmic labile iron pool. *Biometals* **24**: 1179-1187.

Hobman JL & Crossman LC (2015) Bacterial antimicrobial metal ion resistance. *Journal of medical microbiology* **64**: 471-497.

Hoseki J, Yano T, Koyama Y, Kuramitsu S & Kagamiyama H (1999) Directed Evolution of Thermostable Kanamycin-Resistance Gene: A Convenient Selection Marker for Thermus thermophilus. *Journal of biochemistry* **126**: 951.

Ilyas S & Rehman A (2015) Oxidative stress, glutathione level and antioxidant response to heavy metals in multi-resistant pathogen, Candida tropicalis. *Environ Monit Assess* **187**: 4115.

Imlay JA (2008) Cellular defenses against superoxide and hydrogen peroxide. *Annual review of biochemistry* **77**: 755-776.

Imlay JA (2013) The molecular mechanisms and physiological consequences of oxidative stress: lessons from a model bacterium. *Nature reviews Microbiology* **11**: 443-454.

Imlay JA (2014) The Mismetallation of Enzymes during Oxidative Stress*. *Journal of Biological Chemistry* **289**: 28121.

Iwama T, Hosokawa H, Lin W, Shimizu H, Kawai K & Yamagata S (2004) Comparative characterization of the oah2 gene homologous to the oah1 of Thermus thermophilus HB8. *Bioscience, biotechnology, and biochemistry* **68**: 1357-1361.

Jan AT, Ali A & Haq Q (2011) Glutathione as an antioxidant in inorganic mercury induced nephrotoxicity. *Journal of postgraduate medicine* **57**: 72-77.

Jeanmougin F, Thompson JD, Gouy M, Higgins DG & Gibson TJ (1998) Multiple sequence alignment with Clustal X. *Trends in biochemical sciences* **23**: 403-405.

Jeong W, Cha MK & Kim IH (2000) Thioredoxin-dependent hydroperoxide peroxidase activity of bacterioferritin comigratory protein (BCP) as a new member of the thiol-specific antioxidant protein (TSA)/Alkyl hydroperoxide peroxidase C (AhpC) family. *J Biol Chem* **275**: 2924-2930.

Jones DT, Taylor WR & Thornton JM (1992) The rapid generation of mutation data matrices from protein sequences. *Computer applications in the biosciences : CABIOS* **8**: 275-282.

Kennedy MC, Emptage MH, Dreyer JL & Beinert H (1983) The role of iron in the activation-inactivation of aconitase. *Journal of Biological Chemistry* **258**: 11098-11105.

Kobayashi S, Masui R, Yokoyama S, Kuramitsu S & Takagi H (2004) A novel metal-activated L-serine O-acetyltransferase from Thermus thermophilus HB8. *J Biochem* **136**: 629-634.

Kosuge T, Gao D & Hoshino T (2005) Analysis of the methionine biosynthetic pathway in the extremely thermophilic eubacterium Thermus thermophilus. *Journal of bioscience and bioengineering* **90**: 271-279.

Kulkarni RD & Summers AO (1999) MerR Cross-Links to the α, β, and σ 70 Subunits of RNA Polymerase in the Preinitiation Complex at the merTPCAD Promoter † *Biochemistry* **38**: 3362.

Kumar S, Stecher G & Tamura K (2016) MEGA7: Molecular Evolutionary Genetics Analysis Version 7.0 for Bigger Datasets. *Molecular biology and evolution* **33**: 1870-1874.

Larkin MA, Blackshields G, Brown NP*, et al.* (2007) Clustal W and Clustal X version 2.0. *Bioinformatics (Oxford, England)* **23**: 2947-2948.

Latinwo LM, Donald C, Ikediobi C & Silver S (1998) Effects of intracellular glutathione on sensitivity of Escherichia coli to mercury and arsenite. *Biochemical and biophysical research communications* **242**: 67-70.

Lau PCY, Sung CK, Lee JH, Morrison DA & Cvitkovitch DG (2002) PCR ligation mutagenesis in transformable streptococci: application and efficiency. *Journal of microbiological methods* **49**: 193-205.

LaVoie SP, Mapolelo DT, Cowart DM, Polacco BJ, Johnson MK, Scott RA, Miller SM & Summers AO (2015) Organic and inorganic mercurials have distinct effects on cellular thiols, metal homeostasis, and Fe-binding proteins in Escherichia coli. *Journal of biological inorganic chemistry : JBIC : a publication of the Society of Biological Inorganic Chemistry* **20**: 1239-1251.

Ledwidge R, Patel B, Dong A, Fiedler D, Falkowski M, Zelikova J, Summers AO, Pai EF & Miller SM (2005) NmerA, the metal binding domain of mercuric ion reductase, removes Hg2+ from proteins, delivers it to the catalytic core, and protects cells under glutathione-depleted conditions. *Biochemistry* **44**: 11402-11416.

Lee IW, Livrelli V, Park SJ, Totis PA & Summers AO (1993) In vivo DNA-protein interactions at the divergent mercury resistance (mer) promoters. II. Repressor/activator (MerR)-RNA polymerase interaction with merOP mutants. *J Biol Chem* **268**: 2632-2639.

Lemire JA, Harrison JJ & Turner RJ (2013) Antimicrobial activity of metals: mechanisms, molecular targets and applications. *Nat Rev Microbiol* **11**: 371-384.

Lesniak J, Barton WA & Nikolov DB (2002) Structural and functional characterization of the Pseudomonas hydroperoxide resistance protein Ohr. *The EMBO journal* **21**: 6649-6659.

Lesniak J, Barton WA & Nikolov DB (2003) Structural and functional features of the Escherichia coli hydroperoxide resistance protein OsmC. *Protein science : a publication of the Protein Society* **12**: 2838-2843.

Livak KJ & Schmittgen TD (2001) Analysis of Relative Gene Expression Data Using Real-Time Quantitative PCR and the 2−ΔΔCT Method. *Methods* **25**: 402.

Livrelli V, Lee IW & Summers AO (1993) In vivo DNA-protein interactions at the divergent mercury resistance (mer) promoters. I. Metalloregulatory protein MerR mutants. *J Biol Chem* **268**: 2623-2631.

Loi VV, Rossius M & Antelmann H (2015) Redox regulation by reversible protein S-thiolation in bacteria. *Frontiers in Microbiology* **6**.

Lu J & Holmgren A (2014) The thioredoxin antioxidant system. *Free Radical Biology and Medicine* **66**: 75-87.

Lund BO, Miller DM & Woods JS (1991) Mercury-induced H2O2 production and lipid peroxidation in vitro in rat kidney mitochondria. *Biochem Pharmacol* **42 Suppl**: S181-187.

Lund P & Brown N (1989) Up-promoter mutations in the positively-regulated mer promoter of Tn501. *Nucleic acids research* **17**: 5517-5527.

Ma Z, Chandrangsu P, Helmann TC, Romsang A, Gaballa A & Helmann JD (2014) Bacillithiol is a major buffer of the labile zinc pool in Bacillus subtilis. *Molecular Microbiology* **94**: 756-770.

Miller DM, Lund B-O & Woods JS (1991) Reactivity of Hg(II) with superoxide: Evidence for the catalytic dismutation of superoxide by HG(II). *Journal of Biochemical Toxicology* **6**: 293-298.

Moller AK, Barkay T, Abu Al-Soud W, Sorensen SJ, Skov H & Kroer N (2011) Diversity and characterization of mercury-resistant bacteria in snow, freshwater and sea-ice brine from the High Arctic. *FEMS Microbiol Ecol* **75**: 390-401.

Morita R, Nakane S, Shimada A, Inoue M, Iino H, Wakamatsu T, Fukui K, Nakagawa N, Masui R & Kuramitsu S (2010) Molecular Mechanisms of the Whole DNA Repair System: A Comparison of Bacterial and Eukaryotic Systems. *Journal of Nucleic Acids* **2010**: 179594.

Murphy Michael P (2009) How mitochondria produce reactive oxygen species. *Biochemical Journal* **417**: 1-13.

Myhre O, Andersen JM, Aarnes H & Fonnum F (2003) Evaluation of the probes 2′,7′-dichlorofluorescin diacetate, luminol, and lucigenin as indicators of reactive species formation. *Biochemical Pharmacology* **65**: 1575-1582.

Nath KA, Croatt AJ, Likely S, Behrens TW & Warden D (1996) Renal oxidant injury and oxidant response induced by mercury. *Kidney international* **50**: 1032-1043.

Newton GL, Rawat M, La Clair JJ, Jothivasan VK, Budiarto T, Hamilton CJ, Claiborne A, Helmann JD & Fahey RC (2009) Bacillithiol is an antioxidant thiol produced in Bacilli. *Nature chemical biology* **5**: 625-627.

Ni'Bhriain NN, Silver S & Foster TJ (1983) Tn5 insertion mutations in the mercuric ion resistance genes derived from plasmid R100. *J Bacteriol* **155**: 690-703.

Nies DH (1999) Microbial heavy-metal resistance. *Applied microbiology and biotechnology* **51**: 730-750.

Nies DH (2003) Efflux-mediated heavy metal resistance in prokaryotes. *FEMS Microbiology Reviews* **27**: 313.

Norambuena J, Wang Y, Hanson T, Boyd JM & Barkay T (2018) Low molecular weight thiols and thioredoxins are important players in Hg(II) resistance in Thermus thermophilus HB27. *Appl Environ Microbiol*.

O'Halloran TV, Frantz B, Shin MK, Ralston DM & Wright JG (1989) The MerR heavy metal receptor mediates positive activation in a topologically novel transcription complex. *Cell* **56**: 119-129.

Omotayo TI, Rocha JB, Ibukun EO & Kade IJ (2011) Inorganic mercury interacts with thiols at the nucleotide and cationic binding sites of the ouabain-sensitive cerebral electrogenic sodium pump. *Neurochem Int* **58**: 776-784.

Onnis-Hayden A, Weng H, He M, Hansen S, Ilyin V, Lewis K & Guc AZ (2009) Prokaryotic real-time gene expression profiling for toxicity assessment. *Environ Sci Technol* **43**: 4574-4581.

Oram PD, Fang X, Fernando Q, Letkeman P & Letkeman D (1996) The formation of constants of mercury(II)--glutathione complexes. *Chemical research in toxicology* **9**: 709-712.

Oregaard G & Sorensen SJ (2007) High diversity of bacterial mercuric reductase genes from surface and sub-surface floodplain soil (Oak Ridge, USA). *The ISME journal* **1**: 453-467.

Park SJ, Wireman J & Summers AO (1992) Genetic analysis of the Tn21 mer operator-promoter. *J Bacteriol* **174**: 2160-2171.

Parkhill J, Lawley B, Hobman JL & Brown NL (1998) Selection and characterization of mercury-independent activation mutants of the Tn501 transcriptional regulator, MerR. *Microbiology* **144 (Pt 10)**: 2855-2864.

Quastel JH, Stewart CP & Tunnicliffe HE (1923) On Glutathione. IV. Constitution. *The Biochemical journal* **17**: 586-592.

Rao B, Simpson C, Lin H, Liang L & Gu B (2014) Determination of thiol functional groups on bacteria and natural organic matter in environmental systems. *Talanta* **119**: 240.

Rasmussen LD, Zawadsky C, Binnerup SJ, Oregaard G, Sorensen SJ & Kroer N (2008) Cultivation of hard-to-culture subsurface mercury-resistant bacteria and discovery of new merA gene sequences. *Appl Environ Microbiol* **74**: 3795-3803.

Ravel J, DiRuggiero J, Robb FT & Hill RT (2000) Cloning and sequence analysis of the mercury resistance operon of Streptomyces sp. Strain CHR28 reveals a novel putative second regulatory gene. *J Bacteriol* **182**: 2345-2349.

Reeves SA, Parsonage D, Nelson KJ & Poole LB (2011) Kinetic and thermodynamic features reveal that Escherichia coli BCP is an unusually versatile peroxiredoxin. *Biochemistry* **50**: 8970-8981.

Rethmeier J, Rabenstein A, Langer M & Fischer U (1997) Detection of traces of oxidized and reduced sulfur compounds in small samples by combination of different high-performance liquid chromatography methods. *Journal of Chromatography A* **760**: 295-302.

Ritz D & Beckwith J (2001) Roles of thiol-redox pathways in bacteria. *Annual review of microbiology* **55**: 21-48.

Rodríguez-Rojas F, Díaz-Vásquez W, Undabarrena A, Muñoz-Díaz P, Arenas F & Vásquez C (2016) Mercury-mediated cross-resistance to tellurite in Pseudomonas spp. isolated from the Chilean Antarctic territory. *Metallomics* **8**: 108.

ROLAND F. BEERS AIWS (1952) A spectrophotometric method for measuring the breakdown of hydrogen peroxide by catalase. *The Journal of Biological Chemistry* **195**: 133-140.

Rosario-Cruz Z & Boyd JM (2015) Physiological roles of bacillithiol in intracellular metal processing. *Current genetics* **62**: 59-65.

Rosario-Cruz Z, Chahal HK, Mike LA, Skaar EP & Boyd JM (2015) Bacillithiol has a role in Fe-S cluster biogenesis in Staphylococcus aureus. *Molecular microbiology* **98**: 218-242.

Ross W, Park SJ & Summers AO (1989) Genetic analysis of transcriptional activation and repression in the Tn21 mer operon. *J Bacteriol* **171**: 4009-4018.

Saikolappan S, Das K & Dhandayuthapani S (2015) Inactivation of the organic hydroperoxide stress resistance regulator OhrR enhances resistance to oxidative stress and isoniazid in Mycobacterium smegmatis. *J Bacteriol* **197**: 51-62.

Schelert J, Drozda M, Dixit V, Dillman A & Blum P (2006) Regulation of mercury resistance in the crenarchaeote Sulfolobus solfataricus. *J Bacteriol* **188**: 7141-7150.

Schelert J, Dixit V, Hoang V, Simbahan J, Drozda M & Blum P (2003) Occurrence and Characterization of Mercury Resistance in the Hyperthermophilic Archaeon Sulfolobus solfataricus by Use of Gene Disruption. *Journal of Bacteriology* **186**: 427-437.

Shewchuk LM, Verdine GL & Walsh CT (1989) Transcriptional switching by the metalloregulatory MerR protein: initial characterization of DNA and mercury (II) binding activities. *Biochemistry* **28**: 2331-2339.

Shewchuk LM, Verdine GL, Nash H & Walsh CT (1989) Mutagenesis of the cysteines in the metalloregulatory protein MerR indicates that a metal-bridged dimer activates transcription. *Biochemistry* **28**: 6140-6145.

Shewchuk LM, Helmann JD, Ross W, Park SJ, Summers AO & Walsh CT (1989) Transcriptional switching by the MerR protein: activation and repression mutants implicate distinct DNA and mercury(II) binding domains. *Biochemistry* **28**: 2340-2344.

Shimizu H, Yamagata S, Masui R, Inoue Y, Shibata T, Yokoyama S, Kuramitsu S & Iwama T (2001) Cloning and overexpression of the oah1 gene encoding O-acetyl-L-homoserine sulfhydrylase of Thermus thermophilus HB8 and characterization of the gene product. *Biochimica et biophysica acta* **1549**: 61-72.

Solovyev V (2011) *V. Solovyev, A Salamov (2011) Automatic Annotation of Microbial Genomes and Metagenomic Sequences. In Metagenomics and its Applications in Agriculture, Biomedicine and Environmental Studies (Ed. R.W. Li), Nova Science Publishers, p.61-78*.

Song L, Teng Q, Phillips RS, Brewer JM & Summers AO (2007) Lingyun Song1, Quincy Teng2, Robert S. Phillips2,3 John M. Brewer3 and Anne O. Summers1. *Journal of Molecular Biology* **371**: 79.

Spitz DR & Oberley LW (1989) An assay for superoxide dismutase activity in mammalian tissue homogenates. *Analytical Biochemistry* **179**: 8-18.

Steele RA & Opella SJ (1997) Structures of the Reduced and Mercury-Bound Forms of MerP, the Periplasmic Protein from the Bacterial Mercury Detoxification System. *Biochemistry* **36**: 6885-6895.

Summers AO (2009) Damage control: regulating defenses against toxic metals and metalloids. *Current Opinion in Microbiology* **12**: 138.

Swarts DC, Koehorst JJ, Westra ER, Schaap PJ & van der Oost J (2015) Effects of Argonaute on Gene Expression in Thermus thermophilus. *PLoS One* **10**: e0124880.

Tanaka T, Kawano N & Oshima T (1981) Cloning of 3-isopropylmalate dehydrogenase gene of an extreme thermophile and partial purification of the gene product. *Journal of biochemistry* **89**: 677-682.

Thorgersen MP & Downs DM (2008) Analysis of yggX and gshA mutants provides insights into the labile iron pool in Salmonella enterica. *J Bacteriol* **190**: 7608-7613.

Valko M, Morris H & Cronin MTD (2005) Metals, Toxicity and Oxidative Stress. *Current Medicinal Chemistry* **12**: 1161-1208.

Varghese S, Tang Y & Imlay JA (2003) Contrasting sensitivities of Escherichia coli aconitases A and B to oxidation and iron depletion. *J Bacteriol* **185**: 221-230.

Vetriani C, Chew YS, Miller SM, Yagi J, Coombs J, Lutz RA & Barkay T (2005) Mercury adaptation among bacteria from a deep-sea hydrothermal vent. *Applied and environmental microbiology* **71**: 220-226.

Wang D, Huang S, Liu P*, et al.* (2016) Structural Analysis of the Hg(II)-Regulatory Protein Tn501 MerR from Pseudomonas aeruginosa. *Scientific Reports* **6**: 33391.

Wang H & Joseph JA (1999) Quantifying cellular oxidative stress by dichlorofluorescein assay using microplate reader. *Free radical biology & medicine* **27**: 612-616.

Wang X & Horisberger JD (1996) Mercury binding site on Na+/K(+)-ATPase: a cysteine in the first transmembrane segment. *Molecular pharmacology* **50**: 687-691.

Wang X, Zhou X, Zhao J, Zheng Y, Song C, Long M & Chen T (2015) Hydrochemical evolution and reaction simulation of travertine deposition of the Lianchangping hot springs in Yunnan, China. *Quaternary International* **374**: 62-75.

Wang Y, Robison T & Wiatrowski H (2013) The impact of ionic mercury on antioxidant defenses in two mercury-sensitive anaerobic bacteria. *Biometals : an international journal on the role of metal ions in biology, biochemistry, and medicine* **26**: 1023-1031.

Wang Y, Freedman Z, Lu-Irving P, Kaletsky R & Barkay T (2009) An initial characterization of the mercury resistance (mer) system of the thermophilic bacterium Thermus thermophilus HB27. *FEMS Microbiology Ecology* **67**: 118.

Weydert CJ & Cullen JJ (2010) Measurement of superoxide dismutase, catalase and glutathione peroxidase in cultured cells and tissue. *Nat Protoc* **5**: 51-66.

Xu FF & Imlay JA (2012) Silver(I), mercury(II), cadmium(II), and zinc(II) target exposed enzymic iron-sulfur clusters when they toxify Escherichia coli. *Appl Environ Microbiol* **78**: 3614-3621.

Zeng Q, Stalhandske C, Anderson MC, Scott RA & Summers AO (1998) The core metal-recognition domain of MerR. *Biochemistry* **37**: 15885-15895.